THE UNIVERSITY OF MICHIGAN

INDUSTRY PROGRAM OF THE COLLEGE OF ENGINEERING

THE EXPERIMENTAL DETERMINATION OF THE ENTHALPY OF MIXING OF BINARY GASEOUS MIXTURES UNDER PRESSURE

Arun V. Hejmadi

A dissertation submitted in partial fulfillment
of the requirements for the degree of
Doctor of Philosophy
(Chemical Engineering)
in The University of Michigan

December, 1970

IP-836

To Ahalya

ACKNOWLEDGMENTS

I wish to express my appreciation to the people and organizations who contributed to the success of this research:

To Professor John E. Powers, the chairman of my thesis committee, for his constant encouragement and guidance.

To Professor Donald L. Katz for his help, advice and encouragement during this work.

To the members of my thesis committee, Professors Joseph J. Martin, Richard E. Sonntag and Edgar F. Westrum, Jr., for their advice and assistance.

To Andre W. Furtado for many helpful discussions some of which involved this research.

To Dr. David T. Mage and Dr. Millard L. Jones for contributing to the initial phases of design and construction of the equipment.

To others who helped in various phases of this research: Donald Barber, Vasant Bhirud, Peter Fodor, Donald Gatza, Joseph Golba, Vijay Khanna, Dr. Alan Mather and Dr. Victor Yesavage.

To the members of the ORA Instrument Shop: William Rekewitz, Edward Rupke and Herbert Senecal.

To the members of the Instrument Shop of the Chemical and Metallurgical Engineering Department: Cleatis Bolen, Douglas Connell, Erwin Muehlig, Peter Severn and John Wurster.

To the National Science Foundation for two grants without which the project would not have proceeded.

To the Cities Service Oil Company for fellowship support in the latter phases of the work.

To the Chemical and Metallurgical Engineering Department for providing computer time.

To Professor Edgar F. Westrum, Jr., for the use of equipment.

To the National Bureau of Standards for the calibration of standard cells and thermopiles.

To my wife and family for their faith in me.

TABLE OF CONTENTS

	Page
ACKNOWLEDGMENTS	iv
LIST OF TABLES	x
LIST OF FIGURES	xiii
NOMENCLATURE	xv
ABSTRACT	xix
INTRODUCTION	1
EXPERIENCE OF PREVIOUS INVESTIGATORS	3
Excess Property Measurements on Liquids	3
Discussion of Closed-System Calorimeters	7
Discussion of Flow Calorimeters	8
Excess Enthalpy Measurements on Gases	10
Comparison of Flow Calorimetric Techniques for Gases	12
Calorimeter Design	12
Flow and Composition Measurement	13
Mode of Operation	14
Interpretation and Smoothing of Data	15
Prediction Methods	16
Review of Thermodynamic Properties	17
Nitrogen	18
Carbon Dioxide	19
Ethane	21
Oxygen	22
Nitrogen-Carbon Dioxide Mixtures	22
Nitrogen-Ethane Mixtures	24
Nitrogen-Oxygen Mixtures	24

TABLE OF CONTENTS (Continued)

Page

THERMODYNAMIC RELATIONS 28

Thermodynamic Definitions 28

Correlation of Excess Enthalpy with Composition 31

Relations for the Benedict-Webb-Rubin Equation of State 32

Application of First Law of Thermodynamics 35

Primary Corrections 39

Corrections for Impurities 40

Nitrogen-Carbon Dioxide System 41

Nitrogen-Ethane System 44

Secondary Corrections and Smoothing of Data 47

APPARATUS AND EXPERIMENTS 50

APPARATUS 50

Calorimeter 50

Flow Calorimetric Facility 55

Flow System 56

Gas Supply Assembly 60

Constant Temperature Baths 61

Control Panel 63

MEASUREMENTS AND CALIBRATIONS 65

Pressure 65

Pressure Level 65

Differential Pressure 66

Temperature 67

Power 68

TABLE OF CONTENTS (Continued)

Page

Voltage Drop across Calorimeter Heater 68

Current in Calorimeter Heater 70

Flow Rate 71

High Pressure Flow Meters 71

Low Pressure Flow Meter 80

Gas Composition 81

Can Volume Determination 82

Gas Density Measurement 83

PROCEDURE 84

Preparation of the Apparatus 84

Startup 85

Measurements at Steady State 85

Data and Data Reduction 86

RESULTS 89

Interpretation of Calorimetric Data 89

Nitrogen-Carbon Dioxide System 89

Nitrogen-Ethane System 104

Nitrogen-Oxygen System 111

Discussion of Results 114

Check on the Assumption of Adiabaticity 114

Accuracy of the Results 117

Comparisons 120

RECOMMENDATIONS FOR IMPROVEMENT OF EXPERIMENTAL TECHNIQUES IN SUBSEQUENT STUDIES 123

SUMMARY AND CONCLUSIONS 125

TABLE OF CONTENTS (Continued)

	Page
APPENDIX A. ERROR ANALYSIS	127
Compounding of Errors	127
Power Input Measurement	128
Flow Rate Measurement	128
Gas Composition	135
Excess Enthalpy Determinations	138
APPENDIX B. CALIBRATIONS	143
APPENDIX C. TABULATED EXPERIMENTAL DATA AND RESULTS	157
APPENDIX D. SAMPLE CALCULATIONS	171
Volume Determination of Calibration Tank	171
Flow Meter Calibration	177
Enthalpy of Mixing Measurement	184
Nomenclature for Appendix D	196
BIBLIOGRAPHY	202

LIST OF TABLES

Table		Page
I	Investigations of Excess Thermodynamic Properties of Binary Mixtures in the Liquid State at Low Temperatures	4
II	Experimental Investigations of the Enthalpy of Mixing of Gases	11
III	Experimental Investigations on the Binary System Nitrogen-Carbon Dioxide under Pressure	23
IV	Experimental Investigations on the Binary System Nitrogen-Ethane under Pressure	25
V	Some Experimental Investigations on the Binary System Nitrogen-Oxygen under Pressure	27
VI	Key to Sketch of Calorimeter in Figure 2	53
VII	Key to Flow Diagram in Figure 3	59
VIII	Systems Studied and Conditions of Experimental Investigation of this Research	87
IX	Impurity Analyses of Gases Used in This Research	88
X	Examples of Corrections Involved in Data Reduction for the Nitrogen-Carbon Dioxide System	90
XI	Excess Enthalpy Data on Nitrogen-Carbon Dioxide System	92
XII	Regression Coefficients for Smoothing Nitrogen-Carbon Dioxide Excess Enthalpies Versus Composition	96
XIII	Excess Enthalpy Data on Nitrogen-Ethane System	107
XIV	Regression Coefficients for Smoothing Nitrogen-Ethane Excess Enthalpies Versus Composition	111
XV	Excess Enthalpy Data on Nitrogen-Oxygen System	113
XVI	Estimated Limit of Accuracy of the Experimental Measurements	118
XVII	Errors in Determination of Power Input to Calorimeter	129
XVIII	Errors in Volume Determination of Calibration Tank	130
XIX	Errors in Flow Meter Calibration Measurements	132

LIST OF TABLES (Continued)

Table		Page
XX	Errors in Gas Density Analysis Measurements	137
XXI	Estimated Errors Introduced by Primary Corrections for Nitrogen-Carbon Dioxide Mixtures	140
XXII	Estimated Errors Introduced by Secondary Corrections for Nitrogen-Carbon Dioxide Mixtures	141
XXIII	Results of Volume Determinations on Calibration Tank	143
XXIV	Data of Calibrations for Nitrogen Flow Meter	144
XXV	Data of Calibrations for Carbon Dioxide Flow Meter	146
XXVI	Data of Calibrations for Ethane Flow Meter	148
XXVII	Data of Calibrations for Nitrogen and Oxygen Flow Meters Used in Measurements on Nitrogen-Oxygen System	150
XXVIII	Calibration of Dead Weight Gauge	151
XXIX	Calibration of Mercury Barometer	152
XXX	Calibration of Mercury-in-Glass Thermometer	153
XXXI	Calibration of Thermopile	154
XXXII	Calibrated Resistances of Standard Resistors	155
XXXIII	Calibration of Potentiometer Standard Cells	156
XXXIV	Characteristics of Leeds and Northrup Model K-3 Null Potentiometer	156
XXXV	Experimental Enthalpy of Mixing Data on Nitrogen-Carbon Dioxide System	157
XXXVI	Experimental Enthalpy of Mixing Data on Nitrogen-Ethane System	158
XXXVII	Experimental Enthalpy of Mixing Data on Nitrogen-Oxygen System	158
XXXVIII	Primary Corrections for Data on Nitrogen-Carbon Dioxide System	159
XXXIX	Secondary Corrections for Data on Nitrogen-Carbon Dioxide System	160
XL	Primary Corrections for Data on Nitrogen-Ethane System	161

LIST OF TABLES (Continued)

Table		Page
XLI	Secondary Corrections for Data on Nitrogen-Ethane System	162
XLII	Primary Corrections for Data on Nitrogen-Oxygen System	163
XLIII	Values of Heat Capacities and Isothermal Joule-Thompson Coefficients used for Primary Corrections	164
XLIV	Formulae Derived from Benedict-Webb-Rubin Equation of State Used in Calculating Properties	165
XLV	Constants for the Benedict-Webb-Rubin Equation of State	166
XLVI	Sample Results of Volume Determinations on Cans Used for Gas Density Analysis	167
XLVII	Gas Density Analyses of Gravimetrically Prepared Samples	168
XLVIII	Second Virial Coefficients Used in Gas Density Analysis Computations	168
XLIX	Comparison of Compositions from Flow Meter Calibrations and from Gas Density Analysis	169
L	Conversion Factors for SI Units	170
LI	Molecular Weights Used in Computations	170
LII	Formulae for Properties of Nitrogen Used in Computer Programs	172
LIII	Sample Data for Volume Determination of Calibration Tank	173
LIV	Sample Flow Meter Calibration Data	178
LV	Sample Data on Enthalpy of Mixing Measurement	186

LIST OF FIGURES

Figure		Page
1	Schematic for Enthalpy of Mixing Measurements in a Flow Calorimeter	36
2	Enthalpy of Mixing Calorimeter (Key: Table VI)	52
3	Flow Diagram of the Facility (Key: Table VII)	58
4	Control Panel	64
5	Electrical Power Input System for Calorimeter	69
6	Photograph of High Pressure Flow Meter	73
7	Excess Enthalpy Data on Nitrogen-Carbon Dioxide System at 40°C	97
8	Excess Enthalpy Data on Nitrogen-Carbon Dioxide System at 40°C and 500 psia, and Comparisons with Data of Lee and Mather and with B-W-R Equation of State Predictions	98
9	Excess Enthalpy Data on Nitrogen-Carbon Dioxide System at 40°C and 950 psia, and Comparisons with Data of Lee and Mather and with B-W-R Equation of State Predictions	99
10	Excess Enthalpy Data on Nitrogen-Carbon Dioxide System at 31°C	100
11	Excess Enthalpy Data on Nitrogen-Carbon Dioxide System at 31°C and 500 psia, and Comparisons with B-W-R Equation of State Predictions	101
12	Excess Enthalpy Data on Nitrogen-Carbon Dioxide System at 31°C and 950 psia, and Comparisons with B-W-R Equation of State Predictions	102
13	Excess Enthalpy Data on Nitrogen-Ethane System	109
14	Excess Enthalpy Data on Nitrogen-Ethane System and Comparisons with B-W-R Equation of State Predictions	110
15	Excess Enthalpy Measurements on Nitrogen-Carbon Dioxide System as a Function of Reciprocal Flow Rate	116
16	Flow Meter Calibrations for Nitrogen	145

LIST OF FIGURES (Continued)

Figure		Page
17	Flow Meter Calibrations for Carbon Dioxide	147
18	Flow Meter Calibrations for Ethane	149

NOMENCLATURE

A, B	Pure components A and B
A_0, B_0, C_0	Constants in the Benedict-Webb-Rubin equation of state
a,b,c	Constants in the Benedict-Webb-Rubin equation of state
a_n, b_n, c_n	Constants in equation for smoothing excess enthalpies with respect to composition
a_o, b_o, c_o	Constants in equation for smoothing the enthalpy difference ΔH_o with respect to composition
B_{11}, B_N	Second virial coefficient of nitrogen
B_{22}	Second virial coefficient of carbon dioxide
B_{12}	Interaction virial coefficient
C_a, C_b	Connections in power input circuit to calorimeter
C_P	Isobaric heat capacity
C_V	Isochoric heat capacity
d	Internal diameter of tubing used for flow meter
e(z)	Error in variable z
e_c	Voltage across calorimeter heater
F	Flow rate
f	Friction factor
$\underline{H}$	Enthalpy per unit mass or per unit mole
$\overline{H}$	Partial molal enthalpy
ΔH_o	Experimentally measured enthalpy difference at calorimeter outlet conditions
ΔI_{corr}	Correction for impurities
i_c	Current in calorimeter heater
KE	Kinetic Energy
ΔKE_M	Correction for kinetic energy differences
L	Length of flow path in flow meter
M	Molecular weight

m,n	Constants in derivation of equation for correlating results of flow meter calibrations
m	Mass
P	Pressure
ΔP	Pressure drop or difference
ΔP_{corr}	Correction for pressure drop
$\dot{Q}$	Rate of heat leakage to calorimeter
R	Gas constant
R_c	Calorimeter heater
R_{25}	Resistance of standard resistor at 25°C
$R_{T_{res}}$	Resistance of standard resistor at T_{res} °C
R_e, R_i, R_s	Standard resistors
R_f, R_g	Rheostats
R_h	Helipot
Re	Reynolds Number
S_a, S_b	Switches in power input circuit to calorimeter
T	Temperature
ΔT_{corr}	Correction for temperature difference
T_{res}	Temperature of standard resistors
$\bar{u}$	Mean Velocity
$\underline{V}$	Volume per unit mass or per unit mole
V_e	Voltage drop across standard resistor R_e
V_i	Voltage drop across standard resistor R_i
$\dot{W}$	Electrical energy input to calorimeter
$(\dot{W}/F)$	Power to flow ratio or power per unit flow
w	Mass fraction
x	Mole fraction
Y	Group used for error analysis of flow meter calibrations
y	Fraction of impurity in inlet stream to calorimeter

Z	Dependent variable in error analysis
z	Independent variable in error analysis

Subscripts

A,B	Pure component A and pure component B
AB	Mixture of A and B
AM, ABM	Impure A and impure AB
ac	Aerosol can used for gas density analysis
C_2H_6	Ethane
CO_2	Carbon dioxide
c	Critical property
ct	Calibration tank
F	Flow meter
I	Impurities
N	Nitrogen
n	Nominal experimental conditions
O	Oxygen
o	Conditions at calorimeter outlet
P	Constant pressure
r	Reduced property
T	Constant temperature
V	Constant volume
1	Conditions at calorimeter inlet 1
2	Conditions at calorimeter inlet 2

Superscripts

E	Excess property
M	Mixing function

M^x	Ideal mixing function
0	Zero pressure property

Greek Letters

α,γ	Constants in Benedict-Webb-Rubin equation of state
α,β	Temperature coefficients of standard resistor
β_F,δ_F	Constants in correlation equation for flow meter calibrations
η	Viscosity
θ	Time period of gas collection
μ	Adiabatic Joule-Thompson coefficient
ρ	Density
σ	Standard deviation
φ	Isothermal Joule-Thompson coefficient

ABSTRACT

THE EXPERIMENTAL DETERMINATION OF THE ENTHALPY OF MIXING
OF BINARY GASEOUS MIXTURES UNDER PRESSURE

by

Arun Vasudev Hejmadi

Chairman: John E. Powers

Reliable and accurate data on the thermal properties of mixtures are essential for the design of equipment and the testing of enthalpy prediction methods. The importance of the enthalpy of mixing is that it directly measures the solution effect--that is the difference between the enthalpy of the mixture and the enthalpy of its constituents. Thus, the objectives of this research were (1) to design and construct a flow calorimetric facility for the experimental measurement of the enthalpy of mixing of binary gaseous mixtures at elevated pressures, (2) to calibrate and test the equipment and (3) to obtain data on systems of industrial significance and in regions of theoretical importance.

In this flow calorimetric facility, the system brings two gases at the same pressure and temperature to the calorimeter where they are mixed. If there is a decrease in the temperature of the resultant mixture, electrical energy is supplied to the gases to minimize the temperature difference between the inlet pure gases and the outlet mixture stream. If there is an increase in the temperature of the mixture, the calorimeter may be operated without the electrical energy input. The flow rate of each gas is metered prior to entering the calorimeter. Each flow meter was calibrated by flowing for a measured period of time under steady state conditions into a tank of measured volume. The accuracy of

the flow metering was checked by comparing compositions calculated from the flow rates of the two gases with the results of a gas density analysis.

Data were obtained on the following systems at the nominal conditions listed:

(1) Nitrogen-carbon dioxide mixtures at 31°C, 500 psia and 950 psia, and at 40°C at the same pressures at a minimum of four compositions.

(2) Nitrogen-ethane mixtures at 32.38°C and 401 psia at four compositions.

(3) Nitrogen-oxygen mixtures at 25°C and 1001 psia at one composition.

The data on the nitrogen-carbon dioxide system at 31°C and on the nitrogen-ethane system at 32.38°C represent the first enthalpy of mixing measurements made at a reduced temperature of unity of one of the components in a mixture.

The experimental measurements on these three systems were interpreted to yield values of the excess enthalpy at the measured conditions of pressure and temperature at the calorimeter outlet. The excess enthalpies were then normalized to nominal experimental conditions and, finally, smoothed with respect to composition.

Results on the nitrogen-carbon dioxide system at 40°C and 500 psia were used to check on the adiabaticity of the experimental measurements. Ten repetitive measurements made at 0.5 mole fraction nitrogen over a range of flow rates indicated that the heat leak in the calorimeter was less than the experimental precision (0.3 percent).

The estimated accuracy of the data is 0.8 to 2.1 percent for the data on the nitrogen-carbon dioxide and nitrogen-ethane mixtures and ten percent for the data on the nitrogen-oxygen mixtures.

Comparisons were made with experimental results on the nitrogen-carbon dioxide system of another investigator at 40°C and at the same pressures as the present measurements. The excess enthalpy values agreed

within the combined experimental error of both investigations. Excess enthalpy values were calculated from the original Benedict-Webb-Rubin equation of state and were found to deviate five percent or less from the experimental results for the mixtures of nitrogen with ethane and with carbon dioxide.

INTRODUCTION

Most process streams encountered in industry are mixtures of two or more components. Hence, it is important to obtain information on the thermal properties of mixtures.

Very limited quantities of data are available on the enthalpies of mixtures because of the experimental difficulties and the considerable expense involved. Therefore, it is preferable to obtain data in limited and crucial regions--near the two phase envelope or close to the critical point of one of the components--where substantial deviations from ideal solution behavior are anticipated. The thermal property which yields the most information in such regions is the enthalpy of mixing or the excess enthalpy because by definition it measures the deviation from ideal solution behavior.

For the reasons stated earlier, it is not possible to obtain data on the unlimited number of mixtures which may exist. A feasible alternative is to employ an enthalpy prediction method. Before such a method is used, however, it is necessary that its reliability be proved. This may be accomplished by comparing predicted excess enthalpies with the experimentally determined quantities. The enthalpy of mixing is obtained from a prediction method as the difference of two quantities--the enthalpy of the mixture and the enthalpy of the ideal solution of its constituents--both of which are of the same order of magnitude. Hence such a comparison constitutes an extremely severe test of the applicability of a prediction method.

Therefore, the objectives of this research are (1) to design and build a flow calorimetric facility for the experimental determination of the enthalpy of mixing of binary mixtures in the gas phase and under

pressure (2) to calibrate and test the equipment (3) to obtain data on systems of industrial significance and in regions of theoretical importance.

EXPERIENCE OF PREVIOUS INVESTIGATORS

This review covers both sources of data and experimental techniques. References are given to excess property measurements of mixtures of relatively simple molecules in the gaseous and liquid phase. Calorimetric techniques for enthalpy of mixing measurements of liquids and gases are discussed. Enthalpy prediction methods are considered very briefly. A review is presented on the thermodynamic properties of those pure components and mixtures which are relevant to this research.

Excess Property Measurements on Liquids

The measurement of the enthalpy change on mixing liquids at ambient conditions preceded the work at low temperatures. Recently, calorimetric data have been obtained for systems with endothermic (Mrazek and Van Ness,[122] Savini, Winterhalter, Kovach and Van Ness,[146] Savini, Winterhalter and Van Ness[147]) or exothermic enthalpies of mixing (Winterhalter and Van Ness[182]). The systems so investigated generally consist of components (alcohols, aromatics) whose behavior does not approximate that of simple molecules, e.g. argon, krypton, etc.

Measurements of excess properties at low temperatures and low pressures occurred next in chronological order. Table I lists investigations of excess volume, excess enthalpy and excess free energy of binary systems of liquid mixtures of relatively simple molecules. All of these experiments have been performed below -240°F and at pressures lower than 200 psia.

In the references listed in Table I, excess free energies were calculated from volumetric and phase behavior measurements. There have been three different approaches used in excess volume investigations.

TABLE I

INVESTIGATIONS OF EXCESS THERMODYNAMIC PROPERTIES OF BINARY MIXTURES IN THE LIQUID STATE AT LOW TEMPERATURES

System	Property	Year	Author	Reference
He^3-He^4	H^E	1953	Sommers, Keller, Dash	157
CO-CH_4	V^E, G^E	1956	Mathot, Staveley, Young, Parsonage	105
Ar-CH_4	V^E, H^E	1957	Jeener	70
CO-CH_4	H^E	1957	Pool, Staveley	131
N_2-O_2, Ar-O_2	V^E	1958	Blagoi, Rudenko	18
Ar-CH_4	V^E, H^E	1958	Mathot	103
N_2-O_2	V^E, H^E	1960	Knobler, Knaap, Beenakker	80
H_2-D_2	V^E, H^E	1960	Lambert	88
O_2-N_2, O_2-Ar nH_2-nD_2, nH_2-pH_2 nD_2-oD_2	V^E, G^E	1961	Knaap, Knoester, Beenakker	79
Ar-O_2, N_2-O_2	H^E	1961	Knobler, Van Heijningen, Beenakker	81
H_2-D_2, H_2-HD, HD-D_2	H^E	1962	Knaap	78
Ar-CH_4, CO-CH_4	V^E, H^E	1962	Lambert, Simon	89

TABLE I (Continued)

System	Property	Year	Author	Reference
$Ar-O_2$, $Ar-N_2$, N_2-O_2, N_2-CO, $Ar-CO$	V^E, H^E, G^E	1962	Pool, Saville, Herrington, Shields, Staveley	130
$CO-CH_4$, $Ar-CH_4$	V^E, H^E, G^E	1963	Mathot	104
$He-nD_2$	G^E	1963	Simon	154
$CH_4-C_3H_8$	C_P^E	1965	Cutler, Morrison	31
$Ar-CO$, N_2-O_2 $CO-N_2$	V^E, H^E, G^E	1966	Duncan, Staveley	36
$CO-CH_4$, $Ar-CH_4$ N_2-O_2, $Ar-N_2$ N_2-CH_4	G^E	1966	Sprow, Prausnitz	158
$Ar-Kr$	V^E, G^E	1967	Davies, Duncan, Saville, Staveley	33
CH_4-Kr, CH_4-N_2	V^E	1967	Fuks, Bellemans	47
N_2-H_2	V^E	1967	Mastinu	100
oH_2-pH_2, oD_2-pD_2	V^E, H^E	1968	Bakx, Knaap	7
Binary mixtures of CH_4, C_2H_6, C_3H_8 and nC_4H_{10}	V^E	1968	Shan'a, Canfield	152
He^3-He^4	H^E	1969	Seligmann, Edwards, Sarwinski, Tough	150
$Kr-CH_4$	V^E	1969	Calado, Staveley	23

Knaap, Knoester and Beenakker[79] directly measured the volume change which accompanies the mixing of the pure components. In the calorimeter of Jeener[70] constant pressure is maintained in the mixing chamber by external means and excess volume and excess enthalpy are determined simultaneously. The third and most commonly used technique involves calculating excess volumes from density studies on pure components and their mixtures using a pyknometer (e.g. Pool et al.[130]).

The calorimeters employed in making enthalpy of mixing measurements have certain common features. They are all "closed-system" calorimeters. The two pure components are charged into separate chambers which share one common wall made of thin aluminum or copper foil. The liquids are brought into contact by breaking the aluminum or copper foil partition and mechanically stirring the mixture. The cooling which accompanies the mixing process is compensated for by applying a measured potential difference to a resistance wire wound around the mixing chamber. The mixing chamber is enclosed by a vacuum jacket and the entire unit located in a constant temperature bath during the measurements. The main objective of this basically unsteady state technique is to minimize heat losses from the calorimeter to the surroundings by adding a controlled quantity of electrical heat input so as to maintain isothermal conditions in the calorimeter throughout the experiment.

Sommers, Keller and Dash[157] made one of the first enthalpy of mixing measurements. They brought He^3 and He^4 together by breaking a glass vessel containing one component within a flask containing the other pure component. The first enthalpy of mixing calorimeters were reported at about the same time by Pool and Staveley[131] and Jeener.[70] Pool, Saville, Herrington, Shields and Staveley[130] subsequently published

the design of a modified version of their original calorimeter.[131] Knobler, Van Heijningen and Beenakker[81] reported measurements on a calorimeter that eliminated the vapor spaces which existed in calorimeters of other investigators. Knaap[78] modified the calorimeter of Knobler et al.[81] for measuring small values of excess enthalpy such as in the hydrogen-deuterium system.

Discussion of Closed-System Calorimeters

Some of the design and operational problems encountered with closed system calorimeters are outlined in this section. This account is not intended to be exhaustive since detailed discussion of such types of calorimeters are available.[106] The object of this section is to provide a basis on which to compare closed-system calorimeters with flow calorimeters (discussed in next section) with a view to applying them for excess enthalpy measurements under pressure on gases.

There are three areas in which difficulties arise with a closed-system calorimeter. They are:

1. Need for mechanical stirring: The energy injected into the system by mechanical stirring must be accounted for when calculating excess enthalpies. Magnetic stirrers have been used in all calorimeters thus bypassing the need for stirrer shaft packing suitable for low temperatures. In all but the calorimeter of Pool et al.[130,131] the rotor on which the magnetic field acts is separated from the paddle by a long stirrer shaft. To eliminate field effects, Pool et al.[131] switch off the stirrer when making temperature measurements.
2. Constancy of pressure during mixing: Volume changes accompany the mixing process and maintaining the pressure or volume constant introduces errors. The calorimeters of Pool et al.,[130,131] Knobler et al.[81]

and Knaap[78] are essentially constant volume devices. Jeener[70] maintains constant pressure by adding or withdrawing measured quantities of material from the calorimeter. He, therefore, has to make corrections for the mass withdrawn but he also simultaneously determines excess volumes.

3. Corrections for vapor spaces: Some evaporation or condensation of material accompanies the mixing process if there are vapor spaces in the calorimeter. Both Pool et al.[130,131] and Jeener[70] make substantial corrections for this effect when calculating excess enthalpies.

Closed-system calorimeters may be used for measurements on gases without corrections for vapor spaces. However, working with gases introduces some unique problems. Excess enthalpies of gas mixtures are smaller than for liquids except near the critical temperature of one of the components. Hence, large masses of the two gases are necessary to increase the magnitude of the overall heat effect to bring it into a measurable range. This implies larger calorimeters than are used for liquids since gases occupy larger molar volumes than liquids. Mechanical stirring of large volumes of gases and the design and construction of a large calorimeter for high pressure usage introduces considerable difficulty.

Discussion of Flow Calorimeters

A flow calorimeter eliminates or reduces the magnitude of these problems:

1. Need for mechanical stirring: A flow calorimeter can be built with devices (e.g. baffles) which facilitate internal mixing without the need for externally introduced devices (e.g. stirrers). Such devices

usually cause a pressure drop across the calorimeter which must be accounted for when interpreting the data. However, they can be designed to minimize this effect.

2. Constancy of pressure during mixing: The nature of the flow process is such that the calorimeter is at essentially constant pressure regardless of any volume change on mixing.
3. Corrections for vapor spaces: This can be solved by eliminating any dead spaces in the calorimeter where the flowing material can accumulate.

The magnitude of the heat effect (Btu/minute) can be amplified by increasing the flow rate of the two gases rather than increasing the size of the calorimeter. The residence time of the gases can be increased by lengthening the flow path of the gases within the calorimeter.

Flow calorimeters suffer from certain disadvantages. The factor which limits accuracy is the determination of the flow rate. Also, once they are mixed, the gases cannot be recycled to the calorimeter via a compressor without a separation facility. This once-through facility requires large quantities of gases. This entails considerable operational expense especially with costly materials.

Design and construction of a suitable calorimeter presents few special problems especially since generalized criteria for the design and construction of flow calorimeters have been discussed by other investigators.[45,101] The advantages of a flow calorimeter so outweigh the alternative closed-system calorimeter for measurements under pressure that all such enthalpy of mixing determinations on gas mixtures have employed flow calorimetric systems.

Excess Enthalpy Measurements on Gases

Pioneering work was done at Leiden, Netherlands, by Beenakker and associates.[10,11,82,170] They investigated a variety of systems all of which are listed in Table II. Of particular interest are their excess enthalpy measurements on the nitrogen-hydrogen, nitrogen-argon and hydrogen-argon systems because Zandbergen and Beenakker[187] measured excess volumes of the same systems at very similar conditions of pressure and temperature. He utilized a technique closely resembling that of Knaap, Knoester and Beenakker.[79] Lee and Mather[90] report that their results on the nitrogen-hydrogen system agree within three percent with the excess enthalpy values measured by Knoester et al.[82]

Table II presents references to all the excess enthalpy data currently available. The accuracy of this data is believed to be three to five percent with the exception of the data of Kotousov and Baranyuk.[85] The latter are the only investigators among those listed in Table II who did not employ a flow calorimeter. They allowed the counter-current diffusion of the two pure gases along the axis of a tube and recorded temperature and composition profiles with time. Though direct comparison at identical conditions is not possible, their excess enthalpy values are an order of magnitude higher than the extrapolated results of Knoester[82] and Van Eijnsbergen.[170] A flow facility which is under development but from which no data has been reported has been described by Jacobsen and Barieau.[69] This facility is designed to measure excess enthalpies and excess heat capacities of helium-nitrogen mixtures.

This review would be incomplete without the mention of some indirect determinations of excess properties of industrially significant systems: Ernst[42] calculated excess heat capacities of freon mixtures

TABLE II

EXPERIMENTAL INVESTIGATIONS OF THE ENTHALPY OF MIXING OF GASES

System	Temperature °F	Pressure psia	Year	Author	Reference
H_2-N_2	68	440-1200	1962	Beenakker, Coremans	10
H_2-N_2, H_2-Ar, N_2-Ar, CH_4-H_2 Ar-CH_4	-196 to 66	120-1900	1965	Beenakker, Van Eijnsbergen, Knoester, Taconis, Zandbergen	11
H_2-N_2, N_2-Ar H_2-Ar, H_2-N_2-Ar	-196 to 66	450-1900	1967	Knoester, Taconis, Beenakker	82
H_2-CH_4, He-CH_4, CH_4-N_2, He-Ar	-154 to 66	120-1800	1968	Van Eijnsbergen, Beenakker	170
N_2-CH_4	-108 to 104	250-1500	1969	Klein	77
H_2-Ar, H_2-N_2, H_2-CO_2	72	4.4-14.7	1969	Kotousov, Baranyuk	85
N_2-CO_2, H_2-N_2	104 -100 to 68	140-1800 140-2000	1970	Lee, Mather	90

from his own measurements of heat capacities on the pure components and their mixtures. Mather[101] plotted excess enthalpies of a methane-nitrogen mixture between -280 and +40°F at 1000, 1500 and 2000 psia. He calculated these values from his experimentally determined enthalpy values for that mixture and the enthalpy values of the pure components determined by previous investigators. Bhirud and Powers[16] report excess heat capacities of methane-propane mixtures derived from measurements on the mixture and the pure components.

Comparison of Flow Calorimetric Techniques for Gases

The similarities and differences between the experimental and data interpretation techniques used by various investigators are described in this section. The object of these descriptions is to facilitate comparison of previously done work with the present research as it is described in later chapters. The descriptions will be under the following headings:

1. Calorimeter Design
2. Flow and Composition Measurement
3. Mode of Operation
4. Interpretation and Smoothing of Data

Calorimeter Design

The same design principle is used by all investigators. The temperatures of the two pure gases are monitored as they enter the calorimeter. On mixing, a controlled quantity of heat is added to maintain the exiting gas mixture at the same temperature as that of the two inlet gases.

All but Beenakker and coworkers[10,11,82, 170] use a similar mixing capsule. Mixing of the two pure gases is accomplished by Beenakker

and coworkers[10,11,82,170] with perforated baffles placed at right angles to the direction of flow of gas. Heat is supplied via a resistance wire that is wound on the outside of the mixing chamber. The resistance windings are suitably shielded from radiating heat to the surroundings. The mixing capsules used by the other investigators[77,90] consist of concentric cylindrical baffles with the gas being introduced in the innermost baffle. Gas flow is parallel to the cylinder axes and the direction of its flow is reversed when it goes from one baffle to another. The resistance wire for supplying heat is wound on the inner baffles and is in direct contact with the gas.

All the calorimeters except Klein's[77] employ a vacuum jacket for overall insulation. Klein's[77] calorimeter is distinctive in its usage of bakelite and nylon for insulation and for reducing the heat capacity of the calorimeter.

Flow and Composition Measurement

All the investigators measure flow rates by collecting the mixture at atmospheric pressure in a gasometer over a measured period of time.

Beenakker and coworkers[10,11,82,170] use an ingenious flow system which allows them to calculate and control the mixture composition: The gases are stored separately in cylinders of differing internal volumes. One cylinder is charged with gas at a slightly higher pressure than the other. Flow is commenced by opening the valve on the cylinder with the higher pressure in it. Adjustment of a valve downstream from the calorimeter sets the operating pressure in the latter. When the pressure in the two cylinders is equal, the valve on the previously isolated cylinder is opened. The composition of the gas mixture may be calculated from

the ratio of internal volumes of the cylinders and the densities of the gases contained in them.

The flow system employed by Lee and Mather[90] is similar to that of Beenakker and associates. Hence they use the same technique to calculate the composition of the nitrogen-hydrogen mixture. However, the quantitative analysis of their nitrogen-carbon dioxide mixtures was done by gas chromatography. Klein[77] also employed the latter method for analyzing methane-nitrogen mixtures.

Mode of Operation

Beenakker and associates[10,11,82,170] vary the pressure in the calorimeter by allowing the supply cylinders to exhaust continuously. Hence data is obtained at constant temperature with unsteady conditions of pressure in the calorimeter. Excess enthalpy measurements are made at closely spaced values of pressure from 1900 down to 120 psia, which are then corrected for the heat capacity of the calorimeter. Further, with a given set of cylinders, the composition of the gas mixture varies if the ratio of the isothermal compressibilities $\left[\frac{1}{V}\left(\frac{\partial V}{\partial P}\right)_T\right]$ of the two components changes with pressure. For the gases studied by Beenakker and coworkers[11,12,80,170] this correction is small since the gases in the tanks at room temperature are at high reduced temperatures.

Lee and Mather[90] encountered difficulties with their excess enthalpy measurements on nitrogen-carbon dioxide mixtures because the carbon dioxide supply tanks were at room temperature where, due to the proximity of the critical temperature, the compressibility varies rapidly with pressure. For every set of cylinders used, they obtained data at scattered values of pressure and composition.

Klein's[77] calorimetric measurements were at steady state conditions. Pressure regulators controlled the pressure of the gas entering the system from the supply cylinders.

Interpretation and Smoothing of Data

Different techniques are used to compensate for operational variations in pressure, temperature and composition in the data obtained from the three facilities. Beenakker and associates[10,11,82,170] present their raw experimental data in tabular and graphical form and do not attempt to smooth the data. Recently, Hsi and Lu[64] published values of excess enthalpies, excess entropies and excess free energies obtained by graphically smoothing excess enthalpy data of Beenakker et al.[10,11] and Knoester[82] and excess volume data of Zandbergen[187] on the nitrogen-hydrogen, nitrogen-argon and hydrogen-argon systems.

Klein[77] took data as a function of composition at constant temperature and at slightly varying values of pressure. Smoothing this data for pressure and composition variation involved the use of a virial equation of state. The latter was mathematically manipulated and equated to the excess enthalpy. Constants for the equation were determined by a least squares analysis. The equation of state with the regression coefficients was then used to generate smoothed values of excess enthalpy. This approach requires a large number of data points. For example, approximately 40 excess enthalpy values at a given temperature required the evaluation of 16 constants (using up to the fifth virial coefficient) before the standard deviation was less than the experimental uncertainty (3 to 6 percent).

The calorimetric data obtained by Lee and Mather[90] require smoothing over pressure and composition at a given temperature. Their pressure interpolation method involves plotting $\left[\frac{\bar{H}^E}{x(1-x)P}\right]$ versus pressure. At low pressures where molecular interactions are purely binary in

nature, the ordinate is independent of pressure. Even at elevated pressures, this technique reduces the variation of excess enthalpy with pressure by an order of magnitude. It loses its efficacy, however, in high pressure regions where the excess enthalpy versus pressure curve goes through a maximum.

For smoothing with respect to composition, they use plots of $\left[\frac{\underline{H}^E}{x(1-x)}\right]$ versus mole fraction, x . This method reduces the error due to composition interpolation because it changes the parabolic plot of $\underline{H}^E$ against x to a monotonic variation in $\left[\frac{\underline{H}^E}{x(1-x)}\right]$ versus x .

Prediction Methods

Methods for the prediction of the enthalpies of pure components and mixtures have been reviewed by Hobson and Weber,[60,61] Nathan[123] and Mather.[101] Curl and Pitzer[30] developed an enthalpy correlation based on the principle of corresponding states which utilizes three macroscopic parameters: reduced pressure, reduced temperature and acentric factor. A corresponding states treatment based on two molecular parameters was suggested independently by Prigogine[133] and by Scott.[148] Various equations of state, such as the Benedict-Webb-Rubin[12] or the virial equation of state can also be used to determine enthalpies.

Powers[132] and Sehgal et al.[149] have shown by comparisons with other prediction methods and with experimental data that the B-W-R equation[12] is one of the better methods for predicting enthalpy departures, $\underline{H}-\underline{H}^0$, in the gaseous phase for both pure components and mixtures. Hence, it is chosen as the method by which excess enthalpies may be predicted for comparison with the experimental results of this research. This equation is pressure explicit:

$$P = RT\rho + (B_oRT-A - \frac{C_o}{T^2})\rho^2 + (bRT-a)\rho^3 + \frac{c}{T^2}\rho^3(1+\gamma\rho^2)e^{-\gamma\rho^2} + a\alpha\rho^6 \quad (1)$$

and contains eight constants which are usually determined from a least squares fit of PVT data. These constants have been determined for a large number of pure substances--as may be seen in the compilation of constants for 58 compounds by Cooper and Goldfranck.[25] For mixtures, however, constants are less readily available and therefore it is necessary to estimate them from constants for pure substances with mixing rules such as those suggested by Benedict, Webb and Rubin.[13]

Review of Thermodynamic Properties

Raw calorimetric data normally do not directly yield values of the enthalpy of mixing. Some corrections have to be made to the raw data for effects such as Joule-Thompson cooling due to pressure drop across the calorimeter. These corrections, which are discussed in detail in later chapters, require values for the thermodynamic properties of pure components and their mixtures.

The object of this review is to give references to work on pure components and mixtures which are relevant to this research. This consists mainly of references to thermal properties with some mention of more recent investigations of other thermodynamic properties. Unless specified, the references given in this review are to measurements of properties under pressure. This review covers the properties of:

1. Nitrogen
2. Carbon dioxide
3. Ethane
4. Oxygen
5. Nitrogen-carbon dioxide mixtures
6. Nitrogen-ethane mixtures
7. Nitrogen-oxygen mixtures

There are several excellent general reviews available. Reviews of experimental measurements of the thermal properties of pure components have been reviewed by Masi[99] and of mixtures by Mage, Jones, Katz and Roebuck[97] and more recently by Yesavage, Mather, Katz and Powers.[184] Investigations into PVT, thermal and transport properties of several pure components have been reviewed by Wilson, Clark, and Hyman.[181]

Nitrogen

A literature review and compilation of the properties of nitrogen has been made by Din.[34] Lunbeck, Michels and Wolkers[94] calculated the PVT and thermal properties from -193°F to 302°F and up to 90,000 psia. More recently Tsiklis[166] and Tsiklis and Polyakov[168] studied the PVT behavior up to 750°F and 147,000 psia of nitrogen by two different techniques and calculated the thermodynamic properties[169] to the same limits of pressure and temperature.

Second virial coefficients of nitrogen have been reported by Otto,[126] Pfefferle, Goff and Miller[128] and Huff and Reed.[65] Values at low temperatures (-328°F to -185°F) have been listed by Din[34] and measured by Brewer[20] to -240°F.

Heat capacities at constant pressure were measured at and above room temperatures and at high pressures by Workman[183] and Mackey and Krase.[95] The former measured the ratio of the heat capacity at the experimental pressure to the heat capacity at one atmosphere at 78.8°F and 140°F. Mage et al.[97] give enthalpies of nitrogen from 0 to 2000 psia and -250°F to 50°F.

Roebuck and Osterberg[140] measured Joule-Thompson coefficients for nitrogen which were subsequently corrected for an experimental error.[156] Ahlert[2] also measured integral Joule-Thompson coefficients

over a wide range of pressure (0-2400 psia) and temperature (-100°F to +100°F). Data on isothermal Joule-Thompson coefficients have been reported by Ishkin and Kaganer,[68] Gusak,[54] Charnley, Isles and Townley,[24] and Mather, Katz and Powers.[102]

Michels and Gibson[112] give viscosity as a function of pressure (200-15,000 psi) and temperature (78°F-170°F). Kestin and Leidenfrost[74] obtained viscosities of nitrogen at 68°F as a function of pressure on the oscillating-disk viscometer.

Constants for the Benedict-Webb-Rubin equation of state,[12] are reported by Stotler and Benedict,[160] Bloomer and Rao,[19] and Crain and Sonntag.[27]

Carbon Dioxide

Liley[91] reviewed the data up to 1957 and presented tabulations of high temperature and high pressure properties. Subsequently, Newitt, Pai, Kuloor and Huggill[124] compiled and calculated the properties of carbon dioxide between -112°F and 302°F and up to 44,000 psia. Volumetric data on carbon dioxide were obtained by Michels and coworkers[107,108,113] and thermodynamic properties calculated from them have been published by Michels and DeGroot.[111] The most recent compilation and review is the book coauthored by Vukalovich and Altunin.[172] They describe experimental techniques, evaluate the accuracy of the data, and then present tables of thermodynamic and transport properties from the triple point to 1830°F and up to 9100 psia.

A considerable amount of work has been done on carbon dioxide in the USSR. A large volume of work is published in Teploenergetika (Thermal Engineering). A number of density measurements have been reported in that journal since the publication of book by Vukalovich and Altunin[172] but are not directly referred to here as they are too numerous.

Low pressure volumetric data have been reviewed by Vukalovich and Altunin.[172] Second virial coefficients at several temperatures above ambient conditions have been given by Huff and Reed.[65] Pfefferle, Goff and Miller[128] report second and third virial coefficients at 86°F. The data used in this research is that of Michels and Michels.[113]

Constant pressure heat capacities of carbon dioxide were measured by Shrock[153] from 15 to 1000 psia and 150 to 950°F. Koppel and Smith[84] obtained enthalpy differences and heat capacities close to the critical point. Vukalovich and associates[175-179] report heat capacities of carbon dioxide between 68 to 932°F and 76 to 3300 psia. Extremely precise determinations of heat capacity between 50 to 266°F and 1300 to 3700 psia were obtained by Rivkin and Gukov.[136] A total of 171 data points within this range of pressure and temperature permits the accurate determination of the maxima in plots of isobaric heat capacity versus temperature. Recently Altunin and Kutznetsov[3] measured isobaric heat capacities between 62 and 140°F and 150 to 750 psia. Isochoric heat capacity measurements other than those listed by Yesavage et al.[184] are those of Amirkhanov.[4,5,6]

Roebuck, Murrel and Miller[139] measured Joule-Thompson coefficients of carbon dioxide between -60°F and 570°F and up to 3000 psia. Isothermal Joule-Thompson coefficients have been reported by Charnley, Isles and Townley[24] between 32°F and 113°F and 59 and 660 psia. Vukalovich, Altunin, Bulle, Rasskozov and Ertel[173] describe a calorimeter for measuring isothermal Joule-Thompson coefficients for carbon dioxide and report some data.[174]

Viscosity measurements have been made by Michels, Botzen and Schurman[110] by the transpiration method. They review all the work done previous to their own.

Constants for the Benedict-Webb-Rubin equation of state[12] have been calculated by Eakin and Ellington[37] for use in mixture property calculations. Cullen and Kobe[29] give two sets of constants each of which is to be used in a different temperature range. Sass, Dodge and Bretton[144] calculated B-W-R constants for carbon dioxide, ethylene and their mixtures by regressing on compressibility factor data obtained between 122°F to 257°F and up to 7350 psia.

Ethane

Tester[162] has reviewed and compiled the thermodynamic properties of ethane. Michels, Van Straaten and Dawson[116] report PVT data and Michels and Nederbragt[114] report compressibility factors of ethane. Other PVT data on ethane are those of Reamer, Olds, Sage and Lacey,[134] Beattie, Hadlock and Poffenberger[8] and Beattie, Su and Simard.[9]

Early work on second virial coefficients have been reviewed by Tester.[162] Hoover, Nagata, Leland and Kobayashi[62] reviewed the more recent work and presented their own accurate measurements. Data have been reported by Huff and Reed[65] and Michels, Van Straaten, and Dawson.[116]

Sage, Webster and Lacey[143] obtained a large quantity of PVT data. They also determined isochoric heat capacities and Joule-Thompson coefficients but over a small range of pressure and temperature. Saurel[144] has given a single plot of C_p/C_v versus pressure at the critical temperature of ethane. Tsaturyants, Mamedov and Eivazova[165] report isothermal Joule-Thompson coefficients above 116°F. Furtado et al.[48] have measured the effect of both pressure and temperature on the enthalpy of ethane but have not published their results.

Viscosity data on ethane have been reviewed, and selected values given by Eakin, Starling, Dolan and Ellington.[39] Benedict, Webb and

Rubin,[12,14] Opfell, Schlinger and Sage[125] and Eubank and Fort[43] have evaluated constants for the Benedict-Webb-Rubin equation of state.[12]

Oxygen

Hust[66] has authored a bibliography of thermophysical properties of oxygen. Another NBS publication, Circular 564 by Hilsenrath et al.[59] presents calculated thermophysical property values. The volumetric properties of oxygen have been measured by Michels, Schamp and de Graaf,[115] Otto and Holborn,[127] and others.[49,167]

Weber[180] and Goodwin[50] have published calculated values of the thermodynamic functions of oxygen up to 4800 psia and from its triple point to 80°F. The only measurements of isobaric heat capacity under pressure have been those of Workman.[183] Voronel', Chaskin, Popov and Simkin[171] and, more recently, Goodwin and Weber [51,52] have measured isochoric heat capacities in the region surrounding the critical point. Joule-Thompson coefficients have been measured by Brilliantinov[21] at low pressures and by Bennewitz and Andreewa[15] near the critical point of oxygen.

Viscosities in the gas phase under pressure have been reported by Kestin and Leidenfrost[74] and Luken and Johnson.[92] Constants for the B-W-R equation of state[12] have been calculated by Seshadri, Vishwanath and Kuloor.[151]

Nitrogen-Carbon Dioxide Mixtures

The major experimental investigations of the thermodynamic properties are given in Table III. The ice point is the lowest temperature at which PVT work has been done.[87] Low temperature vapor liquid equilibria have been reported by several investigators.[32,72,129] Smith,

TABLE III

EXPERIMENTAL INVESTIGATIONS ON THE BINARY SYSTEM
NITROGEN-CARBON DIOXIDE UNDER PRESSURE

Property	Temperature °F	Pressure psia	Year	Author	Reference
P-V-T-x	32 to 392	760-7600	1940	Krichevsky, Markov	87
P-V-T-x	77 to 257	440-7350	1944	Haney, Bliss	56
P-V-T-x	86	5-1000	1955	Pfefferle, Goff, Miller	128
P-V-T-x	59 to 90	820-2000	1965	Khazanova, Lensevskaya	76
V-L	-60 to 71	up to 2400	1924	Pollitzer, Strebel	129
V-L	up to 86	up to 2900	1939	Abdullaev	1
V-L	43 to 68	150-1600	1945	Mills, Miller	120
V-L	59 to 86	740-1500	1962	Krichevsky, Khazanova, Lensevskaya, Sandalova	86
V-L	-65 to 32	180-2100	1963	Dana, Zenner	32
V-L	-40 to 77	290-2900	1966	Kaminishi, Toriumi	72
S-V	-205 to -115	70-1500	1962	Smith, Sonntag, Van Wylen	155
Joule-Thompson	77 to 167	15-290	1965	Grossman	53
Viscosity	68	15-310	1966	Kestin, Kobayashi, Wood	73

Sonntag and Van Wylen[155] studied solid-vapor phase behavior. Grossman[53] made Joule-Thompson coefficient measurements on nitrogen-carbon dioxide mixtures over a limited range of pressure and temperature. Precise values of the viscosities of several binary mixtures have been measured by Kestin, Kobayashi and Wood[73] using the oscillating-disk viscometer.

Volumetric properties at low pressures were made initially by Fuchs[46] and Trautz and Emert.[164] Measurements of interaction virial coefficients at single values of temperatures were made by Edwards and Roseveare,[41] Lunbeck and Boerboom,[93] Miller and Gorski,[119] Michels and Boerboom,[109] and Pfefferle, Goff and Miller.[128] Data on virial coefficients at several temperatures between -58°F and 392°F have been reported by Zaalishvili,[186] Cottrell et al.[26] Huff and Reed,[65] and Brewer.[20]

Nitrogen-Ethane Mixtures

A list of experimental investigations of the nitrogen-ethane system under pressure are given in Table IV. Reamer, Selleck, Sage and Lacey[135] made PVT measurements up to extreme pressures and from ambient temperatures to 464°F. Sage and Lacey[142] have published tables of thermodynamic properties of nitrogen-ethane mixtures based on that work. The only investigations of thermal properties have been the Joule-Thompson measurements of Head[57] and Stockett and Wenzell.[159] Huff and Reed[65] report virial coefficients of nitrogen-ethane mixtures.

Nitrogen-Oxygen Mixtures

Of the three mixtures of interest here, the largest amount of work has been done on nitrogen-oxygen mixtures. The majority of the investigations have been on mixtures with the composition of air. An

TABLE IV

EXPERIMENTAL INVESTIGATIONS ON THE BINARY SYSTEM NITROGEN-ETHANE UNDER PRESSURE

Property	Temperature °F	Pressure psia	Year	Author	Reference
P-V-T-x	40-464	15-10,000	1952	Reamer, Selleck, Sage, Lacey	135
P-V-T-x, V-L	-290 to 110	50-4000	1955	Eakin, Ellington, Gami	38
V-L	-310 to 90	110-2100	1957	Fastovski, Petrovski	44
V-L	-260 to 90	100-1850	1959	Ellington, Eakin, Parent, Gami, Bloomer	40
V-L	-255 to -220	up to 591	1969	Yu, Elshayal, Lu	185
Joule-Thompson	10 to 190	25 to 590	1960	Head	57
Joule-Thompson	-148 to 77	up to 2500	1964	Stockett, Wenzel	159

extensive bibliography of the thermophysical properties of air have been authored by Hall.[55] Of the few experimental investigations listed in Table V, only the work of Kuenen, Verschoyle and Van Urk[75] and Dodge and Dunbar[35] are not on air. Virial coefficients of nitrogen-oxygen mixtures near room temperature have been given by Miller and Gorski.[119]

TABLE V

SOME EXPERIMENTAL INVESTIGATIONS ON THE
BINARY SYSTEM NITROGEN-OXYGEN UNDER PRESSURE

Property	Temperature °F	Pressure psia	Year	Author	Reference
P-V-T-x	-220 to 68	440-740	1923	Kuenen, Verschoyle, Van Urk	75
P-V-T(air)	-256 to -13	14,700	1954	Michels, Wasenaar, Levelt, de Graaf	117
V-L	-320 to 236	0-440	1927	Dodge, Dunbar	35
Joule-Thompson (air)	14 to 542	0-3200	1925	Roebuck	137
Joule-Thompson (air)	-274 to 32	0-3200	1930	Roebuck	138
Joule-Thompson (air)	53	15-1500	1959	Koeppe	83

THERMODYNAMIC RELATIONS

This chapter presents the mathematical relations which are required to calculate the enthalpy of mixing from measurements such as pressures, temperatures, composition, mixture flow rate and power input in a flow calorimeter.

Basic definitions of mixing and excess functions are presented. Mathematical relations are given for calculating thermodynamic properties from the Benedict-Webb-Rubin equation of state. The first law of thermodynamics is applied to a flow calorimeter in which two reasonably pure gases are mixed. Corrections for impurities are detailed. The expressions used to normalize excess enthalpies to nominal experimental conditions and subsequent smoothing with respect to composition are described.

Thermodynamic Definitions

The enthalpy of mixing and excess enthalpy are defined along with the excess heat capacity and the excess isothermal Joule-Thompson coefficient. The excess enthalpy and excess heat capacity are expressed in terms of enthalpy departures and heat capacity departures for use with the Benedict-Webb-Rubin equation of state.[12]

Thermodynamic mixing functions of binary solutions define the changes in various state functions (e.g. enthalpy, entropy) on mixing pure components at constant pressure and temperature. The enthalpy change on mixing two pure components A and B to form the mixture AB is

$$\underline{H}^M = \underline{H}_{AB} - x_A\underline{H}_A - x_B\underline{H}_B \qquad (2)$$

where x_A and x_B are the mole fractions of A and B respectively. This definition is independent of the nature of the pure components and their molecular interactions.

For ideal solutions, the mixing function is

$$\underline{H}^{M*} = 0 \tag{3}$$

where the superscript star signifies ideal solution behavior.

Excess functions are obtained by subtracting the mixing function of an ideal solution from the value of the mixing function itself. The excess enthalpy at constant pressure and temperature is therefore:

$$\underline{H}^{E} = \underline{H}^{M} - \underline{H}^{M*} \tag{4}$$

Substituting for the enthalpy of mixing, $\underline{H}^{M}$ of Equation (2), and the enthalpy of mixing of the ideal solution, $\underline{H}^{M*}$ of Equation (3), into the last equation yields

$$\underline{H}^{E} = \underline{H}_{AB} - x_A\underline{H}_A - x_B\underline{H}_B \tag{5}$$

The excess enthalpy and the enthalpy of mixing defined as in Equation (5) and (2), respectively, are identical.

The excess enthalpy of a binary mixture at zero pressure, $(\underline{H}^{E})^{0}$, may be written in terms of the zero pressure enthalpies of its constituents as

$$(\underline{H}^{E})^{0} = \underline{H}^{0}_{AB} - x_A\underline{H}^{0}_A - x_B\underline{H}^{0}_B \tag{6}$$

Subtracting $(\underline{H}^{E})^{0}$ from the definition of the excess enthalpy, Equation (5), gives

$$\underline{H}^{E} = (\underline{H}_{AB}-\underline{H}^{0}_{AB}) - x_A(\underline{H}_A-\underline{H}^{0}_A) - x_B(\underline{H}_B-\underline{H}^{0}_B) \tag{7}$$

noting that the excess enthalpy at zero pressure has the value zero. By comparing the last equation with the definition of excess enthalpy, Equation (5), it may be seen that the excess enthalpy may be evaluated either

from enthalpies or from enthalpy departures for the pure components and the mixture. Written in this form, the excess enthalpy can be calculated, from Equation (7), with an equation of state which yields values of enthalpy departure for the pure components and the mixture.

The excess heat capacity and the excess isothermal Joule-Thompson coefficient are obtained starting with the definitions of the heat capacity and isothermal Joule-Thompson coefficient:

$$C_P = \left(\frac{\partial H}{\partial T}\right)_P \tag{8}$$

$$\varphi = \left(\frac{\partial H}{\partial P}\right)_T \tag{9}$$

where the latter may be related to the volumetric properties by the identity:

$$\varphi = \underline{V} - T\left(\frac{\partial V}{\partial T}\right)_P \tag{10}$$

and where the heat capacity and isothermal Joule-Thompson coefficient may be related to the adiabatic Joule-Thompson coefficient, μ , by the identity:

$$\mu = -\frac{\varphi}{C_P} \tag{11}$$

The last two equations will be used later for calculating isothermal Joule-Thompson coefficients for data interpretation.

The excess heat capacity is the derivative of the excess enthalpy with respect to temperature

$$C_P^E = \left(\frac{\partial H^E}{\partial T}\right)_{P,x} \tag{12}$$

Substituting for the excess enthalpy from Equation (5) into the last equation gives

$$C_P^E = \left(\frac{\partial H_{AB}}{\partial T}\right)_{P,x} - x_A\left(\frac{\partial H_A}{\partial T}\right)_P - x_B\left(\frac{\partial H_B}{\partial T}\right)_P \qquad (13)$$

The partial differentials in this equation may be replaced by the heat capacity of the mixture and of the pure components according to Equation (8)

$$C_P^E = C_{P_{AB}} - x_A C_{P_A} - x_B C_{P_B} \qquad (14)$$

The excess heat capacity may be expressed in terms of the heat capacity departures by a procedure similar to the one utilized with excess enthalpies. The expression obtained is

$$C_P^E = (C_{P_{AB}} - C_{P_{AB}}^O) - x_A(C_{P_A} - C_{P_A}^O) - x_B(C_{P_B} - C_{P_B}^O) \qquad (15)$$

where the excess heat capacity is zero at zero pressure. By comparing the last equation with the definition of excess heat capacity, Equation (14), it may be seen that the excess heat capacity, too, may be calculated from either heat capacities or heat capacity departures.

The excess isothermal Joule-Thompson coefficient is the derivative of the excess enthalpy with respect to pressure:

$$\varphi^E = \left(\frac{\partial H^E}{\partial P}\right)_{T,x} \qquad (16)$$

Utilizing a procedure similar to the one used in obtaining Equation (14) for the excess heat capacity, the excess isothermal Joule-Thompson coefficient may be written as:

$$\varphi^E = \varphi_{AB} - x_A\varphi_A - x_B\varphi_B \qquad (17)$$

Correlation of Excess Enthalpy with Composition

The variation of the excess enthalpy with composition at constant pressure and temperature may be correlated with a mathematical expression

which satisfies the Gibbs-Duhem type relation:

$$x_A\left(\frac{\partial \bar{H}_A^E}{\partial x_A}\right)_{P,T} = x_B\left(\frac{\partial \bar{H}_B^E}{\partial x_B}\right)_{P,T} \tag{18}$$

where $\bar{H}_A^E$ and $\bar{H}_B^E$ are the partial molal enthalpies of A and B .

The simplest expression which may be used is the one for regular solutions given by Hildebrand and Scott[58]

$$\frac{H^E}{x(1-x)} = a_n \tag{19}$$

where a plot of excess enthalpy versus the mole fraction of one of the components is a parabola symmetrical about a line through $x = 0.5$.

Since most gas mixtures approximate this behavior, the excess enthalpies may be fitted to a curve which simultaneously represents deviations from regular solution behavior and satisfies the Gibbs-Duhem type relation, Equation (18). One such curve is represented by the equation:

$$\frac{H^E}{x(1-x)} = a_n + b_n(x-0.5) + c_n(x-0.5) \tag{20}$$

Relations for the Benedict-Webb-Rubin Equation of State

This equation of state is used to calculate three thermodynamic properties: enthalpy departure, isothermal Joule-Thompson coefficient and heat capacity departure. The enthalpy departure is used in making corrections for impurities in the nitrogen-ethane mixture data and in calculating excess enthalpies for comparison with the experimental results of this research. The heat capacity departure is utilized in determining the heat capacity of the ethane used in these experiments. Excess isothermal Joule-Thompson coefficients and excess heat capacities used in data interpretation are evaluated from the heat capacity departures and isothermal Joule-Thompson coefficients for pure components and mixtures.

In the following paragraphs, expressions will be given for the three thermodynamic properties, mentioned in the last paragraph, which are suitable for use with a pressure-explicit equation of state (see Equation (1)). That is, the expressions will have only derivatives of pressure with respect to temperature or volume e.g. $\left(\frac{\partial P}{\partial T}\right)_{\underline{V}}$ or $\left(\frac{\partial P}{\partial \underline{V}}\right)_T$

The expression for the enthalpy departure, $\underline{H}-\underline{H}^O$, has been derived by Hougen, Watson and Ragatz[63] as

$$\underline{H} - \underline{H}^O = P\underline{V} - RT - \int_{\infty}^{\underline{V}} \left[P - T\left(\frac{\partial P}{\partial T}\right)_{\underline{V}}\right] d\underline{V} \qquad (21)$$

The relation for the enthalpy departure obtained after performing the mathematical manipulations given in the last equation on the B-W-R equation of state is given in Table XLIV in Appendix C.

The isothermal Joule-Thompson coefficient, φ, has been given in Equation (10) in terms of the differential of volume with respect to temperature, $\left(\frac{\partial \underline{V}}{\partial T}\right)_P$. This equation may be rewritten to handle the pressure explicit B-W-R equation as

$$\varphi = \underline{V} + T\left(\frac{\partial \underline{V}}{\partial P}\right)_T \left(\frac{\partial P}{\partial T}\right)_{\underline{V}} \qquad (22)$$

Performing the differentiations of the last equation on the B-W-R equation gives the equation for the isothermal Joule-Thompson coefficient given in Table XLIV in Appendix C.

The expression for the heat capacity departure is obtained starting with the relation between isobaric and isochoric heat capacities given by Hougen, Watson and Ragatz[63]

$$C_P - C_V = T\left(\frac{\partial \underline{V}}{\partial T}\right)_P \left(\frac{\partial P}{\partial T}\right)_{\underline{V}} \qquad (23)$$

Splitting the differential $(\partial \underline{V}/\partial T)_P$ as before, the last equation may be written:

$$C_P - C_V = -T\left[\left(\frac{\partial P}{\partial T}\right)_V\right]^2\left(\frac{\partial V}{\partial P}\right)_T \qquad (24)$$

Hougen et al.[63] also give the derivative of the isochoric heat capacity with respect to volume as

$$\left(\frac{\partial C_V}{\partial \underline{V}}\right)_T = T\left(\frac{\partial^2 P}{\partial T^2}\right)_{\underline{V}} \qquad (25)$$

Integrating this relation isothermally gives

$$C_V = C_V^0 + T\int_{\infty}^{\underline{V}}\left(\frac{\partial^2 P}{\partial T^2}\right)_{\underline{V}} d\underline{V} \qquad (26)$$

At zero pressure, the isochoric and isobaric heat capacities are related as shown:

$$C_V^0 = C_P^0 - R \qquad (27)$$

Substituting the zero pressure isochoric heat capacity from the last equation into Equation (26) gives

$$C_V = C_P^0 - R + T\int^{\underline{V}}\left(\frac{\partial^2 P}{\partial T^2}\right)_{\underline{V}} d\underline{V} \qquad (28)$$

Substituting for C_V from the last equation into Equation (23) and transposing terms in the resultant expression gives

$$C_P - C_P^0 = -R - T\left[\left(\frac{\partial P}{\partial T}\right)_V\right]^2\left(\frac{\partial V}{\partial P}\right)_T + T\int_{\infty}^{\underline{V}}\left(\frac{\partial^2 P}{\partial T^2}\right)_{\underline{V}} d\underline{V} \qquad (29)$$

Carrying out the differentiations and integrations indicated in the last equation on the B-W-R equation, Equation (1), yields the expression for the heat capacity departure in Table XLIV.

The three expressions for the thermodynamic properties given in Table XLIV require values for the eight empirical B-W-R constants. For the pure components used in this research the constants are given in Table XLV. For mixtures the constants are estimated by combining the pure component constants according to the mixing rules of Benedict et al.[13]

In calculating the excess properties for binary mixtures, for example excess enthalpy, first the enthalpy departures for the mixture and for the two pure components are calculated and then they are subtracted according to Equation (7) given earlier. The excess heat capacity is similarly determined from Equation (15) and the excess isothermal Joule-Thompson coefficient obtained from Equation (17).

Application of First Law of Thermodynamics

The experimental scheme is illustrated in Figure 1. Gas A at flow rate F_A and gas B at flow rate F_B enter the calorimeter at almost identical conditions (P_1,T_1) and (P_2,T_2) respectively. If the gases cool on mixing then enough electrical heat input, $\dot{W}$, is supplied to make the temperature of the exiting gas mixture, T_o, almost identical with the inlet gas temperatures, T_1 and T_2. This is the case for the nitrogen-carbon dioxide and nitrogen-ethane systems but when nitrogen and oxygen are mixed there is evolution of heat and the outlet temperature is higher than the inlet temperatures. For measurements with the latter system, the calorimeter may be operated without any power input i.e. $\dot{W} = 0$. There is a small pressure drop across the calorimeter hence the outlet pressure, P_o, is slightly lower than inlet pressures, P_1 and P_2.

The mathematical derivation which follows is applicable to all three systems. Since the gases used contained some impurities, relations are obtained here for mixing two impure gases and corrections for impurities made later. Henceforth the added subscript M refers to the impure gas stream and the absence of M implies that the gas stream is assumed to be pure, e.g., the subscript A is pure A and the subscript AM is impure A.

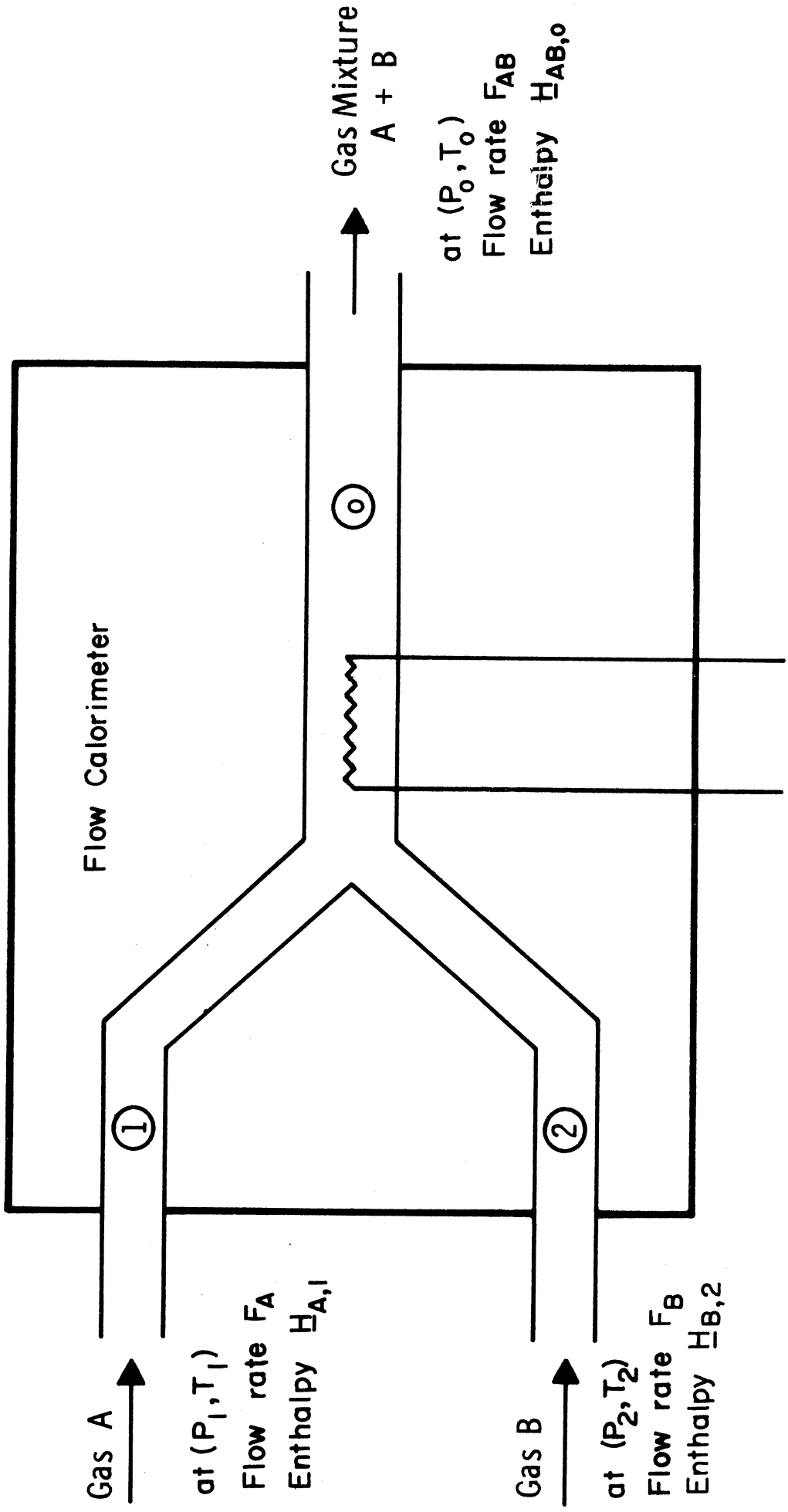

Figure 1. Schematic for Enthalpy of Mixing Measurements in a Flow Calorimeter.

Neglecting potential energy effects, the first law of thermodynamics when applied to the system illustrated in Figure 1, at steady state, yields

$$\frac{\dot{W}-\dot{Q}}{F_{ABM}} = \frac{F_{AM}}{F_{ABM}} \underline{H}_{AM,1} + \frac{F_{BM}}{F_{ABM}} \underline{H}_{BM,2} - \underline{H}_{ABM,o} + \frac{F_{AM}}{F_{ABM}} KE_{AM,1} + \frac{F_{BM}}{F_{ABM}} KE_{BM,2} - KE_{ABM,o} \qquad (30)$$

where F_{ABM} is the total flowrate of both gases and $\dot{Q}$ is the rate of heat leakage to the calorimeter. The heat leak term is the most difficult term to evaluate numerically in Equation (30). Hence the prime criterion in the design and operation of the enthalpy of mixing calorimeter is to make the heat leak negligible. For purposes of calculation, the assumption is made that the experiments are carried out under adiabatic conditions:

$$\dot{Q} = 0 \qquad (31)$$

The results of the experimental verification of this assumption of adiabaticity are discussed in the chapter entitled "Results."

The kinetic energy, KE , of a given stream is calculated per unit mass of that stream and expressed in terms of the average velocity, $\bar{u}$, of the stream. For example, the kinetic energy of the impure stream B at (T_2,P_2) is

$$KE_{BM} = \frac{1}{2} \bar{u}^2_{BM,2}$$

where

$$\bar{u}_{BM,2} = \frac{F_{BM}}{(\rho_{BM,2})(\text{cross-sectional area of flow})} \qquad (32)$$

and $\rho_{BM,2}$ is the density of impure B at (P_2,T_2). Substituting the assumed value of $\dot{Q} = 0$ and abbreviating the differences in kinetic energy by

$$\Delta KE_M = \frac{F_{AM}}{F_{ABM}} KE_{AM,1} + \frac{F_{BM}}{F_{ABM}} KE_{BM,2} - KE_{ABM,o} \qquad (33)$$

reduces Equation (30) to

$$\frac{\dot{W}}{F_{ABM}} = \frac{F_{AM}}{F_{ABM}} \underline{H}_{AM,1} + \frac{F_{BM}}{F_{ABM}} \underline{H}_{BM,2} - \underline{H}_{ABM,o} + \Delta KE_M \qquad (34)$$

The first three terms on the right hand side of Equation (34) represent an enthalpy difference between three streams that are at differing pressures and temperatures. A similar enthalpy difference can be defined at the outlet conditions of the calorimeter, (T_o, P_o), as

$$\Delta H_o = \underline{H}_{ABM,o} - \frac{F_{AM}}{F_{ABM}} \underline{H}_{AM,o} - \frac{F_{BM}}{F_{ABM}} \underline{H}_{BM,o} \qquad (35)$$

Adding Equation (34) to (35) and transposing $\dot{W}/F_{ABM}$ gives

$$\Delta H_o = - \frac{\dot{W}}{F_{ABM}} + \frac{F_{AM}}{F_{ABM}} (\underline{H}_{AM,1} - \underline{H}_{AM,o}) + \frac{F_{BM}}{F_{ABM}} (\underline{H}_{BM,2} - \underline{H}_{BM,o}) + \Delta KE_M \qquad (36)$$

The two terms on the right hand side of Equation (36) that represent enthalpy differences can be expressed in terms of the calorimeter inlet and outlet pressures and temperatures:

$$\Delta H_o = - \frac{\dot{W}}{F_{ABM}} + \frac{F_{AM}}{F_{ABM}} \int_{P_o}^{P_1} (\varphi_{AM} dP)_{T_1} + \frac{F_{AM}}{F_{ABM}} \int_{T_o}^{T_1} (C_{P_{AM}} dT)_{P_o}$$
$$+ \frac{F_{BM}}{F_{ABM}} \int_{P_o}^{P_2} (\varphi_{BM} dP)_{T_2} + \frac{F_{BM}}{F_{ABM}} \int_{T_o}^{T_2} (C_{P_{BM}} dT)_{P_o} + \Delta KE_M \qquad (37)$$

The energy balance as expressed by Equation (37) may be used directly if power is supplied to the calorimeter. If there is no power input, then the energy balance, Equation (37), may be used after setting the power input to zero, $\dot{W} = 0$.

Primary Corrections

Experimental measurements give values of the power input, $\dot{W}$, and the flow rate of the mixture, F_{ABM}, from which may be calculated the power per unit flow or the power/flow ratio, $(\dot{W}/F)$.

$$(\dot{W}/F) = \frac{\dot{W}}{F_{ABM}} \tag{38}$$

The excess enthalpy at calorimeter outlet conditions, $\underline{H}^E_o$, is obtained by applying four corrections to the power/flow ratio. Collectively, these corrections are called primary corrections. They are:

1. Correction for pressure drop across the calorimeter expressed by

$$\Delta P_{corr} = \frac{F_{AM}}{F_{ABM}} \varphi_{AM}[P_1-P_o] + \frac{F_{BM}}{F_{ABM}} \varphi_{BM}[P_2-P_o] \tag{39}$$

The two terms in this equation are the integrated forms of the terms involving pressure drop in the energy balance, Equation (37).

2. Correction for temperature difference across the calorimeter described by

$$\Delta T_{corr} = \frac{F_{AM}}{F_{ABM}} C_{P_{AM}}[T_1-T_o] + \frac{F_{BM}}{F_{ABM}} C_{P_{BM}}[T_2-T_o] \tag{40}$$

which are the integrated forms of the terms involving temperature difference in the energy balance equation.

The pressure and temperature differences are sufficiently small (maximum values of about 0.1°C and 0.4 psi) to justify assuming that the values of C_P and φ are constant during the integration. The numerical values of the properties are obtained at nominal experimental conditions from literature sources which will be referred to in the chapter entitled "Results." Only for oxygen, the isothermal Joule-Thompson coefficient is calculated from a slightly different form of Equation (10)

$$\varphi = \underline{V}\left[1 - \underline{V}T\left(\frac{\partial P}{\partial T}\right)_\rho \Big/ \left(\frac{\partial P}{\partial \rho}\right)_T\right] \qquad (41)$$

using the tabulations by Weber(180) of volume and the differentials, $\left(\frac{\partial P}{\partial T}\right)_\rho$ and $\left(\frac{\partial P}{\partial \rho}\right)_T$, obtained from his own PVT data.

3. Correction for kinetic energy differences between incoming and outgoing gases, ΔKE_M, detailed in Equation (33). This term, too, occurs in the energy balance, Equation (37). Density data is needed on impure A and B and on their mixture.

These three corrections are applied to $(\dot{W}/F)$, the power to flow ratio, to obtain the enthalpy difference, ΔH_o. This enthalpy difference is the enthalpy change which takes place with the isothermal, isobaric mixing of the impure streams of A and B at calorimeter outlet conditions, (T_o, P_o). To determine the enthalpy of mixing of pure A and B it is necessary to make one more correction.

4. Correction for impurities in the substances under study. This correction is applied to the enthalpy difference, ΔH_o, to obtain the excess enthalpy, $\underline{H}_o^E$, of the mixture of the two major components in the stream exiting the calorimeter.

$$\underline{H}_o^E = \Delta H_o + \Delta I_{corr} \qquad (42)$$

where ΔI_{corr} is the correction for impurities. The nitrogen-carbon dioxide system uses the experimentally obtained enthalpy differences, ΔH_o, whereas the nitrogen-ethane system requires an enthalpy prediction technique to make this correction.

Corrections for Impurities

The mathematical manipulations required to extract the excess enthalpy, $\underline{H}_o^E$, from the measurable enthalpy difference, ΔH_o, will be derived in this section. The two cases of the nitrogen-carbon dioxide

system and the nitrogen-ethane system will be considered separately. To maintain continuity with the previous development, the subscripts used will be A and B . A is assumed to signify nitrogen and B the other component, ethane or carbon dioxide.

Nitrogen-Carbon Dioxide System

As indicated in Table IX, the nitrogen used in this research contains only 0.02 mole percent oxygen and the carbon dioxide contains 0.05 and 0.09 mole percent nitrogen and oxygen, respectively. Both streams are relatively pure and contain one principal impurity--oxygen. As will be described, the impurity corrections for the data on the nitrogen-carbon dioxide system are based on certain assumptions regarding the major impurity oxygen, and the implementation of these corrections require the experimental results of this very research.

The enthalpy change on mixing nitrogen and oxygen was measured in the course of this research and found to be at least two orders of magnitude smaller than the excess enthalpy values of the other two systems. Therefore, since the amount of oxygen impurity is small, the nitrogen stream is assumed to be pure. Based on the same results, it seems reasonable to assume that the excess enthalpy of the oxygen-carbon dioxide system is very similar to that of the nitrogen-carbon dioxide system at the conditions of experimental measurements of the present research. Since the fraction of oxygen impurity in the carbon dioxide is small, for purposes of making impurity corrections, the oxygen is lumped with the nitrogen and the carbon dioxide stream is assumed to contain only one impurity--0.14 mole percent nitrogen.

For this system, the measurable quantity, ΔH_o , which was defined in Equation (35) for mixing impure A and B streams must be

modified to

$$\Delta H_o = \underline{H}_{AB,o} - \frac{F_{BM}}{F_{AB}} \underline{H}_{BM,o} - \frac{F_A}{F_{AB}} \underline{H}_{A,o} \qquad (43)$$

where A is pure nitrogen, BM is carbon dioxide with only nitrogen as impurity, and AB is the nitrogen-carbon dioxide mixture.

The enthalpies of the impure carbon dioxide and the nitrogen-carbon dioxide mixtures may be defined in terms of the excess enthalpies (as in Equation (5)) $\underline{H}^E_{BM,o}$ and $\underline{H}^E_o$, respectively:

$$\underline{H}_{BM,o} = \underline{H}^E_{BM,o} + y_A \underline{H}_{A,o} + y_B \underline{H}_{B,o} \qquad (44)$$

$$\underline{H}_{AB,o} = \underline{H}^E_o + x_A \underline{H}_{A,o} + x_B \underline{H}_{B,o} \qquad (45)$$

where y_A and y_B are the mole fractions of nitrogen and carbon dioxide in the latter feed stream.

Substituting for $\underline{H}_{BM,o}$ and $\underline{H}_{AB,o}$ from Equation (44) and (45) in the expression for ΔH_o, Equation (43), and collecting coefficients of $\underline{H}_{A,o}$ and $\underline{H}_{B,o}$ yields

$$\Delta H_o = \underline{H}^E_o - \frac{F_{BM}}{F_{AB}} [\underline{H}^E_{BM,o}] + \underline{H}_{A,o} \left[x_A - y_A \frac{F_{BM}}{F_{AB}} - \frac{F_A}{F_{AB}}\right]$$
$$+ \underline{H}_{B,o} \left[x_B - y_B \frac{F_{BM}}{F_{AB}}\right] \qquad (46)$$

A mass balance on A and B entering and leaving the system gives

$$F_A + y_A F_{BM} = x_A F_{AB} \qquad (47)$$

$$y_B F_{BM} = x_B F_{AB} \qquad (48)$$

Substituting for the mole fraction of A, x_A from Equation (47), and the mole fraction of B, x_B from Equation (48), into the expression

for ΔH_o , Equation (46), reduces the coefficients of $\underline{H}_{A,o}$ and $\underline{H}_{B,o}$ to zero. Transposing terms in Equation (46), the excess enthalpy of the exit stream, $\underline{H}^E_o$, may be expressed as

$$\underline{H}^E_o = \Delta H_o + \frac{F_{BM}}{F_{AB}} \left[\underline{H}^E_{BM,o}\right] \tag{49}$$

Comparing this equation with Equation (42) in which the application of the impurity correction was originally expressed yields

$$\Delta I_{corr} = \frac{F_{BM}}{F_{AB}} \left[\underline{H}^E_{BM,o}\right] \tag{50}$$

The excess enthalpy of the impure carbon dioxide stream, $\underline{H}^E_{BM,o}$, required to estimate the impurity correction is obtained from the experimentally determined enthalpy difference, ΔH_o . The enthalpy difference is fitted to an equation similar to Equation (20).

$$\frac{\Delta H_o}{x_N(1-x_N)} = a_o + b_o(x_N-0.5) + c_o(x_N-0.5)^2 \tag{51}$$

where x_N is the mole fraction of nitrogen and a_o, b_o and c_o are determined by a least squares analysis. Since the carbon dioxide stream is assumed to contain only nitrogen and since the fraction of this impurity is small, the excess enthalpy of the impure carbon dioxide stream, $\underline{H}^E_{BM,o}$, is equated to the enthalpy difference, ΔH_o , and substituted in the last equation along with mole fraction impurity $x_N = y_A$:

$$\underline{H}^E_{BM,o} = y_A(1-y_A)[a_o + b_o(y_A-0.5) + c_o(y_A-0.5)^2] \tag{52}$$

The excess enthalpy of the impure carbon dioxide feed stream $\underline{H}^E_{BM,o}$ is evaluated by substituting the mole fraction impurity nitrogen, (in this case its value is $y_A = 0.0014$), in the last equation and the impurity correction, ΔI_{corr} , determined from Equation (50).

Nitrogen-Ethane System

The ethane used in this investigation has ethene, propene and propane as impurities as indicated in Table IX. Whereas it was possible to make use of binary enthalpy of mixing data to account for nitrogen as an impurity in carbon dioxide, the presence of several impurities other than nitrogen necessitates another approach, which is outlined below.

The enthalpy difference, ΔH_o, for this system is defined in a similar way as for the nitrogen-carbon dioxide system, Equation (43),

$$\Delta H_o = \underline{H}_{ABM,o} - \frac{F_A}{F_{ABM}} \underline{H}_{A,o} - \frac{F_{BM}}{F_{ABM}} \underline{H}_{BM,o} \qquad (53)$$

assuming that the nitrogen is pure and that the impurities are in the ethane feed and in the nitrogen-ethane mixture stream.

The excess enthalpy of the nitrogen-ethane mixture, as defined in Equation (5), may be written in terms of the molar flow rates of A and B as

$$\underline{H}_o^E = \underline{H}_{AB,o} - \frac{F_A}{F_{AB}} \underline{H}_{A,o} - \frac{F_B}{F_{AB}} \underline{H}_{B,o} \qquad (54)$$

where $$x_A = \frac{F_A}{F_{AB}} \quad \text{and} \quad x_B = \frac{F_B}{F_{AB}}$$

Multiplying the expression for ΔH_o, Equation (53), by $\frac{F_{ABM}}{F_{AB}}$, subtracting it from Equation (54) for $\underline{H}_o^E$, and writing the resultant expression explicitly in $\underline{H}_o^E$ gives

$$\underline{H}_o^E = \underline{H}_{AB,o} - \frac{F_B}{F_{AB}} \underline{H}_{B,o} + \frac{F_{ABM}}{F_{AB}} \Delta H_o - \frac{F_{ABM}}{F_{AB}} \underline{H}_{ABM,o} + \frac{F_{BM}}{F_{AB}} \underline{H}_{BM,o} \qquad (55)$$

The flow rates of the impure ethane and nitrogen-ethane streams may be written as the sum of the flow rate of impurities, F_I, and the flow rate of the remainder

$$F_{ABM} = F_{AB} + F_I \qquad (56)$$

$$F_{BM} = F_B + F_I \tag{57}$$

where F_B is the flow rate of pure ethane and F_{AB} is the flow rate of the impurity-free binary nitrogen-ethane stream.

Substituting for F_{ABM} and F_{BM} from the last two equations in the expression for $\underline{H}_o^E$, Equation (55), and regrouping terms gives

$$\underline{H}_o^E = \Delta H_o \left[\frac{F_I+F_{AB}}{F_{AB}}\right] + \frac{F_B}{F_{AB}}\left[\underline{H}_{BM,o} - \underline{H}_{B,o}\right] + \left[\underline{H}_{AB,o} - \underline{H}_{ABM,o}\right] + \frac{F_I}{F_{AB}}\left[\underline{H}_{BM,o} - \underline{H}_{ABM,o}\right] \tag{58}$$

By transposing terms in Equation (42), the correction for impurities, ΔI_{corr}, may be expressed as the difference between the excess enthalpy, $\underline{H}_o^E$, and the enthalpy difference, ΔH_o,

$$\Delta I_{corr} = \underline{H}_o^E - \Delta H_o \tag{59}$$

Substituting for the excess enthalpy at calorimeter outlet conditions, $\underline{H}_o^E$, from Equation (58) in the last equation and performing the subtraction of Equation (59) gives the impurity correction:

$$\Delta I_{corr} = \frac{F_I}{F_{AB}}[\Delta H_o] + \frac{F_B}{F_{AB}}[\underline{H}_{BM,o} - \underline{H}_{B,o}] + [\underline{H}_{AB,o} - \underline{H}_{ABM,o}] + \frac{F_I}{F_{AB}}[\underline{H}_{BM,o} - \underline{H}_{ABM,o}] \tag{60}$$

Evaluation of the impurity correction, requires values for the enthalpy difference, ΔH_o, and the six enthalpy terms in Equation (60). The former is determined experimentally. The six enthalpy terms are estimated from the Benedict-Webb-Rubin equation of state.[12,13,14] An equation of state, however, yields values of the enthalpy departure rather than values of the enthalpy itself (See Equation (21)). As will be shown, it is sufficient to use enthalpy departures in place of the six enthalpy terms in Equation (60) to evaluate the impurity correction.

The equation for the impurity correction, Equation (60), was derived from Equation (53) for the enthalpy difference, ΔH_o, and from Equation (54) for the excess enthalpy. Earlier in the chapter, it was shown that the excess enthalpy can be calculated from enthalpy departures. It will now be shown that the enthalpy difference, ΔH_o, can also be calculated from enthalpy departures.

The enthalpy difference at zero pressure is

$$\Delta H_o^o = \underline{H}_{ABM,o}^o - \frac{F_A}{F_{ABM}} \underline{H}_{A,o}^o - \frac{F_{BM}}{F_{ABM}} \underline{H}_{BM,o}^o \qquad (61)$$

The zero pressure enthalpy of the impure nitrogen-ethane mixture may be written in terms of the zero pressure enthalpies of its constituents:

$$\underline{H}_{ABM,o}^o = \frac{F_A}{F_{ABM}} \underline{H}_{A,o}^o + \frac{F_B}{F_{ABM}} \underline{H}_{B,o}^o + \frac{F_I}{F_{ABM}} \underline{H}_{I,o} \qquad (62)$$

noting that the excess enthalpy at zero pressure is zero and where the subscript I refers collectively to all the impurities. In a similar way the zero pressure enthalpy of the impure ethane may be written as

$$\underline{H}_{BM,o}^o = \frac{F_B}{F_{BM}} \underline{H}_{B,o}^o + \frac{F_I}{F_{BM}} \underline{H}_{I,o}^o \qquad (63)$$

Substituting for $\underline{H}_{ABM,o}^o$ and $\underline{H}_{BM,o}^o$ from the last two equations into Equation (61) for the zero pressure enthalpy difference gives

$$\Delta H_o^o = \frac{F_A}{F_{ABM}} \underline{H}_{A,o}^o + \frac{F_B}{F_{ABM}} \underline{H}_{B,o}^o + \frac{F_I}{F_{ABM}} \underline{H}_{I,o}^o - \frac{F_A}{F_{ABM}} \underline{H}_{A,o}^o - \frac{F_{BM}}{F_{ABM}} \left[\frac{F_B}{F_{BM}} \underline{H}_{B,o}^o + \frac{F_I}{F_{BM}} \underline{H}_{I,o}^o \right] \qquad (64)$$

All the terms in the last equation cancel out reducing the zero pressure enthalpy difference to zero. This implies that the enthalpy difference, ΔH_o, like the excess enthalpy, $\underline{H}_o^E$, may be calculated with enthalpy departures only, and further implies that the impurity correction, ΔI_{corr} requires only enthalpy departures for its evaluation.

Therefore, the impurity correction for the nitrogen-ethane mixtures is determined by substituting the values for the enthalpy departures, calculated from the B-W-R equation, instead of the enthalpy terms in Equation (60). The expression for the enthalpy departure for the B-W-R equation of state is given in Table XLIV. The B-W-R constants for the pure components are given in Table XLV and the mixture constants are determined from them using the mixing rules of Benedict et al.(13)

Secondary Corrections and Smoothing of Data

The primary corrections described in the previous sections of this chapter serve to yield values of $\underline{H}_o^E$, the excess enthalpy at the experimentally determined conditions of pressure and temperature at the calorimeter outlet. It is necessary to make a second set of adjustments to the excess enthalpy $\underline{H}_o^E$, to obtain a normalized excess enthalpy $\underline{H}_n^E$. These adjustments, called secondary corrections, compensate for the operational variation in temperature and pressure level (± 0.05°C and ± 3 psi) at the calorimeter outlet. The normalized excess enthalpy at nominal experimental conditions (T_n, P_n) is obtained from the excess enthalpy at calorimeter outlet conditions (T_o, P_o) using the equation

$$\underline{H}_n^E = \underline{H}_o^E + \int_{P_o}^{P_n} (\varphi^E \, dP)_{T_o} + \int_{T_o}^{T_n} (C_P^E \, dT)_{P_n} \qquad (65)$$

where C_P^E and φ^E have been defined earlier in Equations (14) and (17), respectively. The actual calculations are carried out on the integrated form of the last equation

$$\underline{H}_n^E = \underline{H}_o^E + \varphi^E[P_n - P_o] + C_P^E[T_n - T_o] \qquad (66)$$

with the thermodynamic excess properties being assumed constant over the integration.

As explained, thermodynamic data are required on the variation of excess enthalpy with temperature and pressure, respectively. In the absence of experimental data, these quantities are estimated using the Benedict-Webb-Rubin equation of state. The heat capacity and the isothermal Joule-Thompson coefficient are estimated from the equations in Table XLIV for the pure components with the constants given in Table XLV. For the mixtures, the equations in Table XLIV are used with the mixture constants being calculated from the pure component constants using the mixing rules of Benedict et al.[13] The excess heat capacity and the excess Joule-Thompson coefficient are calculated by substituting the values of the thermodynamic properties so obtained in the expressions given earlier in this chapter for these quantities, Equation (15) and (17) respectively. The excess properties predicted by the B-W-R equation are believed to be of doubtful accuracy (estimates of accuracy will be given in chapter entitled "Results"). The thermodynamic properties are evaluated at the nominal experimental conditions and are assumed to be constant over the pressure and temperature differences of Equation (66).

In the chapter entitled "Results," the experimental results on the nitrogen-ethane mixtures are presented both with and without impurity corrections. When impurity corrections are made, the secondary corrections on the binary nitrogen-ethane mixtures are made as described. For the case where impurity corrections are not made, the "excess" heat capacity and "excess" Joule-Thompson coefficient are calculated from the following equations at nominal experimental conditions:

$$C_P^{E'} = C_{P_{ABM,n}} - \frac{F_A}{F_{ABM}} C_{P_{A,n}} - \frac{F_{BM}}{F_{ABM}} C_{P_{BM,n}} \qquad (67)$$

$$\varphi^{E'} = \varphi_{ABM,n} - \frac{F_A}{F_{ABM}} \varphi_{A,n} - \frac{F_{BM}}{F_{ABM}} \varphi_{BM,n} \qquad (68)$$

where A is pure nitrogen, BM is impure ethane and ABM is the impure nitrogen-ethane mixture. The heat capacities and the isothermal Joule-Thompson coefficients in the above equations are the derivatives at nominal experimental conditions of the enthalpy terms in Equation (53) for the enthalpy difference, ΔH_o , of nitrogen-ethane mixtures. The prime in the above equations indicates that these are not true excess properties. However, they are used just like "true" excess properties for normalizing the data as described in earlier paragraphs.

The values of excess enthalpy normalized to nominal temperature and pressure are correlated with the mole fraction of nitrogen, x_N , using Equation (20) written previously

$$\frac{H_n^E}{x_N(1-x_N)} = a_n + b_n(x_N-0.5) + c_n(x_N-0.5)^2 \qquad (69)$$

where x_N is the mole fraction of nitrogen. The constants a_n, b_n and c_n are obtained by a regression analysis.

APPARATUS AND EXPERIMENTS

In this flow calorimetric facility, the system brings two gases at the same temperature and pressure to the calorimeter where they are mixed. A measured quantity of electrical energy is added to the gases in the calorimeter to minimize the temperature difference between the incoming pure gases and the exiting mixture stream. Each pure gas stream is metered individually, hence both the flowrate and the composition of the mixture are determined simultaneously.

The experimental details of these measurements are given in this chapter. The design of the flow calorimeter used to make these measurements is presented. The facility in which it is incorporated is described. An account is given of the mode of operation of this facility.

APPARATUS

A description is given here of the calorimeter and the flow calorimetric facility. Measurements and procedures are presented in later sections.

Calorimeter

The design of the calorimeter is based on several factors. The heat leak to and from the calorimeter must be minimized. The calorimeter must have a low heat capacity so it can respond quickly to changes in experimental conditions. The pure gases which enter the calorimeter must be adequately mixed so that the exit mixture is of uniform composition. Simultaneously, the pressure drop generated by internal mixing devices must be small. Differences in kinetic energy between the pure gases entering and the mixture leaving the calorimeter must be minimized. The experience of previous investigators[45,71,96,98] with flow calorimeters

for isobaric heat capacity measurements heavily influenced the design and construction of this calorimeter. Especially valuable was the work of Faulkner[45] who in his thesis gives an excellent review of various aspects of calorimeter design and instrumentation.

A sketch of the calorimeter is given in Figure 2 with the key on Table VI. The pure gases A and B enter the calorimeter through ports 1 and 2, respectively, via 3/8-inch tubing union tees. The temperature difference between the gases entering is measured by duplicate six junction copper-constantan thermopiles which are inserted in thermowells 4. The temperature difference between the gas entering port 1 and the outlet mixture is monitored by similar duplicate thermopiles inserted in thermowells 11a and 11b. The bottoms of the thermowells are packed with Apiezon-N grease to improve thermal contact.

The pressure is measured via 1/8-inch tubing pressure taps 5 and 6 for the inlet gases and 10 for the outlet mixture. The 1/8-inch tubes are welded to sleeves which are concentric to the 3/8-inch tubing carrying the gas. The gas pressure is transmitted to the sleeves through six 1/32-inch diameter holes equally spaced on the circumference of the 3/8-inch tubing. The six holes are at the same location along the axis of the 3/8-inch tubing as the multiple junctions of the thermopiles inserted in the coaxial thermowells, in order that the pressure and temperature be measured at the same point.

The pure gases flow through two concentric tubes and are mixed at the point labeled 7 within the mixing chamber. Reversing the direction of flow, the gas mixture then passes into the annular space, 8, between the outer most of the two concentric tubes and a thin (0.01 inch thick) copper cylinder. The latter is the first of four concentric cylindrical baffles (other three baffles not shown in Figure 2) over

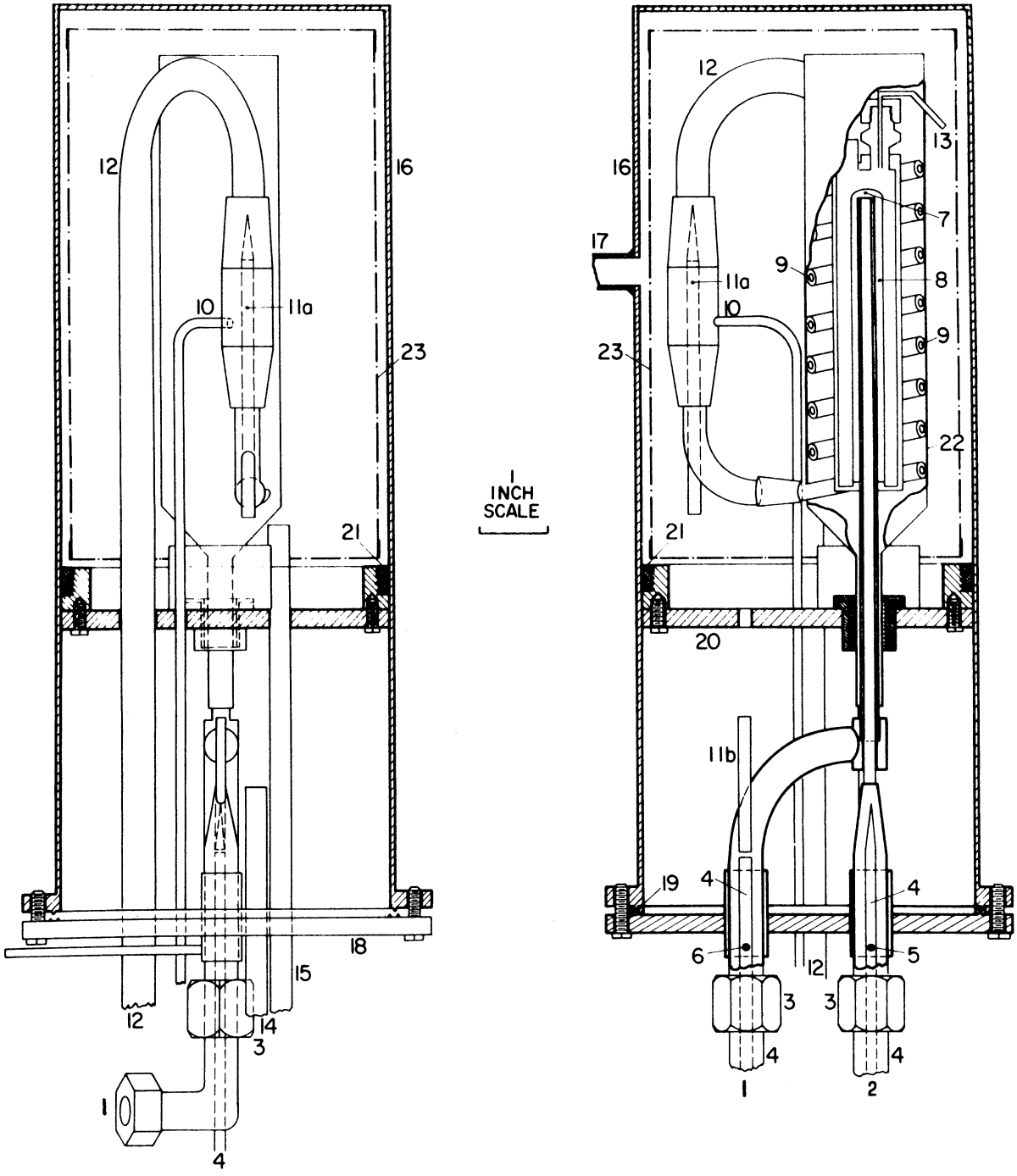

Figure 2. Enthalpy of Mixing Calorimeter. (Key: Table VI)

TABLE VI

KEY TO SKETCH OF CALORIMETER IN FIGURE 2

1. Gas inlet A
2. Gas inlet B
3. 3/8-inch tubing union tees
4. Thermocouple wells to measure differential temperature at inlet
5. Inlet pressure tap--Gas A
6. Inlet pressure tap--Gas B
7. Mixing point of Gases A and B
8. Annular space for flow of gas mixture
9. Helical tubes carrying mixed gases to outlet tubes
10. Outlet pressure tap--mixture A+B

11a. Outlet thermocouple well

11b. Inlet thermocouple well to measure temperature differential between gas inlet and gas outlet. Thermocouple junctions placed in wells 11a and 11b

12. Gas outlet tube
13. Heater leads
14. Tube for housing thermocouple lead
15. Tube for housing heater leads
16. Outer vacuum jacket
17. Vacuum line
18. Bottom flange
19. Teflon gasket
20. Teflon mechanical partition
21. Brass collar with coarse interrupted threads. Collar attached to outer jacket
22. Gold-plated thin copper shield
23. Silver-plated thin copper shield

Note: Sketch on right shows details of inlet assembly and mixing chamber.

which the gas mixture flows back and forth. In passing from one baffle to the next the mixture flows through approximately 30 symmetrically distributed holes of 1/32-inch diameter located at alternate ends of the hemispherical ends of the baffles. Detailed drawings of similar baffles have been given by Faulkner.[45] The only difference is that the cluster of holes in each of these baffles are located at the opposite end of the baffles shown by Faulkner. From the top of the outermost baffle, the gas mixture passes into a helical 1/4-inch diameter tube, 9, which leads it to the outlet measuring station. The gas mixture exits the calorimeter via tube 12. This tube is made as long as possible to minimize heat conduction along it.

The first two of these baffles is wound with 180 ohms of insulated Nichrome wire. Heater leads, 13, are brought into the mixing capsule through a conax gland. The two remaining baffles and the helical tube serve to equilibrate the mixture. An externally goldplated copper radiation shield, 22, is in contact with the helical tube and facilitates regenerative heat transfer.

A silver plated copper shield, 23, completely surrounds the mixing chamber and the outlet measuring station and isolates them from the line of sight of the surroundings as well as the gas inlet assembly. A single junction copper-constantan thermocouple measures the temperature difference between the skin of the shield and the exit tube, 12. The shield, 23, is supported by three small copper pins which rest on the teflon partition, 20. Very little, if any heat is conducted away from the shield through these supports and through the teflon partition. The partition is bolted to a circular brass ring. Interrupted threads on the brass ring mate with similar threads on a brass collar, 21, which is attached to the outer jacket, 10, of the calorimeter.

A vacuum jacket, 16, surrounds the mixing chamber, and the measuring stations. The vacuum serves to minimize conductive and convective heat transfer between the calorimeter and the surroundings. Twelve symmetrically placed socket head screws squeeze a teflon gasket, 19, between the bottom flange, 18, and the flange on the vacuum jacket. An operational vacuum level of one to four microns Hg is maintained within the jacket with a vacuum pump.

Conductive heat transfer along the thermopile wires is minimized by using 30-gauge wire and making the distance between the two sets of six junctions about four feet in length. The 30-gauge copper lead wires are brought out of the calorimeter bath through a 1/4-inch O.D. stainless tube, 14, about three feet long welded to the bottom flange, 18. The copper wires are threaded through teflon tubing before inserting them in the 1/4-inch tube. At the end of the 1/4-inch tube, the wires are soldered to the Covar sealed pins of an octal plug. A vacuum tight seal is maintained by soft-soldering the octal plug and the tubing to an annular stainless steel cylindrical adaptor. The 22-gauge copper lead wires from the calorimetric heater are brought out of the calorimeter via a similar stainless steel tubing, 15, and octal plug arrangement.

Flow Calorimetric Facility

The flow calorimetric facility supplies the two gases to the calorimeter where measurements are made under steady state conditions. The flow system is described by tracing the path followed by the two gases from the supply cylinders to the exhaust system. Details of the gas supply assembly, the conditioning baths and the control panel follow separately.

Flow System

A flow diagram is presented in Figure 3 with the key on Table VII. The two gases under investigation are supplied from cylinders, 1 and 2. These cylinders are manifolded, as shown, to dampen the rate of decrease of supply pressure caused by continuous withdrawal of gas. Manually operated pressure regulators, 3, set the pressure of the gas entering the flow metering section at about 1100 psia (except for ethane flow metering pressure of 500 psia). In the case of ethane and carbon dioxide only, the gas is heated with heating tapes wound onto the pressure regulator and gas supply tubing to prevent it from condensing when it is throttled from supply to flow metering pressure.

The flow rate of each gas is metered separately in high pressure flow meters, 5 and 6, which are located in the flow meter bath. The temperature of the bath is maintained at 25°C for the nitrogen-oxygen system and at 45°C for the other two systems.

The gases are preconditioned prior to entering the bath by heating tapes wrapped onto the tubing. The power input to the heating tapes is adjusted to maintain the gas temperature within ± 1 to 2°C of the bath temperature. Gas temperatures are monitored by single junction copper-constantan thermocouples, 13, inserted into the gas streams through conax glands. On entering the bath, the gases flow through 50 feet of copper conditioning coils.

Traces of oil and gross particles are filtered out by passing the gases through glass-wool filled bombs (not shown in Figure 3) before they enter the bath. Micron filters, 4, on the gas inlet, outlet and pressure taps to the flow meter further cleanse the gas and prevent deposition of particles within the flow meters.

The gases are throttled from the flow metering pressure to the required pressure in the calorimeter by metering valves, 21. Preheating by heating tapes on the tubing, 12, prevents condensation. Ball valves, 22, are used as on-off valves as they provide negligible resistance to flow. They occur at this and other points in the flow path of the gases wherever throttling or metering valves are located.

The temperatures of the gases entering the calorimeter bath, which are measured by thermocouples, 13, are brought to within ± 1 to 2°C of the bath temperature by controlling electrical power input to heating tapes, 12, wound on the tubing. Gas temperatures are equalized with the bath temperature by passing each of the gases through 50 feet of copper coils in the bath. The two gases are mixed within the calorimeter. The difference in temperature between the mixture exiting the calorimeter and the two pure gases entering it is rendered negligible by passing the mixture over heated resistance wire within the calorimeter.

On leaving the calorimeter bath, the gas mixture is preheated with heating tape, 12, to prevent condensation when it is throttled to 75 psia pressure by pressure reducing valve, 18. Valving is provided at this point to withdraw mixture samples at a pressure of 75 psia for composition analysis.

Again, the mixture is preconditioned as described earlier before entering the flow meter bath. The two flow meter baths in Figure 3 are in reality a single bath. They are drawn as shown for clarity in the flow diagram. The low pressure flow meter, 19, is not calibrated but used only for operational control. A glass wool bomb located prior to entering the bath, and micron filters, 4, at the flow meter remove oil and particulate matter from the gas mixture.

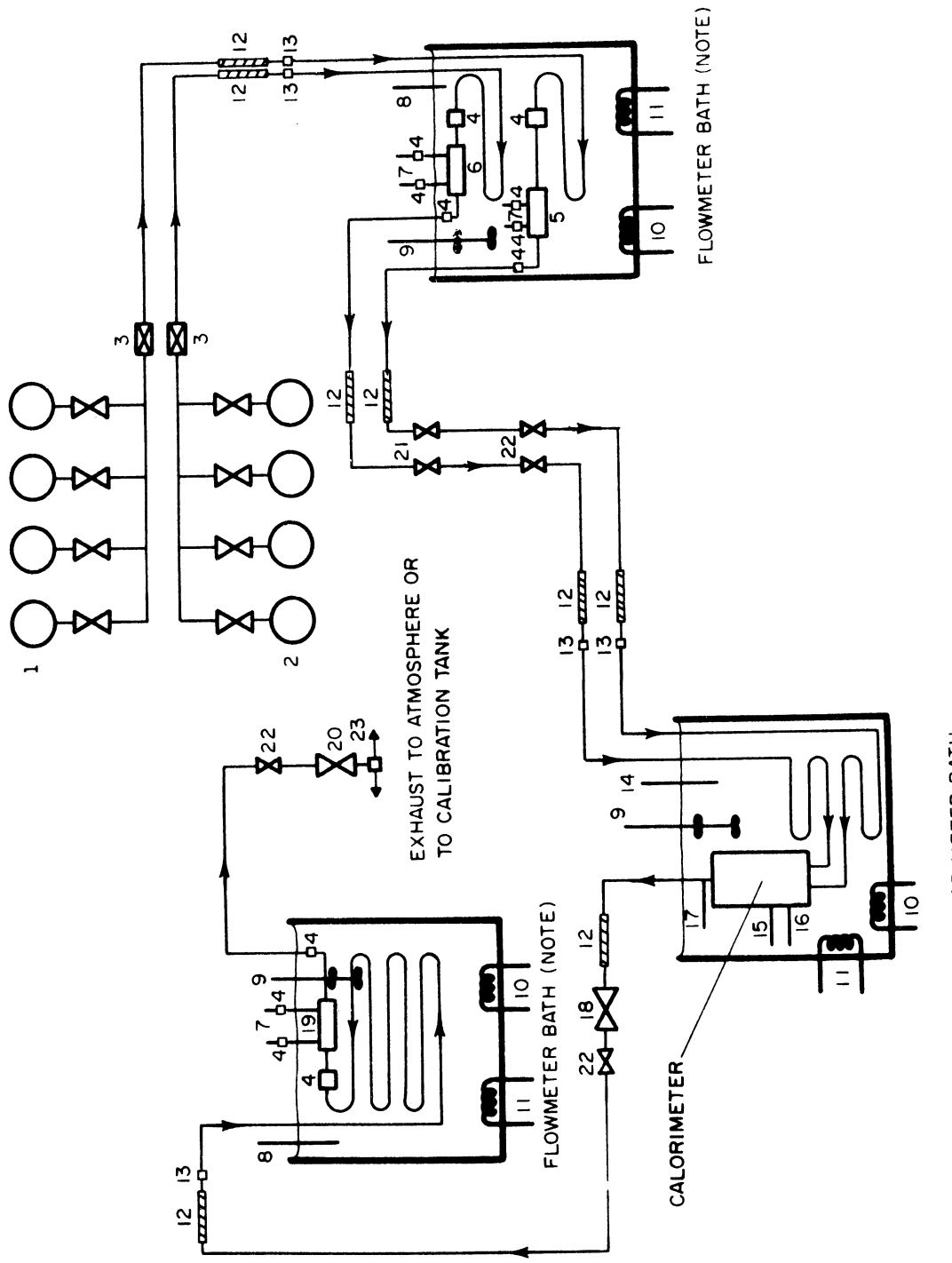

Figure 3. Flow Diagram of the Facility. (Key: Table VII)

TABLE VII

KEY TO FLOW DIAGRAM IN FIGURE 3

1. Gas A tanks
2. Gas B tanks
3. Pressure regulator
4. Micron filter
5. High pressure flow meter
6. High pressure flow meter
7. Pressure taps
8. Thermometer
9. Stirrer
10. Controlled heat input
11. Cooling water or compressed air
12. Heating tapes
13. Thermocouples
14. Thermometer
15. Inlet pressure tap--Gas A
16. Inlet pressure tap--Gas B
17. Mixture outlet pressure tap
18. Pressure reducing valve
19. Meriam flow meter--mixture A+B
20. Flow metering valves
21. Metering valves
22. Ball valves
23. Two-way outlet solenoid valve

The mixture is throttled to atmospheric pressure through flow metering valves, 20. It is then vented through a two way solenoid valve, 23. During normal operation, with the solenoid valve switch off, the gas mixture is vented to a tunnel located beneath the laboratory floor. A fan at the end of the tunnel exhausts the gas mixture to the air outside the building. When the solenoid valve switch is thrown, the mixture is diverted to a calibration tank. The latter is a tank whose volume (about six cubic feet) has been measured accurately. It is used only during flow meter calibrations to measure flow rate by collecting the gas in it over a measured period of time.

Gas Supply Assembly

Each of the nitrogen and oxygen supply cylinders are filled with about 250 standard cubic feet of gas at approximately 2300 psig. Seven cylinders are connected to the supply manifold of each gas. Gas is withdrawn from the manifolded cylinders with a resultant decrease in pressure level of 30 to 40 psi/hour till an internal pressure of 1200 to 1300 psig is reached after which they are replaced with fresh cylinders.

Both the ethane and carbon dioxide in the supply cylinders are in coexisting liquid and gaseous phases. The ethane cylinders contain about 30 pounds at 350 psig whereas there is 50 pounds of carbon dioxide at about 850 psig. The cylinders after manifolding are heated with heating tapes to raise the gas pressure to the required level. The four manifolded ethane cylinders are kept at 700 psig. The carbon dioxide in the six cylinders is maintained at about 1300 psig. Variacs control the power input to the heating tapes to sustain the pressures at these levels within $\pm$ 50 psi.

Constant Temperature Baths

There are three constant temperature baths: The cooling water bath, the flow meter bath, and the calorimeter bath.

1. Cooling Water Bath: This bath, as its name implies, supplies cooling water at a controlled temperature. Water is recirculated by a floor-mounted centrifugal pump to a 50-gallon drum, fastened to the wall near the roof. Cooling water is tapped from the exhaust of this pump. An overflow drain on the drum maintains a constant head of water. The temperature of the water draining from the bottom of the drum into the pump is measured by a temperature sensing probe. A pneumatic error signal is transmitted by it to an air-pressure controlled valve which regulates the amount of water entering the drum to control the temperature of the water in the recirculating system. A constant amount of heat is supplied by a 2000-watt immersion heater in the drum. Once steady conditions are achieved, the cooling water temperature does not vary by more than a few tenths of a degree.
2. Flow Meter Bath: It consists of a 27-inch long by 15-inch wide by 25-inch deep stainless steel bath insulated with 2-inch thick styrofoam blocks on the side and bottom and with 1 1/2-inch thick styrofoam on the top. The assembly is enclosed in a 1/2-inch thick plywood box.

The bath fluid water is stirred by a Lightnin' 10X mixer. A 100-watt tubular heater, used for on-off control, and a 300-watt tubular heater, for continuous heat input, are immersed in the water. These two low lag heaters consist of a resistance wire packed with high thermal conductivity material within 5/16-inch copper tubing. The temperature of the bath is sensed by a mercury-to-wire Philadelphia

Scientific and Glass thermoregulator. Lead wires from the thermoregulator are connected to a Fisher transistor relay.

Cooling water tapped from the centrifugal pump is returned to the cooling water bath after it is circulated through a copper coil (50 feet in length) submerged in the flow meter bath. The constant flow rate and relatively invariant temperature of the cooling water provides for a fixed heat removal rate. The heat input from the continuous-input heater can be controlled with a variac till it provides slightly less heat than can be extracted by the cooling source. The temperature of the bath can then be maintained within ± 0.01°C with on-off mode control by regulating the heat input from the on-off heater to 10-20 watts.

3. Calorimeter Bath: The working space in the calorimeter bath is an 18-inch long by 12-inch wide by 22-inch deep stainless steel tank. Eight-inch thick styrofoam insulation on the sides and bottom of the tank is supported by a 1/2-inch thick plywood box. The top consists of a stainless steel plate divided into two halves and covered with four inches of styrofoam.

Since all the measurements are close to room temperature, the only bath fluid used is water. Stirring is accomplished by an explosion proof Lightnin' Model NC-4 portable mixer with an EVS unit for varying the agitation rate. Cooling for the bath is provided by passing compressed air at an inlet pressure of 50 psig through a submerged copper coil 50 feet in length. A 300-watt knife heater connected to a powerstat supplies a constant heat input to the bath. The variable heat input is supplied to a 100-watt tubular heater by a Bayley Model 121 proportional controller. The temperature sensor for this controller

is a nickel resistance thermometer in a stainless steel sheath. In the bath described, the controller was capable of operating at a band width of 0.01°C without temperature instability once the gas streams (e.g. nitrogen, ethane, etc.) had attained steady flow and temperature conditions. The degree of control achieved is ± 0.002°C.

Control Panel

The constant temperature baths and much of the high pressure tubing is enclosed by a 10-foot high, L-shaped, 1/4-inch thick steel barricade. Almost all the instruments used are either fastened to or are located in front of the long arm of the L-shaped barricade which is termed the control panel. A photograph of this control panel is given in Figure 4.

Four separate pressure manifolds consisting of flush-mounted valves connected by 1/8-inch copper tubing are located on the face of the long arm of the L-shaped barricade. Two of these manifolds connect the two high pressure flow meters to their individual high pressure manometers and Heise gauges. One manifold is for measuring the pressure and pressure drop in the calorimeter. The fourth one is connected to the instrumentation for the low pressure flow meter.

The switches for the 110-volt electrical power are mounted on a transite board bolted to the control panel. The electrical measuring equipment (power supply, K-3 potentiometer, etc. described later) are placed separately on a wooden table. A 12-position Leeds and Northrup type 31-3 rotary selector switch which is mounted on the transite board permits the reading of voltages from several sources (e.g. four thermopiles in calorimeter) on the K-3 potentiometer. The pressure regulators and valves for controlling the pressure and flow rate of the flowing gas

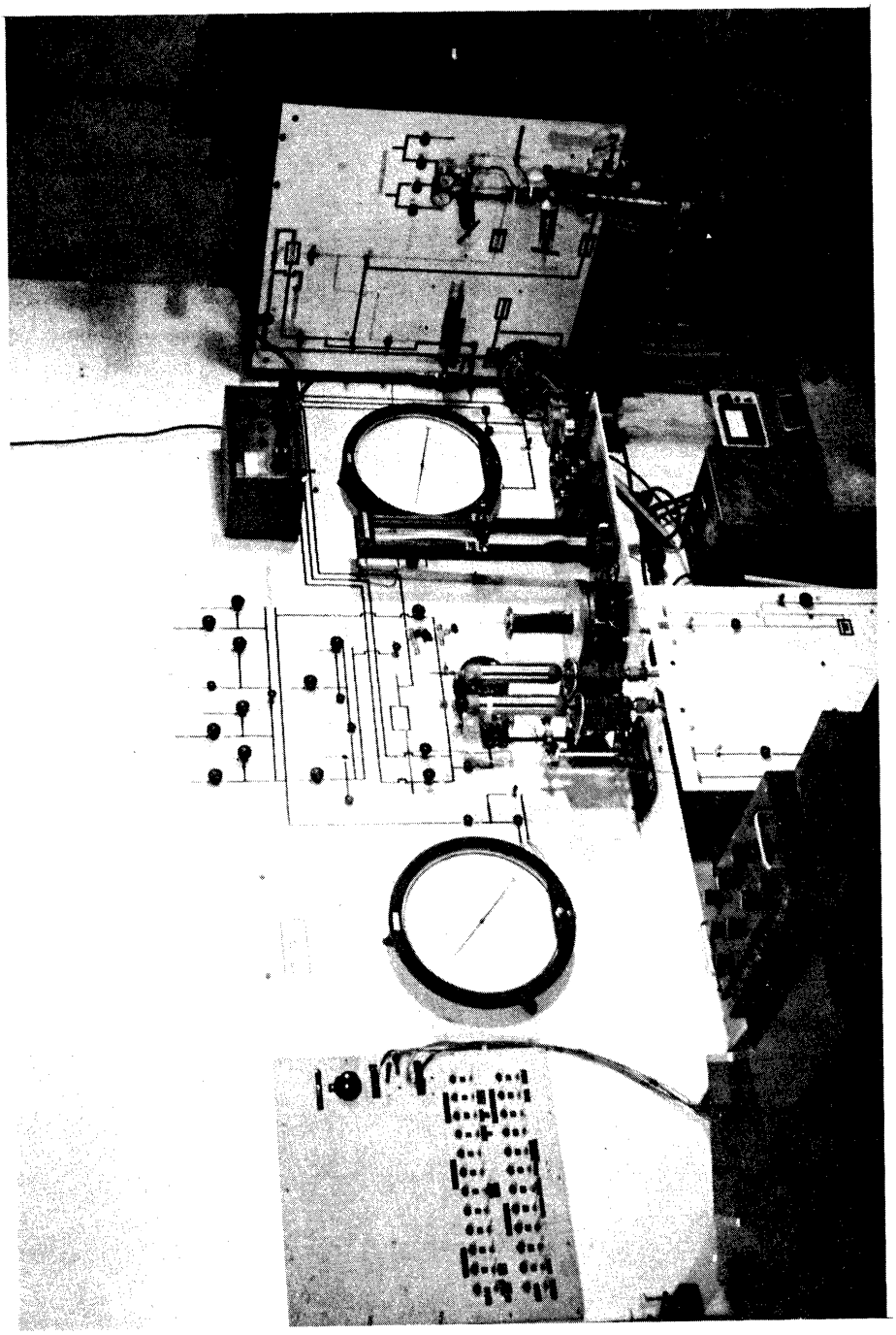

Figure 4. Control Panel.

streams are mounted on an auxiliary aluminum panel board beside the control panel and at right angles to it.

MEASUREMENTS AND CALIBRATIONS

The prime measurements are pressure, temperature, power, flow rate and composition.

Pressure

Both pressure level and pressure drop are measured in the calorimeter.

Pressure Level

The pressure is measured at the calorimeter outlet tap, 10 (Figure 2), with a Mansfield and Green type 13Q dead weight gauge with a smallest measurable pressure increment of 0.1 psi. The nominal pressure reading on the dead weight gauge is corrected by a procedure outlined by Cross[28] (See Appendix D for sample calculation), which accounts for local gravity, air bouyancy on the brass weights and thermal expansion of the piston. Local gravity is 980.314 gals at the Natural Science Building on the Main Campus of the University of Michigan. After being corrected for latitude and elevation[22] of the Automotive Laboratory on North Campus, gravity is taken to be 980.317 gals. Effects due to elastic distortion (less than .01 psi) and surface tension of the oil (0.002 psi) are neglected. Corrections are also made from a calibration certificate traceable to the National Bureau of Standards provided by the manufacturer (See Appendix B, Table XXVIII).

The oil which lubricates the piston-cylinder assembly of the dead weight gauge is separated from the gas in the system by a mercury-filled U-leg. The mercury is visible in two Penberthy X-500 sight glasses

mounted on the end of a U-shaped stainless steel tube. Differences in the mercury levels can be read to 1/16-inch off transparent graduated scales fastened to the sight glasses. When making pressure measurements, the difference in mercury levels in the two arms is always kept at less than 1/16-inch (0.03 psi) by pumping in or draining oil. Metering valves on both the oil and gas side facilitate the gradual increase or decrease of pressure applied to the column of mercury. Traps are provided to prevent the mercury from blowing over into the system.

The measurements on the dead weight gauge are corrected for oil head (0.075 psi) but not for the small difference in mercury levels (less than 0.03 psi) or for the gas head between the calorimeter and the U-leg (less than 0.01 psi). After accounting for uncertainties in the various corrections to the gauge pressure measurement the precision is believed to be ± 0.2 psi and the accuracy ± 0.3 psi.

The gauge pressure readings are converted to absolute pressure readings with atmospheric pressure measurements on an Eberbach catalog No. 5070 Fortin-type mercury barometer with a vernier scale with 0.01 inch smallest division. Pressure readings are corrected for scale and mercury expansion, local gravity and zero error using standard techniques described by Brombacher, Johnson and Cross.[22] The zero error was determined by calibrating the barometer against a standard barometer (see Appendix B, Table XXIX). The accuracy of the measurement after accounting for uncertainties in the corrections and including capillarity error is estimated as ± 0.02 inches Hg. This error contributes negligibly to the absolute pressure value.

Differential Pressure

Pressure drops between pairs of taps 5, 6 and 10 in the calorimeter (Figure 2) are read in a Meriam high pressure manometer with dibutyl

phthalate manometric fluid (specific gravity ~1.04) and measured by a telescope-cathetometer arrangement to ± 1 cm.

Temperature

The temperature of the calorimeter bath is measured with a mercury-in-glass Fisher Scientific thermometer (No. 3C3642) graduated in 0.1°C intervals between -1°C and 51°C. Emergent stem corrections were made as outlined by Swindells.(161) An accompanying National Bureau of Standards calibration certificate (See Table XXX, Appendix B) estimates the inaccuracy of the corrections as less than ± 0.03°C. Based on the 0.1°C graduations, it is estimated that a temperature change of ± 0.025°C within a ± 0.05°C band is detectable on this thermometer.

The temperature of the gas stream entering the port labelled 1 in the sketch of the calorimeter (Figure 2) is assumed to be equal to the bath temperature. Temperature differences are measured between the two inlet streams by a pair of six junction copper-constantan thermopiles. Likewise the temperature difference between the inlet and outlet gases are measured by duplicate six junction copper-constantan thermopiles. One of the latter thermopiles was calibrated by the National Bureau of Standards (See Appendix B, Table XXXI) with an accuracy of ± 0.5 microvolt.

The output from the thermopiles is measured on a K-3 null potentiometer with a No. 9834 D.C. Null Detector both of which are manufactured by the Leeds and Northrup Company. The limit of accuracy on these instruments is ± 0.5 microvolts (Table XXXIV) which corresponds to a temperature difference of ± 0.002°C which is equal to the thermopile calibration accuracy.

Combining the accuracy of the thermopile calibration and potentiometer with the ± 0.002°C calorimeter bath control, the accuracy of the

temperature difference measurement is believed to be ± 0.006°C. The estimated inaccuracy in the measurement of the temperature of the gas at the calorimeter outlet is ± (0.03+0.006) or about ± 0.04°C with differences in temperature being detectable to ± (0.025+0.006) or about ± 0.03°C.

Power

The power to the calorimeter is supplied by a Kepco CK40-0.8M D.C. power supply with output voltage regulation of ± 0.01 percent. The scheme used to supply and measure the power to the calorimeter heater is shown in Figure 5. A pot within the Kepco power supply unit (not shown in Figure 5) is used for coarse adjustment of its power output. Fine adjustments are achieved by varying the setting on the 40-turn helipot, R_h. The degree of resolution on the final adjustments can be changed by altering the resistance of the rheostats, R_f and R_g.

The power input to the calorimeter is

$$\dot{W} = (e_c)(i_c) \tag{70}$$

where e_c is the voltage drop across and i_c is the current flowing through the calorimeter heater.

Voltage Drop across Calorimeter Heater

The potential drop, V_e, is measured across the standard resistor, R_e. The accurate evaluation of the voltage drop across the calorimeter, e_c, requires values for the resistance of the wires connecting the calorimeter heater, R_c, to the standard resistors, R_e and R_s. The connections, C_a and C_b are made close to where the heater leads emerge from the conax gland within the calorimeter, 13 (in Figure 2). The resistance of the lead wires between the calorimeter heater, R_c,

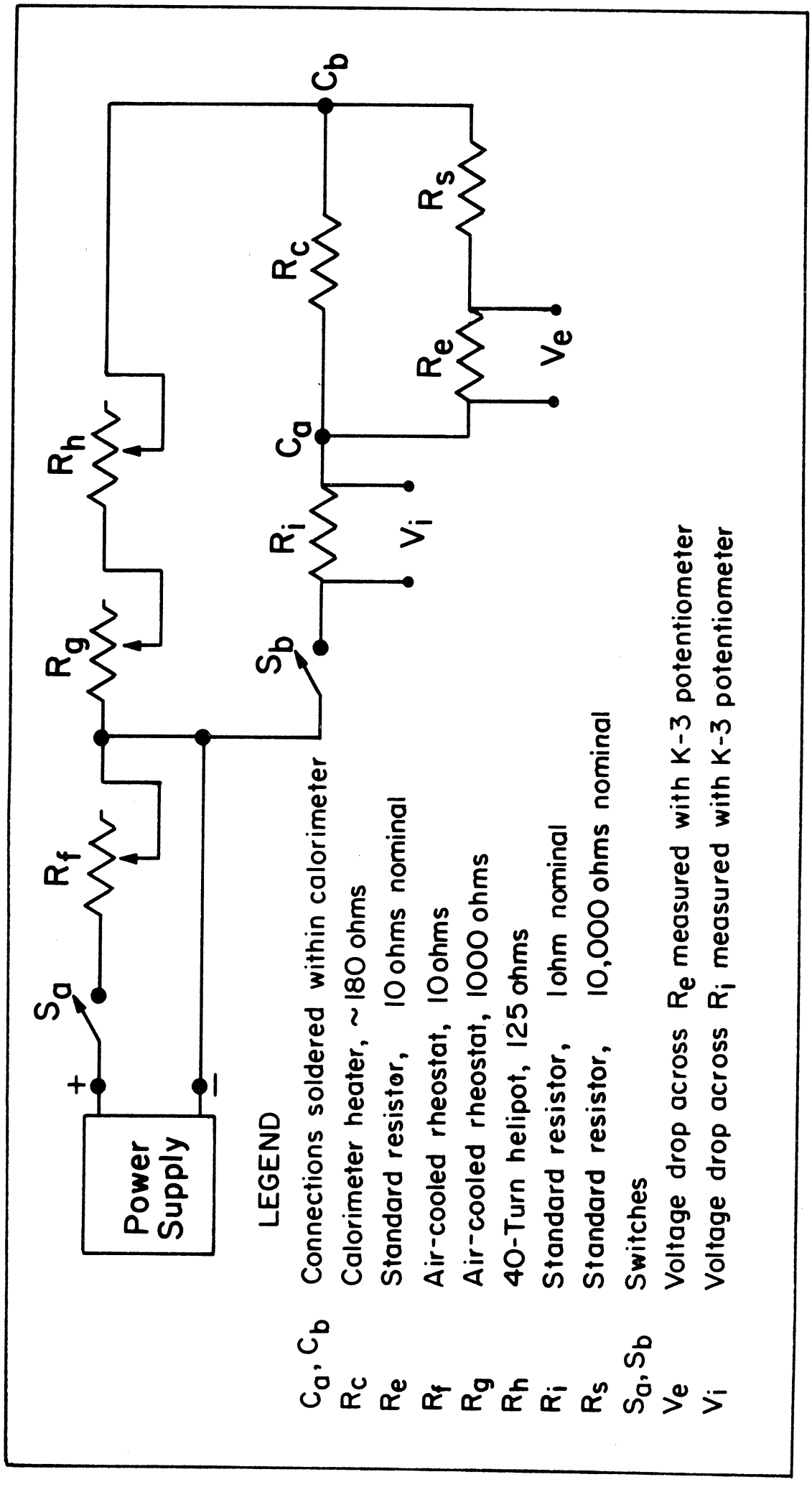

Figure 5. Electrical Power Input System for Calorimeter.

and the connections, C_a and C_b, is negligible (less than 0.01 ohms) compared to the resistance of the heater itself (180 ohms). The wires between the standard resistors and the connections, C_a and C_b are chosen so that they contribute negligibly (about 0.1 ohms) to the overall resistance of that arm (approximately 10,010 ohms).

Neglecting the resistance of the connecting wires, the voltage drop across the combined standard resistors, R_e and R_s, can be calculated from V_e and equated to the voltage drop, e_c,

$$e_c = \frac{(R_s+R_e)}{R_e} V_e \tag{71}$$

Current in Calorimeter Heater

Inspection of the power input system, Figure 5, reveals that the current passing through the one ohm standard resistor, R_i, is divided between the calorimeter heater and the arm with standard resistors, R_e and R_s. The current flowing through the two standard resistors, R_e and R_s, is equal and it is

$$i_{R_e} = \frac{V_e}{R_e} \tag{72}$$

where $i_{R_e} = i_{R_s}$. Subtracting the current, i_{R_e}, in the arm parallel to the calorimeter heater from that flowing through the one ohm standard resistor yields i_c, the current in the calorimeter heater:

$$i_c = \frac{V_i}{R_i} - \frac{V_e}{R_e} \tag{73}$$

The electrical energy input to the calorimeter is calculated by substituting the expression for i_c, Equation (73), and e_c, Equation (71), in the relation for the power input, Equation (70)

$$\dot{W} = \left(\frac{V_i}{R_i} - \frac{V_e}{R_e}\right)\left(\frac{R_s+R_e}{R_e}\right) V_e \quad \text{watts} \tag{74}$$

The two voltages V_e and V_i are measured on the K-3 potentiometer. Its operating characteristics are given in Table XXXIV in Appendix B. A Leeds and Northrup 7309 standard cell used in these measurements is checked at frequent intervals against a similar standard cell calibrated by the National Bureau of Standards (See Appendix B, Table XXXIII).

All the measurements made during this research were at calorimeter power input levels which caused a rise in temperature of the resistors of only 3°C to 4°C. The temperature of each standard resistor is measured by single junction thermocouples inserted in tubes that penetrate the oil which submerges the resistance coils. Both the values of the resistances and the temperature coefficients are listed in Table XXXII, Appendix B.

Flow Rate

Metering of the flow rate is the most critical of all the measurements since it is the factor which limits the accuracy of the entire set of measurements. The high pressure flow meters and the low pressure flow meter are described separately.

High Pressure Flow Meters

The two high pressure flow meters and their workings are discussed under four separate headings:

1. Description
2. Measurements
3. Calibration
4. Correlation

Description:

Each of the high pressure flow meters is made out of 1/8-inch O.D. x 0.040-inch I.D. stainless steel tubing 13 inches long. The pressure

drop is measured across two #80 drill holes 6 inches apart and 3 1/2 inches from the ends of the tubing. Two lengths of 1/8-inch O.D. x 1/16-inch I.D. tubes heliarc welded to the tubing at the location of the #80 drill holes serve as pressure taps. Argon is blown through all the tubing while heliarc welding to prevent the formation of blisters. To maintain a uniform inner surface, after the welding operation, the whole length of the tube is smoothed with medium lapping compound on music wire. A photograph of the flow meter is given in Figure 6.

In the bath, the flow meter is held rigid sandwiched between two brass plates to prevent any change in flow pattern which would cause a change in its flow characteristics. Two Nupro micron in-line filters are attached to the ends of the flow tubing with Swagelok fittings. The filter brackets and flow meter sandwich are bolted to a common base plate. There are micron filters on the pressure taps as well.

Measurements:

The pressure at the inlet pressure tap is measured on a 0-1500 psi temperature-compensated Heise Bourdon tube gauge with 1 psi smallest division. The Heise gauge is calibrated frequently against the dead weight gauge described earlier. The accuracy of the pressure measurement with the Heise gauge is estimated to be $\pm$ 1 psi.

The pressure drop is registered with di butyl phthalate manometric fluid (specific gravity $\sim$1.04) in a Meriam high pressure manometer. Only in the case of the nitrogen-oxygen system, mercury was used as the manometric fluid. A maximum pressure drop of 100 cm is measurable with a telescope-cathetometer arrangement capable of reading differences in heights of $\pm$ 0.01 cm.

The Meriam Instrument Company who supplied the di butyl phthalate also supplied data on its thermal expansion characteristics. The temperature

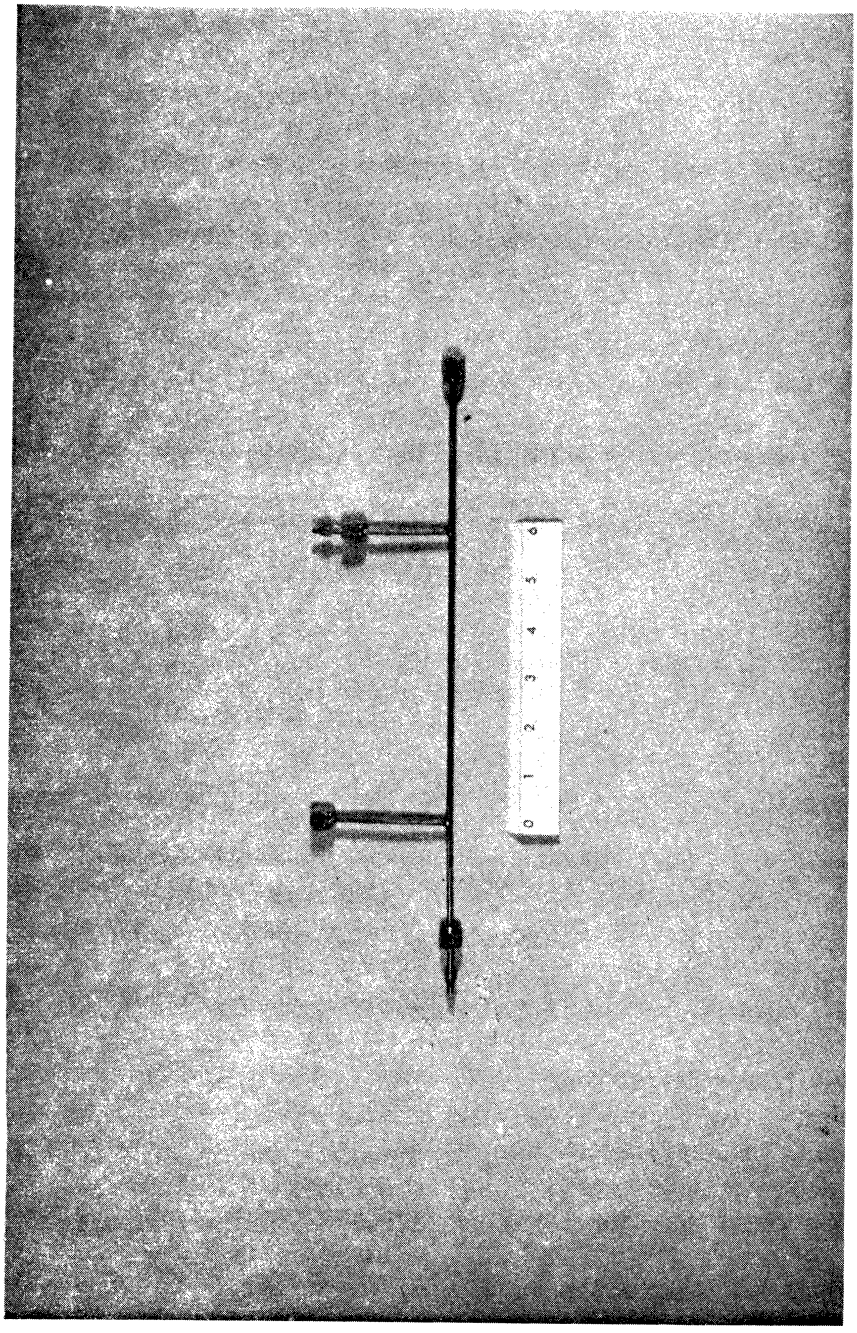

Figure 6. Photograph of High Pressure Flow Meter.

of the fluid is measured by a mercury thermometer taped with insulation onto the outside of the well on the manometers. As both manometers operate at room temperatures, this does not introduce substantial error. The accuracy of the pressure drop is estimated to be ± 0.04 cm.

At the conditions of 1100 psia and 45°C (bath temperature) in the flow meters, the carbon dioxide is in the gaseous state but it is possible for condensation to occur in the pressure tap lines that are at room temperature. Hence the 15 feet of pressure tap lines that lead from the flow meters to the manifold are wrapped with electrical heating tape. To prevent condensation inside the manifold and the high pressure manometer, they are filled with nitrogen under pressure instead of being heated. Occasional flushing with nitrogen is required while setting the flow rates during the initial phases of operating the flow meters but not when steady conditions are approached.

Calibration:

The calibration of the flow meters may be divided into three phases. The first phase consists of developing a means for measuring the flow rate of the gas through the flow meter. The second phase consists of calibrating the flow meter with this device and the third consists of correlating the pressure and pressure drop with the flow rate.

1. Flow Rate Determination: The device chosen is a copper tank (henceforth called calibration tank) whose volume is about six cubic feet. First the instrumentation used on the calibration tank will be described. Then the procedure for determining its volume and finally the manner in which it is utilized for measuring flow rates will be detailed.

The tank is located in a stirred water bath. The temperature of the water bath is measured with a mercury-in-glass thermometer which

has been calibrated against the NBS certified thermometer. Gas temperatures are measured at two vertical locations in the tank with calibrated copper-constantan thermocouples inserted in a 1/4-inch stainless steel tube. The output from the thermocouples is read on the K-3 potentiometer.

When it is used to calibrate the flow meters, the absolute pressure of 20 mm Hg in the initially evacuated tank is measured by a mercury vacuum manometer to ± 0.5 mm Hg. After the tank is filled with gas, the pressure of about 30 inches of water gauge is read to ± 0.05 inches on a 36-inch King manometer filled with di butyl phthalate manometric fluid. During the volume determination of the calibration tank, the vacuum manometer is replaced by a McLeod gauge, and the pressure above atmospheric read on the 36-inch King manometer with mercury as the manometric fluid. The absolute pressure in the tank is determined from the gauge pressure in the tank and atmospheric pressure read on the Eberbach barometer described earlier.

The first step in determining the volume of the calibration tank is to evacuate the tank to about 20 microns Hg. The pressure and temperatures are noted when the temperature of the gas and of the stirred water differ by less than 0.05°C. Two aluminum cylinders containing pure nitrogen are used to charge 320 g of gas into the tank. Both cylinders are weighed before and after releasing nitrogen. Pressures and temperatures are again recorded when the three temperature measurements agree within 0.05°C. The volume of the tank is calculated from the pressures, temperatures, mass of nitrogen and virial coefficient data of Otto.[126] Four such volume measurements (See Table XXIII, Appendix B) yielded an average volume of 0.422 ft^3 with a standard deviation of 0.2 percent.

When the calibration tank is utilized for calibration of the flow meters a procedure is used which is similar to the one described

for determining the volume. The gas in the system is allowed to enter the tank through a two-way solenoid valve, (23 in Figure 3) via a short length of copper tubing. A timer capable of measuring time intervals of 10,000 seconds to 0.1 second is connected to the switch for the solenoid valve. The tank is initially evacuated to about 20 mm Hg and pressures and temperatures noted after thermal equilibration between the gas in the tank and the water in the bath. When steady state conditions are achieved in the flow meters, the switch on the solenoid valve is thrown. This simultaneously starts the timer and allows gas to enter the calibration tank. When the tank is full, the solenoid valve is deactivated which stops the timer as well. When the gas temperature differs from the water temperature by less than 0.05°C, values of the temperatures and pressure are recorded.

2. Calibration Procedure: Each flow meter is calibrated separately. The pressure in the flow meter is adjusted to about 1100 psia by regulators, 3 (Figure 3). The level of pressure in the calorimeter section is varied till there is sonic flow through metering valve, 21, and pressure reducing valve, 18, while maintaining 60 psi at the low pressure flow meter. Critical flow is also maintained across each of the two metering valves that comprise the flow metering valves, 20.

The need for two flow metering valves was dictated by experience. Originally only one flow metering valve was used. Before the solenoid valve switch is thrown there is atmospheric pressure in the tank (20 mm Hg). During calibration the pressures in both the tank and at the valve exit rise from the initial pressure (20mm Hg) to just above atmospheric pressure. With one valve, this change in back pressure caused the flow rate and hence the pressure and pressure drop in the flow meters to change continuously.

To combat this affect, two flow metering valves were used with the pressure in the line between them being maintained at about 30 psig which assisted in sustaining critical flow across both valves. This worked satisfactorily with the nitrogen flow meter. To maintain steady conditions in the carbon dioxide flow meter, however, it was found necessary to continuously adjust the second valve so as to hold constant the pressure level in the low pressure flow meter section. The degree of adjustment required decreased when two vacuum pumps were attached in parallel to the atmospheric exhaust port of the two-way solenoid valve.

When steady state conditions have been achieved in the flow meters, the switch on the solenoid valve is thrown and the flow rate determined as described earlier. During the period of gas collection, readings of pressure level and pressure drop in the flow meters are taken every minute.

The readings on the various instruments are punched on IBM cards and fed to a computer program which calculates values for the flow rate, pressure and pressure drop and values of viscosity and density of the gas at the conditions in the flow meter.

3. Correlation: The results from the computer program are correlated by a modified version of the universal friction factor law:[17]

$$\frac{1}{\sqrt{f}} = 4.07 \log_{10} \mathrm{Re}\sqrt{f} - 0.40 \qquad (75)$$

The modification consists of lumping all the dimensional constants (tube length, diameter, etc.) and the unit conversion factors together into two unknown constants, β_F and δ_F, and expressing the previous equation in terms of the flow rate, pressure, pressure drop, viscosity and density.

The unknown constants in the modified equation are determined from the flow meter calibration results. The derivation of the modified equation is described below:

The friction factor is defined as

$$f = \frac{1}{2}\frac{d}{L} \cdot \frac{\Delta P_F}{\rho_F \bar{u}^2} \tag{76}$$

in terms of the tube diameter, d, the tube length, L, the pressure drop, ΔP_F, density, ρ_F, and mean velocity, $\bar{u}$.

The mean velocity is written in terms of the flow rate, F, and the density, ρ_F, and the cross-sectional area of flow, $\frac{\pi d^2}{4}$, as

$$\bar{u} = \frac{F4}{\rho_F \pi d^2} \tag{77}$$

Substituting for $\bar{u}$ from (77) in the previous equation for friction factor gives

$$f = \frac{1}{2}\frac{d}{L} \cdot \frac{\Delta P_F}{\rho_F} \cdot \rho_F^2 \frac{\pi^2 d^4}{F^2 16} \tag{78}$$

Collecting the constant terms into a single constant, n yields

$$f = n^2 \left(\frac{\rho_F \Delta P_F}{F^2}\right) \quad \text{where} \quad n = \frac{1}{2}\frac{d^5}{L}\frac{\pi^2}{16} \tag{79}$$

The Reynolds number is

$$Re = \rho_F \frac{\bar{u}d}{\eta_F} \tag{80}$$

Substituting for the mean velocity, $\bar{u}$ from Equation (77) into the last equation gives

$$Re = \frac{4F}{\rho_F \pi d^2} \rho_F \frac{d}{\eta_F}$$

$$= \frac{4}{\pi d}\left(\frac{F}{\eta_F}\right) \tag{81}$$

Substituting for Reynolds number, Re , and friction factor, f , from Equations (81) and (79) respectively into the friction factor Equation (75) gives

$$\frac{F}{\sqrt{\rho_F \Delta P_F}} \frac{1}{n} = 4.07 \log_{10} \left[n \left(\frac{\sqrt{\rho_F \Delta P_F}}{F} \right) \frac{4}{\pi d} \left(\frac{F}{\eta_F} \right) \right] - 0.40 \qquad (82)$$

The constants within the $\log_{10}$ term may be combined thus:

$$m^{\frac{1}{2}} = \frac{n4}{\pi d} \qquad (83)$$

and the base 10 logarithm term written in terms of natural logarithms. Making these changes in Equation (82) yields

$$\frac{F}{\sqrt{\rho_F \Delta P_F}} \frac{1}{n} = \frac{4.07}{2.303} \ln \left[m^{\frac{1}{2}} \frac{\sqrt{\rho_F \Delta P_F}}{\eta_F} \right] - 0.40 \qquad (84)$$

This expression is further modified by squaring the term within the square brackets and collecting all the constant terms

$$\frac{F}{\sqrt{\rho_F \Delta P_F}} = \left\{ \frac{4.07}{2.303} \cdot \frac{n}{2} \cdot \right\} \ln \left[\frac{\rho_F \Delta P_F}{\eta_F^2} \right] + \left\{ \frac{4.07}{2.303} \cdot \frac{n}{2} \ln[m] - 0.40 \right\} \qquad (85)$$

This equation expresses a linear relationship between the two measurable variables $\frac{F}{\rho_F \Delta P_F}$ and $\ln \frac{\rho_F \Delta P_F}{\eta_F^2}$. This linear relation may also be written as

$$\frac{F}{\sqrt{\rho_F \Delta P_F}} = \beta_F \ln \left[\frac{\rho_F \Delta P_F}{\eta_F^2} \right] + \delta_F \qquad (86)$$

where β_F and δ_F are the two constant terms in the previous Equation (85). The last equation is the modified friction factor equation used to correlate the results.

Data from the following sources are used to correlate the results of flow meter calibrations:

Carbon dioxide: Density and second virial coefficient data of Michels and Michels[113] and viscosity data of Michels, Botzen and Schurman.[110]

Ethane: Densities from tabulations by Tester,[162] viscosity values given by Eakin, Starling, Dolan and Ellington[39] and second virial coefficients reported by Michels, Van Straaten and Dawson.[116]

Nitrogen: For the calibrations used with the nitrogen-carbon dioxide system, density tabulations by Din,[34] viscosity data of Michels and Gibson[112] and second virial coefficients reported by Otto.[126]

Oxygen: For the flow meter calibrations utilized for the nitrogen-oxygen system, data on compressibility factors and second virial coefficients given by Hilsenrath et al.[59] and data on viscosity reported by Kestin and Leidenfrost[74] on both nitrogen and oxygen.

The computer program for data reduction calculates values for the two variables $\frac{F}{\sqrt{\rho_F \Delta P_F}}$ and $\frac{\rho_F \Delta P_F}{\eta_F^2}$. A regression analysis on all the flow meter calibrations yields the two constants β_F and δ_F.

The results of the flow meter calibrations for all the gases are presented in Appendix B in a series of Tables XXIV through XXVII and Figures 16 through 18. The flow meters for all the gases are calibrated at a nominal pressure of 1100 psia except ethane for which nominal flow metering pressure is 500 psia.

Low Pressure Flow Meter

This is a laminar flow device made by the Meriam Instrument Company. The pressure drop across it is read to ± 0.006 inches by a National Instrument Laboratory 20-inch water manometer. The pressure in the flow meter is read on a King 130-inch manometer to ± 0.05 inches Hg.

The low and high pressure flow meters can be calibrated simultaneously by a procedure described earlier. During calibration of the carbon dioxide flow meter, the second of the two flow metering valves, 20 in Figure 3, is adjusted continuously so as to maintain constant

pressure at the low pressure flow meter as mentioned earlier. However, the response of the water manometer is too slow to give correct values of the pressure drop across it. Therefore, the low pressure flow meter was not calibrated. It was used only to check on steady state conditions during the enthalpy of mixing measurements and during the flow meter calibration.

Gas Composition

The composition of the mixture which exits the calorimeter can be calculated from the flow rates of the two gases entering it. In order to provide an independent check on this calculated composition, samples of nitrogen-carbon dioxide mixtures were collected during enthalpy of mixing measurements and analyzed by a modified gas density technique.

The sample bomb is a 370 cc capacity aerosol can to which is soft soldered a small, light valve. Before collecting the sample, the can is evacuated to about 30 microns Hg with the pressure being read on a thermocouple vacuum gauge. The mixture sample at about 60 psig is tapped just downstream of the pressure reducing valve, 18 in Figure 3. Gas pressure in the can is measured to $\pm$ 0.05 inches Hg on a 130-inch King manometer. During the pressure measurement, the can is held at a fixed temperature by immersion in a constant temperature water bath. The temperature of this bath is set at 25°C with the NBS calibrated thermometer and regulated to 0.1°C with on-off control.

Each can weighs about 160 g and holds approximately 1.8 g of nitrogen at 100 inches Hg gauge. The can is weighed on a Christian Becker balance whose weights have been corrected against a set of NBS calibrated weights.

Can Volume Determination

Before analyzing the mixture sample it is necessary to determine the internal volume of the aerosol can. This procedure is initiated by evacuating the can and filling it to 120 inches Hg gauge pressure with nitrogen. The can is brought to 25°C by immersing it in the bath for about half an hour. The copper line between the manometer and the aerosol can is flushed out with the gas in the can to prevent impurities from diffusing into the nitrogen. As a further precaution, the pressure in the manometer is set slightly below the can pressure, which is now about 100 inches Hg gauge. After the valves connecting the manometer and the can are opened, the pressure on the manometer is noted every minute. Five minutes after the pressure reaches a steady level, atmospheric pressure is noted and the valves on the can and in the pressure manifold are closed. The can is removed from the bath, detached from the copper line, rinsed with acetone, dried and weighed. The can is evacuated to 30 microns Hg and reweighed. To ensure thermal equilibration with the room conditions, the can is placed in the balance room for 30 minutes prior to each weighing. Two successive weighings are made which usually differ by less than 0.4 mg. An identical can with an internal pressure of 15 psia is weighed along with the sample can to check for changes in atmospheric conditions. The change in weight of the identical can (about 0.5 mg) gives the buoyancy correction which should be applied to the sample can.

The volume of the can is calculated from the mass of gas, its pressure, temperature and the virial coefficient of nitrogen.[109] The change in internal volume with pressure of several cans was also determined. The can is placed in a large mouthed jar completely filled with water. The level of water is noted in a graduated 5 cc pipette inserted in the rubber stopper of the jar. The change of the water level in the

pipette with pressure in the can is noted and the change in can volume with pressure calculated as 0.007 cc/psi. Repeated pressurizing also showed that the can does not suffer any permanent expansion at pressures up to 65 psig.

The results of volume determinations on two aerosol cans are given in Table XLVI, Appendix C. The volumes reported have been normalized to 70 psia. Measurement Number 2 on can 30 and can 31 was done with the carbon dioxide used in the enthalpy of mixing measurements. Difficulties were encountered in a number of cans due to leaks (mostly vacuum leaks) in the soft solder and at the valves and fittings. For this reason and because each can volume measurement takes four to six hours, the volume of the remaining cans was determined just once.

Gas Density Measurement

The technique used for gas density analysis is identical with that used for can volume measurements. The can with the sample is immersed in the bath. Gas pressure is adjusted to within ± 3 inches Hg of the pressure of can volume determination and its value is measured on the 130-inch manometer. The second virial coefficients of nitrogen,[109] carbon dioxide[109] and its mixtures[93] used in calculating the compositions are given in Table XLVIII in Appendix C.

A check was performed on the analytical technique before it was used. A mixture of known composition was made up by gravimetric analysis. Two cans were evacuated and weighed. They were filled simultaneously with nitrogen from a pressure regulator on a nitrogen cylinder to a predetermined pressure and both cans weighed. Carbon dioxide was introduced into the two cans so that both cans were at the same final pressure and the cans reweighed. The gases were mixed for 48 hours by

placing the cans under a heat lamp. After making buoyancy corrections, the composition in the cans was calculated with a maximum inaccuracy of 0.08 percent from the mass of nitrogen and carbon dioxide introduced. Because of the filling procedure used, the composition in both cans was almost equal. The gas in the cans was then analyzed by the gas density technique. The results are presented in Table XLVII, Appendix C. The volume of can 14 was determined just once whereas the volume of can 30 was measured three times (Table XLVI). The probable accuracy of the gas density measurements is discussed in Appendix A.

PROCEDURE

There are three phases into which the operation of the facility may be divided:

1. Preparation of the Apparatus
2. Startup
3. Measurements at Steady State

These will be described briefly and followed by a section entitled

4. Data and Data Reduction

Preparation of the Apparatus

Preparations start a day previous and continue to the time that gas flow is commenced. Valves and fittings are tested for leaks under pressure. The baths are controlled at the required temperature. The heating tapes, calorimeter power input circuit and all the thermocouples and thermopiles are checked for open circuits and for shorts to ground. The aerosol cans are evacuated continuously for several hours till the time that they are used to collect samples.

Prior to starting gas flows, the Heise gauges are calibrated against the dead weight gauge. Readings are then taken of the level of fluids in all the manometers at zero pressure drop and the calorimeter bath temperature is checked with the NBS calibrated thermometer. Micrometer vernier handles on all the valves which control flows are set at predetermined values.

Startup

The valves on the nitrogen cylinders are opened and the pressure in the flow meter set at about 1100 psia with regulators, 3 (Figure 3). The flow rate is fixed approximately with metering valve, 21, on the nitrogen line. The calorimeter pressure is set at about the value of the partial pressure of nitrogen in the desired mixture.

The flow of carbon dioxide is initiated similarly. Further simultaneous adjustments are required in both the metering valves, 21, and the pressure reducing valve, 18, to achieve the desired pressure and composition in the calorimeter. The latter can be set to within ± 1-2 mole percent of a preselected value. The pressure level at the calorimeter outlet is set at ± 3 psi of the preselected nominal pressure. Next, the power supply is switched on and adjusted to a precalculated setting.

Measurements at Steady State

Steady conditions are achieved one to two hours after commencing gas flows. Several minor checks and adjustments (e.g. valve settings, bath temperatures, etc.) are made towards the end of this period. Invariance of the flow rate of the two gases as determined by the pressure and pressure drop in the high pressure flow meters (5 and 6) can be checked by similar readings on the low pressure mixture flow meter, 19.

The final adjustments consist of varying the power input to the calorimeter. A desk calculator is used to calculate settings on the power supply and the helipot. The calorimeter itself can attain steady state within 15 to 20 minutes after a change in the input power setting if the initial values of the inlet-outlet gas temperatures differ by no more than 0.5°C.

Data is taken under steady state conditions when the temperature difference between the inlet and outlet gases to the calorimeter is less than about 0.05°C. Readings on all instruments are taken every two minutes over a four- to six-minute period. For the nitrogen-carbon dioxide system, the gas mixture is sampled for analysis. Readings of power input and pressure drop in the calorimeter are taken at the conclusion of the other measurements.

When the gas flow is stopped, several measurements are repeated: The Heise gauges are recalibrated against the dead weight gauge; the temperature of the calorimeter bath is rechecked with the NBS calibrated thermometer; and zero level readings are made on all the manometers.

Data and Data Reduction

After the measurements described are complete, all instrument readings are transferred to punched cards. The reduction of the data is then carried out on the IBM 360/67 computer. Several computer programs are used which perform the calculations outlined in the chapter entitled "Thermodynamic Relations."

Measurements of the enthalpy of mixing were performed on three systems which along with the conditions of experimental measurements are listed in Table VIII. The purity of the gases used is listed in Table IX. The data obtained on these three systems is listed in Tables XXXV, XXXVI

and XXXVII in Appendix C. The results after interpretation of calorimetric measurements are given in the series of Tables XXXVIII to XLII in Appendix C. A sample calculation is detailed in Appendix D.

TABLE VIII

SYSTEMS STUDIED AND CONDITIONS OF EXPERIMENTAL INVESTIGATION OF THIS RESEARCH

System	Nominal Experimental Conditions			Number of Experimental Measurements at Each (P_n,T_n)
	Temperature T_n °C	°F	Pressure P_n psia	
N_2 - CO_2	40	104	500	15
	40	104	950	4
	31	87.8	500	4
	31	87.8	950	4
N_2 - C_2H_6	32.38	90.28	401	4
N_2 - O_2	25	77	1001	5

TABLE IX

IMPURITY ANALYSES OF GASES USED IN THIS RESEARCH

Gas	Constituent		Mole Percent
Nitrogen	Nitrogen		99.98
	Oxygen		0.02
		Total	100.00
Carbon dioxide	Carbon dioxide		99.86
	Oxygen		0.09
	Nitrogen		0.05
		Total	100.00
Ethane	Ethane		99.22
	Propene		0.41
	Propane		0.32
	Ethene		0.05
		Total	100.00
Oxygen	Oxygen		99.80
	Argon		0.11
	Nitrogen		0.09
		Total	100.00

RESULTS

This chapter presents details of the interpretation of calorimetric data on the nitrogen-carbon dioxide, nitrogen-ethane and nitrogen-oxygen systems. The results are given in both tubular and graphical form, and are compared with available data on the systems as well as with values calculated from an equation of state. The precision and accuracy of the measurements are considered.

Interpretation of Calorimetric Data

Direct calorimetric measurements give the pressures and temperatures of the two gases entering and the mixture exiting the calorimeter. These are then combined with the power input and flow rate measurement through a set of primary and secondary corrections to yield values of the excess enthalpy. This data interpretation is discussed separately for each system.

Nitrogen-Carbon dioxide System

Two examples are given in Table X of the primary and secondary corrections involved in data reduction for the nitrogen-carbon dioxide system. The numerical values of the corrections (in Btu/lb) are given in Tables XXXVIII and XXXIX in Appendix C.

Primary Corrections:

Heat capacity data are required to make the correction for non-isothermal operation of the calorimeter (See Equation (40)). The tabulations by Din[34] for nitrogen and Vukalovich and Altunin[172] for carbon dioxide are employed for this purpose. This correction averages about 0.5 percent with a maximum of 1.2 percent.

TABLE X

EXAMPLES OF CORRECTIONS INVOLVED IN DATA REDUCTION FOR THE NITROGEN-CARBON DIOXIDE SYSTEM

Nominal Experimental Conditions	T_n °C	40	31
	P_n psia	500	950
Actual Experimental Conditions	T_o °C	40.033	31.010
(Conditions at outlet of calorimeter)	P_o psia	498.5	952.6
Mole fraction Nitrogen		0.518	0.725
Electrical heat input to calorimeter, $(\dot{W}/F)$, Btu/mol		82.3	259.0
		Percent Corrections	
Primary corrections: Applied to $(\dot{W}/F)$			
(a) For pressure drop across calorimeter		-0.22	-0.03
(b) For non-isothermal operation		-0.07	-0.10
(c) For kinetic energy difference of incoming and outgoing gases		-0.8×10^{-4}	0.5×10^{-5}
(d) For impurities in carbon dioxide		0.37	0.48
	Total	0.08	0.35
$\underline{H}_o^E$ at experimental conditions (T_o, P_o), Btu/mol		82.3	259.9
Secondary Corrections: Applied to $\underline{H}_o^E$ at (T_o, P_o)			
(e) For normalizing to P_n		0.34	-0.86
(f) For normalizing to T_n		0.03	0.04
	Total	0.37	-0.82
$\underline{H}_n^E$ normalized to (T_n, P_n), Btu/mol		82.6	257.8

Joule-Thompson coefficients of carbon dioxide and nitrogen reported by Roebuck et al.[139,140] are combined with the above mentioned heat capacities values according to Equation (11) to obtain the isothermal Joule-Thompson coefficients used in making the pressure drop correction (See Equation (39)). The values of the thermodynamic properties are given in Table XLIII in Appendix C. This correction decreases with increased density of the gases flowing through the calorimeter as can be seen in the two examples in Table X. The pressure drop correction ranges between 0.03 and 0.22 percent with an average value of 0.1 percent.

Kinetic energy corrections (See Equation (33)) are calculated using the density tabulations on nitrogen by Din,[34] tabulations on carbon dioxide by Newitt et al.[124] and mixture compressibility factor data of Haney and Bliss.[56] As illustrated in Table X this correction is always very small with a maximum contribution to the power/flow ratio of 10^{-4} percent.

Impurities are accounted for by a technique, detailed in the chapter entitled "Thermodynamic Relations," which utilizes the experimental measurements of this very research. The impurity analysis of nitrogen and carbon dioxide is done with a mass spectrometer and the results are given in Table IX. Corrections calculated, assuming the nitrogen to be pure and the carbon dioxide to contain 0.14 mole percent nitrogen, range between 0.3 and 0.8 percent with an average contribution of 0.5 percent.

Numerical values of the four corrections which comprise the primary corrections are listed in Table XXXVIII, Appendix C. Their sum is listed as a percent correction to the power per unit flow, $(\dot{W}/F)$, in Table XI along with the resultant excess enthalpy at calorimeter outlet conditions after primary corrections.

TABLE XI

EXCESS ENTHALPY DATA ON NITROGEN-CARBON DIOXIDE SYSTEM

Mol Fr Nitrogen	Power Flow (W/F) Btu/mol	Primary Corrections Percent	$\underline{H}^E_o$ at (T_o, P_o) Btu/mol	Secondary Corrections Percent	$\underline{H}^E_n$ at (T_n, P_n) Btu/mol	$\frac{(\underline{H}^E_n - \underline{H}^E_{smoothed}) \times 100}{\underline{H}^E_n}$ Percent
Nominal Experimental Conditions: T_n = 40°C P_n = 500 psia						
0.288	76.8	0.35	77.0	-0.58	76.6	0.47
0.339	80.4	0.12	80.5	0.02	80.5	-0.49
0.437	84.5	-0.48	84.1	0.11	84.2	-0.33
0.481	83.7	-0.00	83.7	-0.02	83.7	-0.38
0.482	83.9	-0.55	83.4	0.46	83.8	-0.16
0.484	84.0	0.34	84.3	-0.31	84.0	0.11
0.491	83.9	0.00	83.9	-0.14	83.8	0.08
0.503	82.9	0.16	83.0	0.16	83.1	-0.21
0.508	84.3	-0.89	83.5	0.04	83.5	0.47
0.509	83.2	-0.29	83.0	0.59	83.5	0.45
0.510	83.3	-0.60	82.8	0.79	83.4	0.44

TABLE XI (CONTINUED)

Mol Fr Nitrogen	Power / Flow ($\dot{W}/F$) Btu/mol	Primary Corrections Percent	H^E_o at (T_o,P_o) Btu/mol	Secondary Corrections Percent	H^E_n at (T_n,P_n) Btu/mol	$(H^E_n - H^E_{smoothed})\times 100 / H^E_n$ Percent
0.518	82.3	0.08	82.3	0.37	82.6	-0.09
0.525	82.4	0.10	82.5	0.20	82.6	0.31
0.575	79.9	-0.29	79.7	0.01	79.7	0.56
0.670	69.5	-0.15	69.4	0.01	69.4	-0.35
	Nominal Experimental Conditions:		T_n = 40°C		P_n = 950 psia	
0.220	269.1	-0.32	268.2	0.45	269.4	0.76
0.358	302.9	0.92	305.7	-0.86	303.0	-0.64
0.516	281.8	-0.33	280.9	1.36	284.7	0.94
0.732	187.7	0.59	188.8	1.02	190.7	-0.14
	Nominal Experimental Conditions:		T_n = 31°C		P_n = 500 psia	
0.228	77.6	-0.15	77.4	0.04	77.5	-0.02
0.363	95.7	0.16	95.8	-0.78	95.1	0.35

TABLE XI (CONTINUED)

Mol Fr Nitrogen	Power Flow ($\dot{W}/F$) Btu/mol	Primary Corrections Percent	H_o^E at (T_o,P_o) Btu/mol	Secondary Corrections Percent	H_n^E at (T_n,P_n) Btu/mol	$\frac{(H_n^E - H_{n\,smoothed}^E) \times 100}{H_n^E}$ Percent
0.485	97.1	0.33	97.4	-0.96	96.5	-0.29
0.729	70.2	0.38	70.5	0.55	70.9	0.02
	Nominal Experimental Conditions: T_n = 31°C P_n = 950 psia					
0.239	419.1	-0.01	419.0	1.63	425.9	1.17
0.310	440.1	0.54	442.4	0.20	443.3	-0.76
0.489	409.5	0.18	410.2	0.70	413.1	0.93
0.725	259.0	0.35	259.9	-0.82	257.8	-0.06

Secondary Corrections and Tabulated Results:

Secondary corrections compensate for operational variations in calorimeter outlet pressure level of ± 3 psi and outlet temperature level of ± 0.05°C. There are no experimental data available on the excess heat capacity and the excess isothermal Joule-Thompson coefficient of nitrogen-carbon dioxide mixtures. Hence, these properties are calculated using the original Benedict-Webb-Rubin equation[12] of state with Bloomer and Rao's[19] constants for nitrogen and Cullen and Kobe's[29] constants for carbon dioxide (See Table XLV, Appendix C) and with the mixing rules suggested by Benedict et al.[13] for their mixtures. Values of φ^E calculated in this manner at 40°C agree within ten percent at 500 psia and 30 percent at 950 psia with values obtained by differentiating Lee and Mather's data.[90]

The average contribution of the correction for pressure level at 500 psia which is about 0.2 percent at 40°C and 0.5 percent at 31°C increases to about 0.7 percent at 950 psia at both temperatures. This increase is due to the rise in the value of the excess properties caused by the increased proximity of the critical point of carbon dioxide. For example at 31°C and 0.49 mole fraction nitrogen, the value of φ^E is 0.32 Btu/(mol psi) at 500 psia and 1.5 Btu/(mol psi) at 950 psia. However, the percent correction does not reflect the five-fold rise in the value of φ^E because the magnitude of the excess enthalpy also increases with pressure. The contribution for normalizing temperature levels averages 0.03 percent at 500 psia and 0.2 percent at 950 psia at both temperatures. The percent contribution due to the application of secondary corrections to the excess enthalpy at calorimeter outlet conditions and the resultant normalized excess enthalpies, $\underline{H}_n^E$, are listed in Table XI. The numerical values of the corrections are given in Table XXXIX, Appendix C.

Values of the excess enthalpies are smoothed with respect to composition by a least squares analysis of the data after primary and secondary corrections have been applied. The equation used is one which has been given in the chapter entitled "Thermodynamic Relations":

$$\frac{\underline{H}_n^E}{x_N(1-x_N)} = a_n + b_n(x_N-0.5) + c_n(x_N-0.5)^2 \qquad (69)$$

Coefficients for this equation are listed in Table XII along with the average and standard deviations. The percent deviation of every individual experimental point from this curve is listed in the last column of Table XI.

Graphical Results:

The results of the excess enthalpy measurements are plotted in the Figures 7 through 9 for the data at 40°C and in Figures 10 through 12 for the data at 31°C. The open and solid circles in these figures are experimental values of the normalized excess enthalpy, $\underline{H}_n^E$.

In Figures 7 and 10, the excess enthalpy is plotted as a function of composition. The solid lines in these figures are obtained from

TABLE XII

REGRESSION COEFFICIENTS FOR SMOOTHING NITROGEN-CARBON DIOXIDE EXCESS ENTHALPIES VERSUS COMPOSITION

Nominal Experimental Conditions		Regression Coefficients			Percent Arithmetic Average Absolute Deviation from Experimental Points	σ Percent
T	P	a_n	b_n	c_n		
40	500	333.909	-140.093	181.668	0.32	0.40
40	950	1147.29	-1082.50	1457.65	0.57	1.29
31	500	384.931	-155.828	185.099	0.19	0.45
31	950	1617.85	-2023.96	2623.85	0.70	1.72

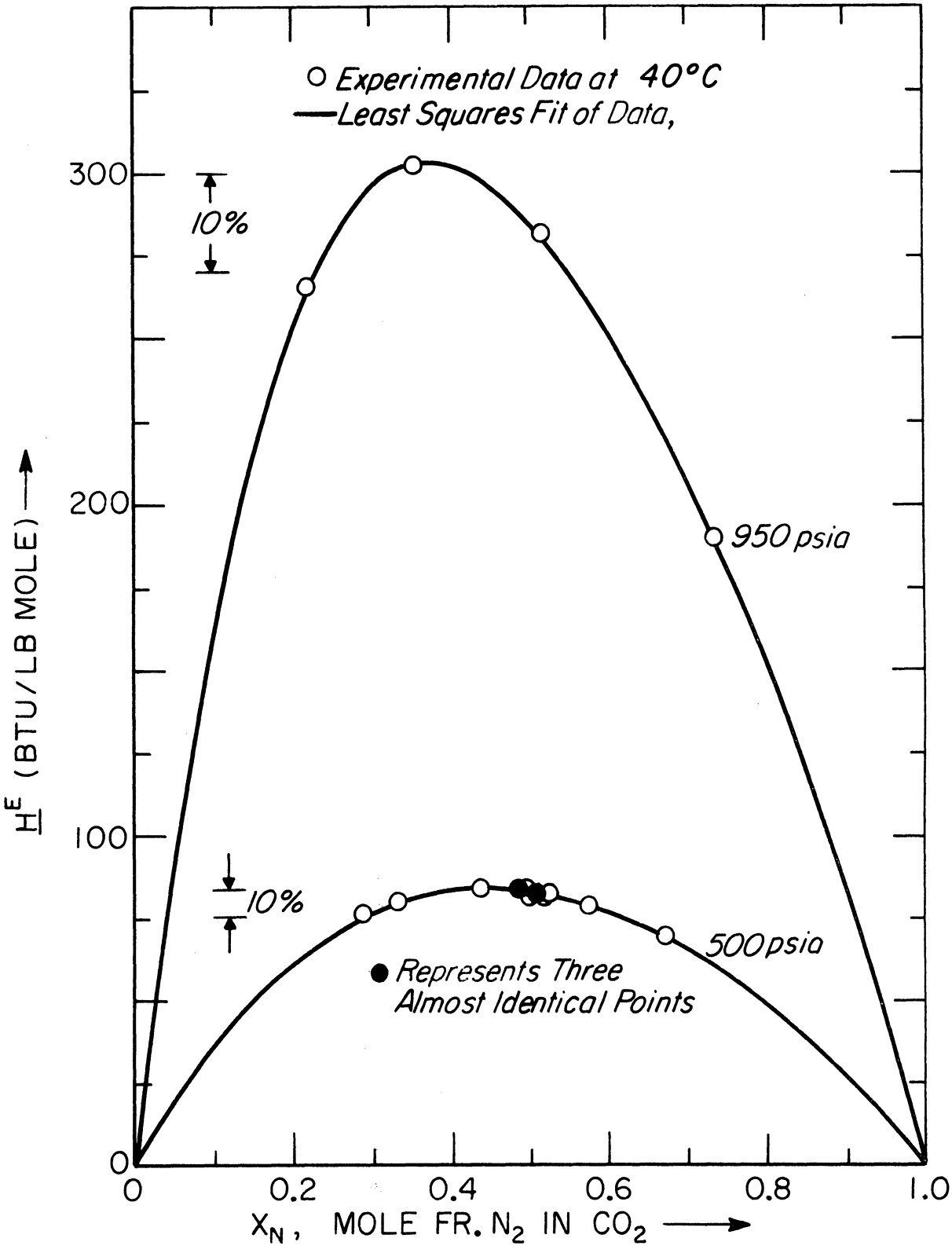

Figure 7. Excess Enthalpy Data on Nitrogen-Carbon Dioxide System at 40°C.

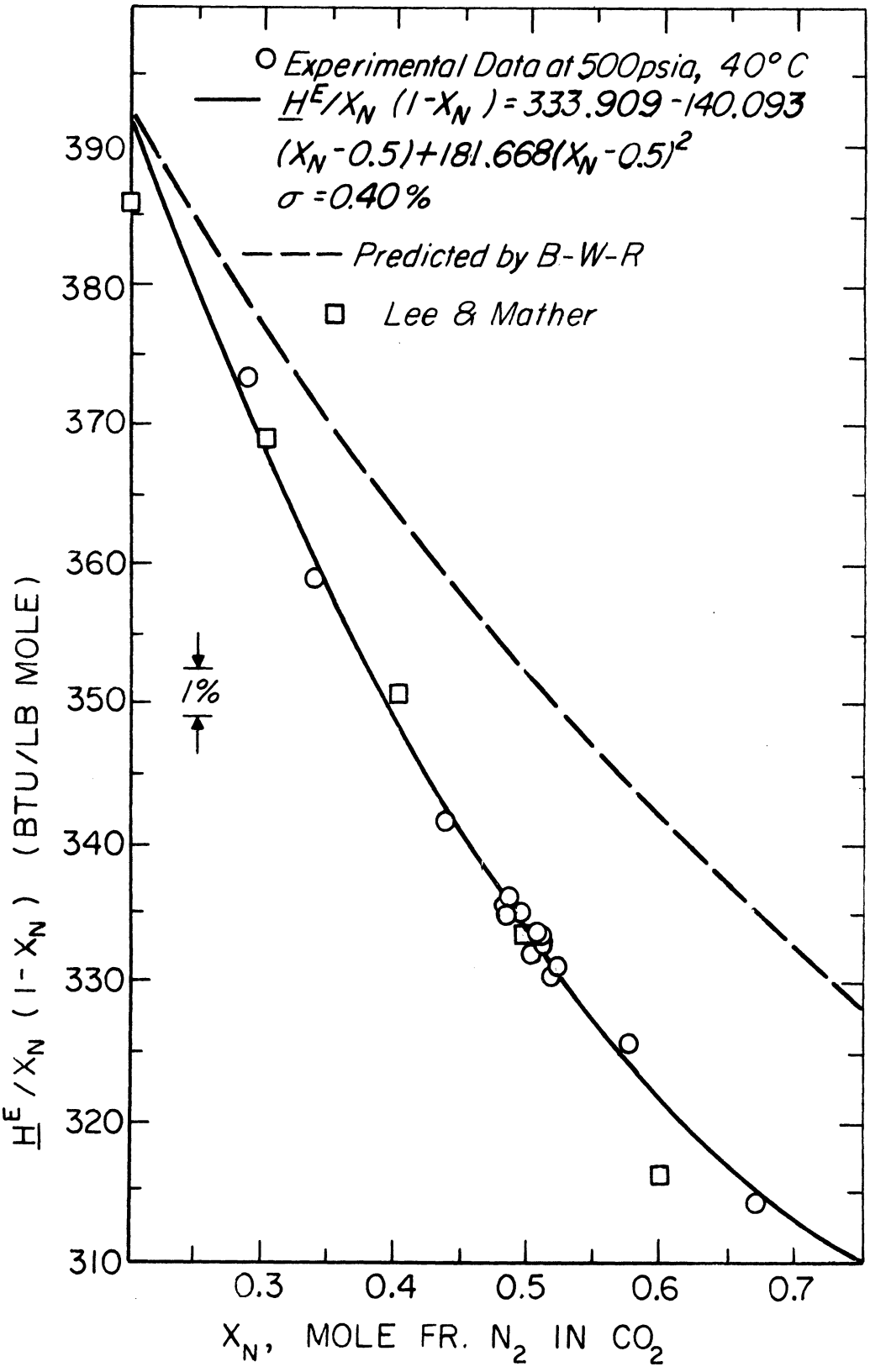

Figure 8. Excess Enthalpy Data on Nitrogen-Carbon Dioxide System at 40°C and 500 psia, and Comparisons with Data of Lee and Mather and with B-W-R Equation of State Predictions.

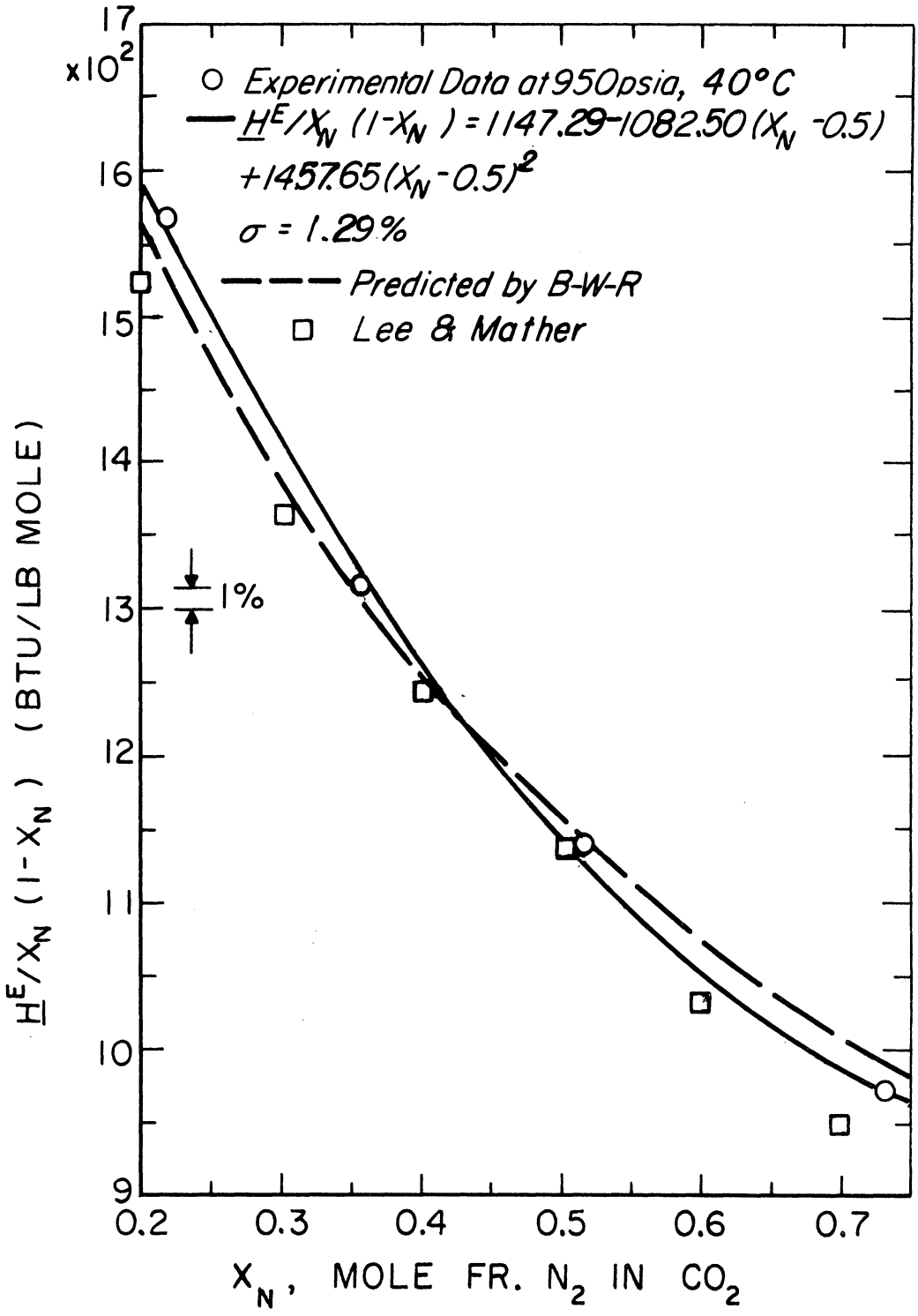

Figure 9. Excess Enthalpy Data on Nitrogen-Carbon Dioxide System at 40°C and 950 psia, and Comparisons with Data of Lee and Mather and with B-W-R Equation of State Predictions.

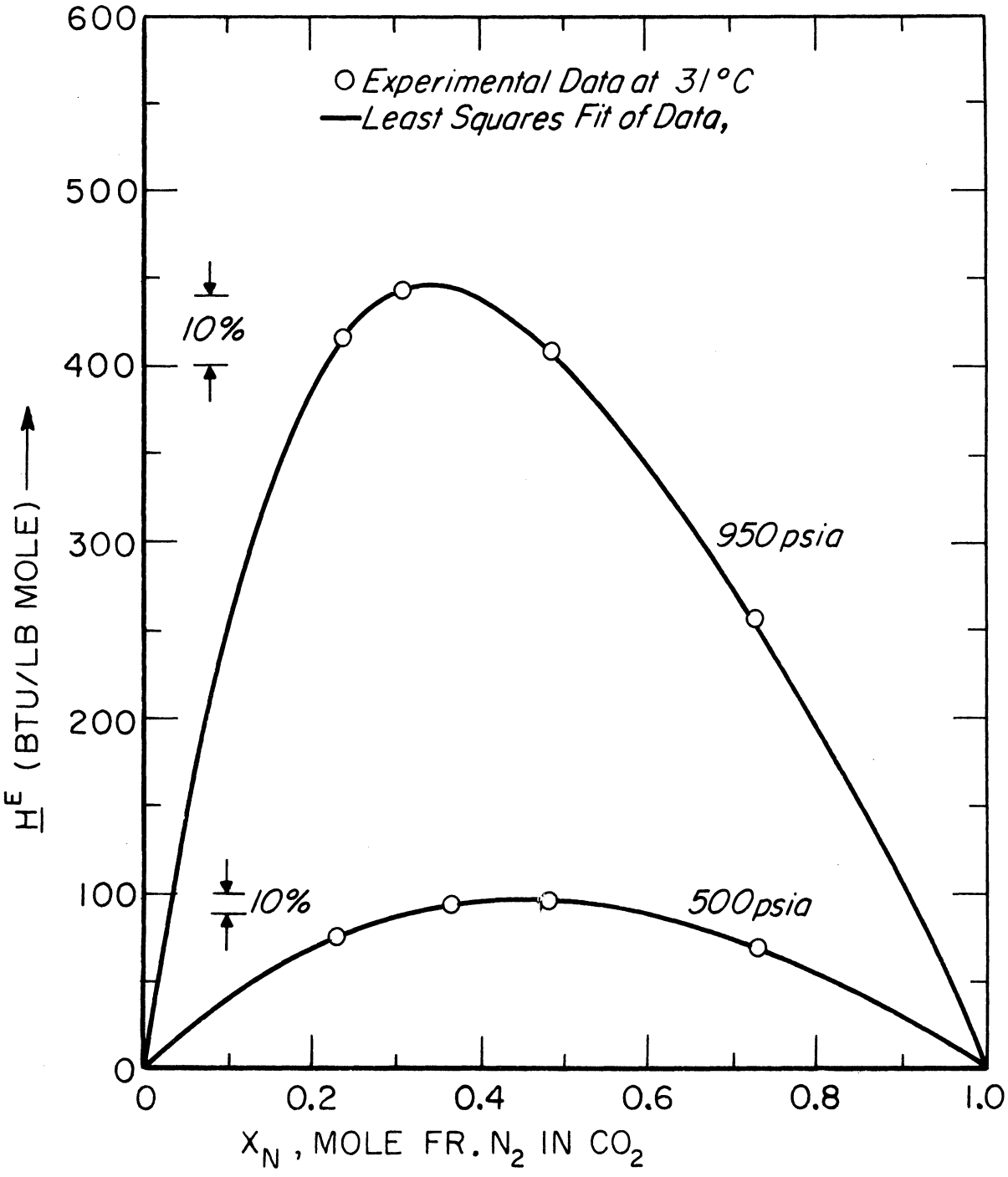

Figure 10. Excess Enthalpy Data on Nitrogen-Carbon Dioxide System at 31°C.

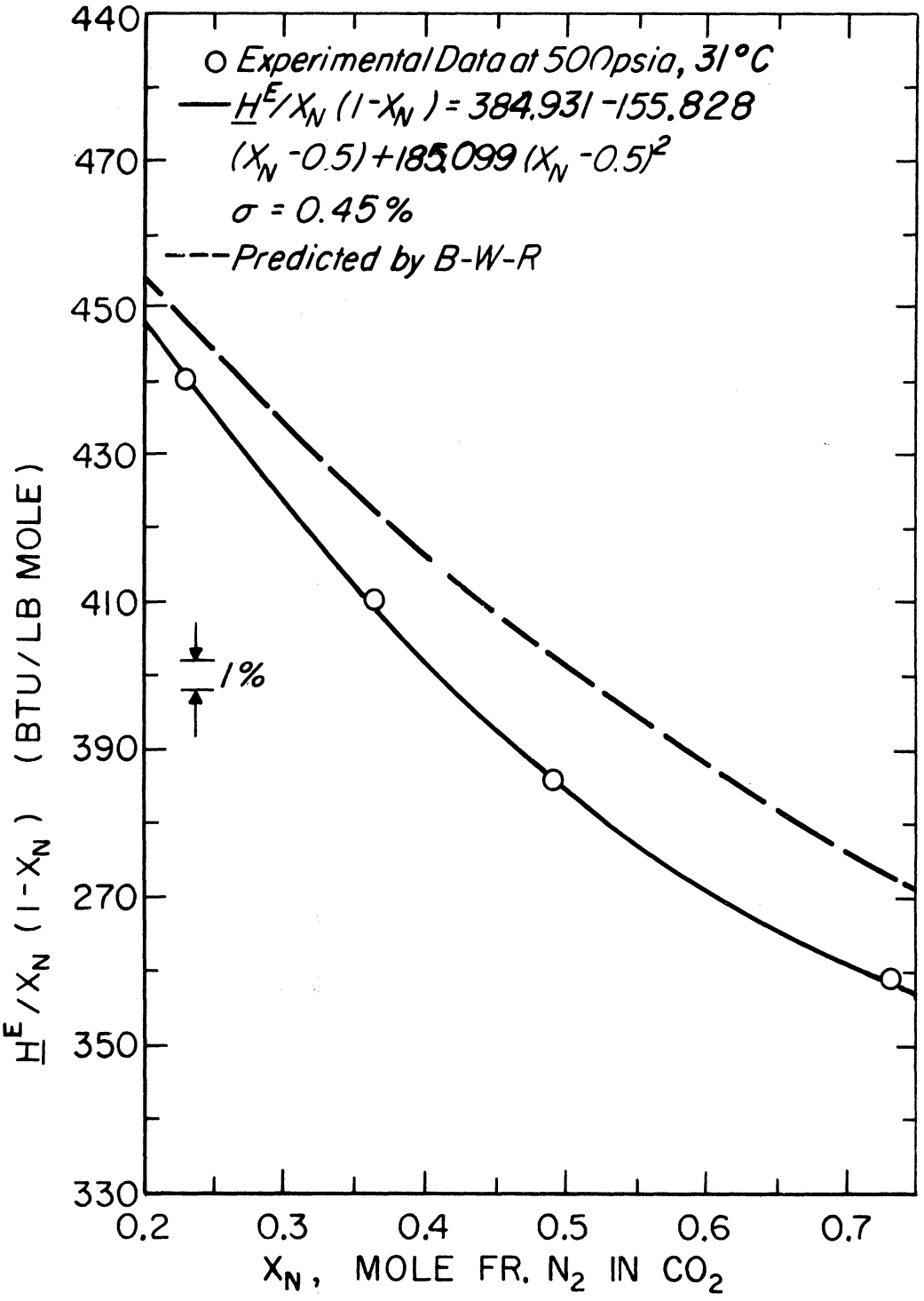

Figure 11. Excess Enthalpy Data on Nitrogen-Carbon Dioxide System at 31°C and 500 psia, and Comparisons with B-W-R Equation of State Predictions.

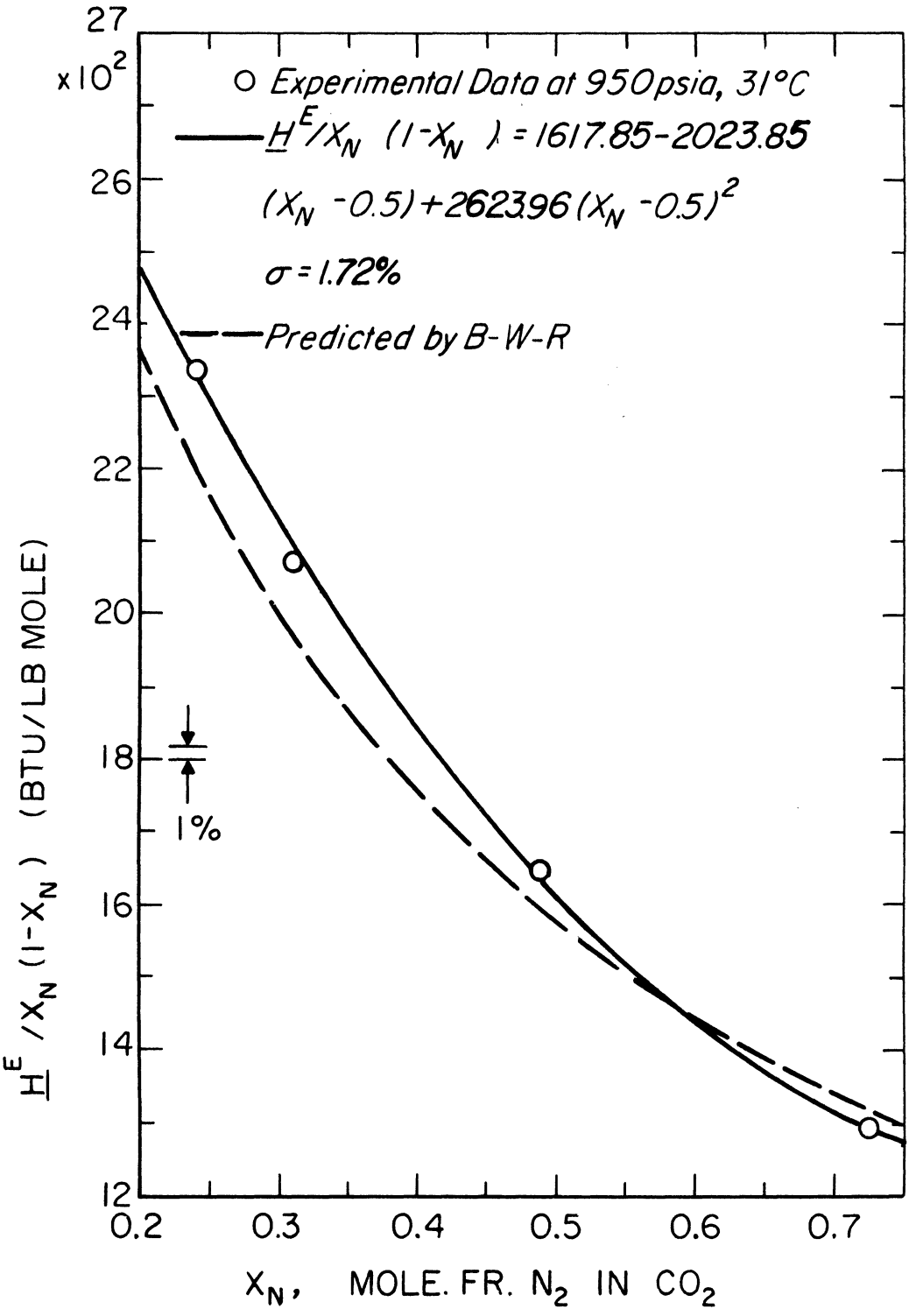

Figure 12. Excess Enthalpy Data on Nitrogen-Carbon Dioxide System at 31°C and 950 psia, and Comparisons with B-W-R Equation of State Predictions.

the equation

$$\underline{H}^E_n = x_N(1-x_N)(a_n + b_n(x_N-0.5) + c_n(x_N-0.5)^2) \qquad (87)$$

with the constants listed in Table XII.

In the same two figures, the effect of the relative vicinity of the critical point of carbon dioxide (T_c = 31°C and P_c = 1071 psia) may be seen by examining the location and value of the maxima in the curves which represent the composition-smoothed results. Within experimental accuracy, the excess enthalpies at 500 psia (P_r = 0.47 of carbon dioxide) at both 40°C(T_r = 1.15) and 31°C(T_r = 1.0) reach a maximum value at the same mole fraction value of 0.443. The corresponding value of the peak at this composition increases from 84.5 Btu/mol to 97.3 Btu/mol with the decrease in temperature. The deviation from the symmetrical parabola increases with increasing pressure and decreasing temperature. For the data at the higher pressure of 950 psia (P_r = 0.89) the location at which this peak occurs shifts from 0.370 mole fraction at 40°C to 0.340 at 31°C. The value of the peak rises from 306.0 to 450.8 Btu/mol--a sharper increase than at 500 psia for the same temperature change.

The results are presented in different but related plots in Figures 8, 9, 11 and 12. The abscissae in these plots are the same as in the previously discussed ones but the ordinates are $\left[\frac{\underline{H}^E}{x_N(1-x_N)}\right]$. The curves in these figures are obtained from Equation (69) with the constants from Table XII.

In plots of $\left[\frac{\underline{H}^E}{x_N(1-x_N)}\right]$ against x_N, the intercepts at $x_N = 0$ and $x_N = 1$ are the slopes of the curves of $\underline{H}^E$ versus x_N at the same mole fractions. The values of the intercepts cannot be determined from the plots in Figures 8, 9, 11 and 12 because the curves are

not drawn to those limits of composition. However, the intercepts may be evaluated from Equation (69) by substituting these mole fraction values:

$$\frac{\underline{H}^E}{x_N(1-x_N)} = a_n - \frac{b_n}{2} + \frac{c_n}{4} \qquad (88)$$

at $x_N = 0$, and

$$\frac{\underline{H}^E}{x_N(1-x_N)} = a_n + \frac{b_n}{2} + \frac{c_n}{4} \qquad (89)$$

at $x_N = 1$.

The effect of the critical point of carbon dioxide may be seen in these figures as well. The regression line through the data points is skewed most for the conditions closest to the critical point of carbon dioxide.

Nitrogen-Ethane System

The methods used for the reduction of the data on the nitrogen-ethane system are identical with the ones outlined for the nitrogen-carbon dioxide system with the exception of the technique for correcting for impurities.

Primary Corrections:

The sources of data used for nitrogen are the same ones referred to earlier in the discussion of the nitrogen-carbon dioxide system.

In the absence of experimental data at elevated pressures, ethane heat capacities used in correcting for non-isothermal operation are obtained from the Benedict-Webb-Rubin equation of state[12] with zero pressure heat capacity tabulations of Rossini et al.[141] The B-W-R constants used for the impure ethane are obtained using the mixing rules of Benedict et al.[14] on the constants listed in Table XLV in Appendix C. Adiabatic Joule-Thompson coefficients of Sage, Webster and Lacey[143] for

ethane are combined with the heat capacity values according to Equation (11) to obtain isothermal Joule-Thompson coefficients for making the pressure drop correction. The pressure drop correction varies between 0.11 to 0.13 percent and the temperature difference correction ranges from 0.43 to 0.58 percent.

Tabulations of density by Tester[162] on ethane and by Sage and Lacey[142] on nitrogen-ethane mixtures are employed for the kinetic energy difference correction. This correction never exceeds 10^{-4} percent.

The enthalpy change on mixing the impure nitrogen and ethane streams at calorimeter outlet conditions, ΔH_o (obtained by applying corrections for pressure drop, temperature difference and kinetic energy difference to the power/flow ratio), is listed in the fourth column of Table XIII under the heading "Multicomponent System." Henceforth this enthalpy change will be referred to as the excess enthalpy of the multicomponent system signifying that no corrections have been made for the ethene, propene and propane in the ethane used in this research (which amount to about 0.8 mole percent--See Table IX). The enthalpy change on mixing pure nitrogen and pure ethane, termed the "Binary System," is obtained by applying impurity corrections to the excess enthalpies at calorimeter outlet conditions for the multicomponent system.

The method employed in making impurity corrections has been described in the chapter entitled "Thermodynamic Relations." The equation for the impurity correction derived there is

$$\Delta I_{corr} = \frac{F_I[\Delta H_o]}{F_{AB}} + \frac{F_B}{F_{AB}}[\underline{H}_{BM,o}-\underline{H}_{B,o}] + [\underline{H}_{AB,o}-\underline{H}_{ABM,o}]$$

$$+ \frac{F_I}{F_{AB}}[\underline{H}_{BM,o}-\underline{H}_{ABM,o}] \qquad (60)$$

which assumes that the nitrogen is pure and corrections are made for the impurities in ethane only. In this equation, the flow rates and the enthalpy difference, ΔH_o , are obtained experimentally but a prediction method is required to estimate the enthalpies of the various streams. The enthalpy departures, $\underline{H} - \underline{H}^o$, may also be used in place of the enthalpies (as explained in the chapter "Thermodynamic Relations") and these are obtained from the Benedict-Webb-Rubin equation of state[12] with the constants[14] listed in Table XLV and with the mixing rules suggested by Benedict et al.[13]

The last term is the one that contributes the most (about 60 percent) to the impurity correction, ΔI_{corr} . The magnitude of this term increases with the increase in the fraction of impurities in ethane and with an increase in the difference between the enthalpy of the impure ethane, $\underline{H}_{BM,o}$, and the enthalpy of the impure nitrogen-ethane mixture, $\underline{H}_{ABM,o}$. In this case the substantial fraction of the impurities and the proximity of the ethane to its two-phase region causes the impurity correction to range from 0.9 to 1.6 percent. This is reflected in the increased contribution of the primary corrections for the "Binary System" over those for the "Multicomponent System" given in column three of Table XIII. The excess enthalpies after primary corrections for the nitrogen-ethane mixtures are listed in the fourth column of the same table.

The interpreted results with and without impurity corrections are presented for three reasons. First, because the interpreted results on the binary system are less accurate than those on the multicomponent system because of the estimated 30 percent uncertainty in the impurity correction introduced by the enthalpy prediction method (the accuracy of the results is discussed in Appendix A and summarized later in this chapter).

TABLE XIII

EXCESS ENTHALPY DATA ON NITROGEN-ETHANE SYSTEM

Mol Fr Nitrogen	Power Flow ($\dot{W}/F$) Btu/mol	Primary Corrections Percent	$\underline{H}^E_o$ at (T_o,P_o) Btu/mol	Secondary Corrections Percent	$\underline{H}^E_n$ at (T_n,P_n) Btu/mol	$\frac{(\underline{H}^E_n - \underline{H}^E_{smoothed})x100}{\underline{H}^E_n}$ Percent
Multicomponent System, Nominal Experimental Conditions: T_n = 32.38°C, P_n = 401 psia						
0.767	90.4	-0.69	89.8	-0.02	89.8	0.03
0.576	133.7	-0.57	133.0	0.17	133.2	-0.10
0.423	146.4	-0.61	145.5	-0.05	145.4	0.11
0.276	131.8	-0.56	131.0	-0.29	130.7	-0.04
Binary System, Nominal Experimental Conditions: T_n = 32.38°C, P_n = 401 psia						
0.769	90.4	-2.33	88.2	-0.02	88.2	0.03
0.578	133.7	-1.93	131.0	0.17	131.2	-0.11
0.425	146.4	-1.73	143.5	-0.05	143.5	0.12
0.277	131.8	-1.47	129.5	-0.28	129.2	-0.04

Second, this procedure demonstrates that corrections can be made for impurities in the feed stream on which enthalpy of mixing data is not available. Finally, using cheaper, less pure gas, results of diminished accuracy may be obtained with considerably lower operating costs.

Secondary Corrections and Tabulated Results:

For both the binary and the multicomponent systems, the values for the excess heat capacities and the excess Joule-Thompson coefficients are obtained from the B-W-R equation[12,13] with the constants listed in Table XLV. The uncertainty in these values are estimated to be ± 30 percent. The variation in the calorimeter outlet pressure is ± 0.5 psi and outlet temperature is ± 0.006°C as may be seen in Table XXXVI, Appendix C. This variation is much smaller than for the data on the nitrogen-carbon dioxide system. Hence, the maximum correction for pressure level is 0.28 percent and the correction for temperature level never exceeds 0.02 percent. The secondary corrections along with the normalized excess enthalpies, $\underline{H}_n^E$, are listed in Table XIII. The latter values are smoothed with respect to composition by fitting the data to Equation (69). The regression coefficients as well as the average and standard deviation are listed in Table XIV. The deviation of each experimental point from the regression curve is listed in the last column of Table XIII.

Graphical Results:

The results are presented graphically in Figures 13 and 14 in plots similar to those employed for the nitrogen-carbon dioxide data. In both figures the excess enthalpies of the binary system as well as the multicomponent system are shown. The circles represent the data, after primary and secondary corrections, on the multicomponent system and the squares represent similarly treated data on the binary system. The curves

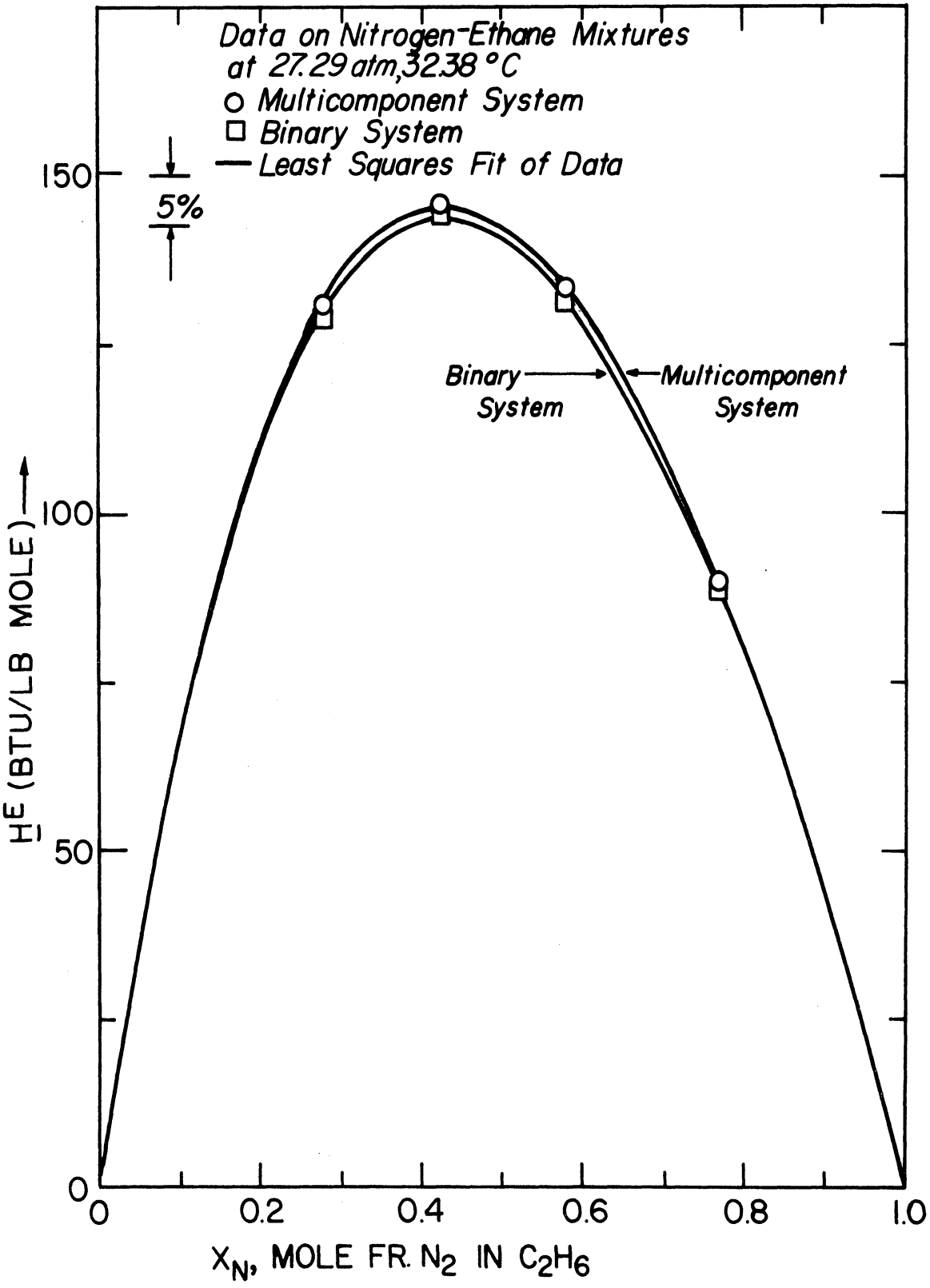

Figure 13. Excess Enthalpy Data on Nitrogen-Ethane System.

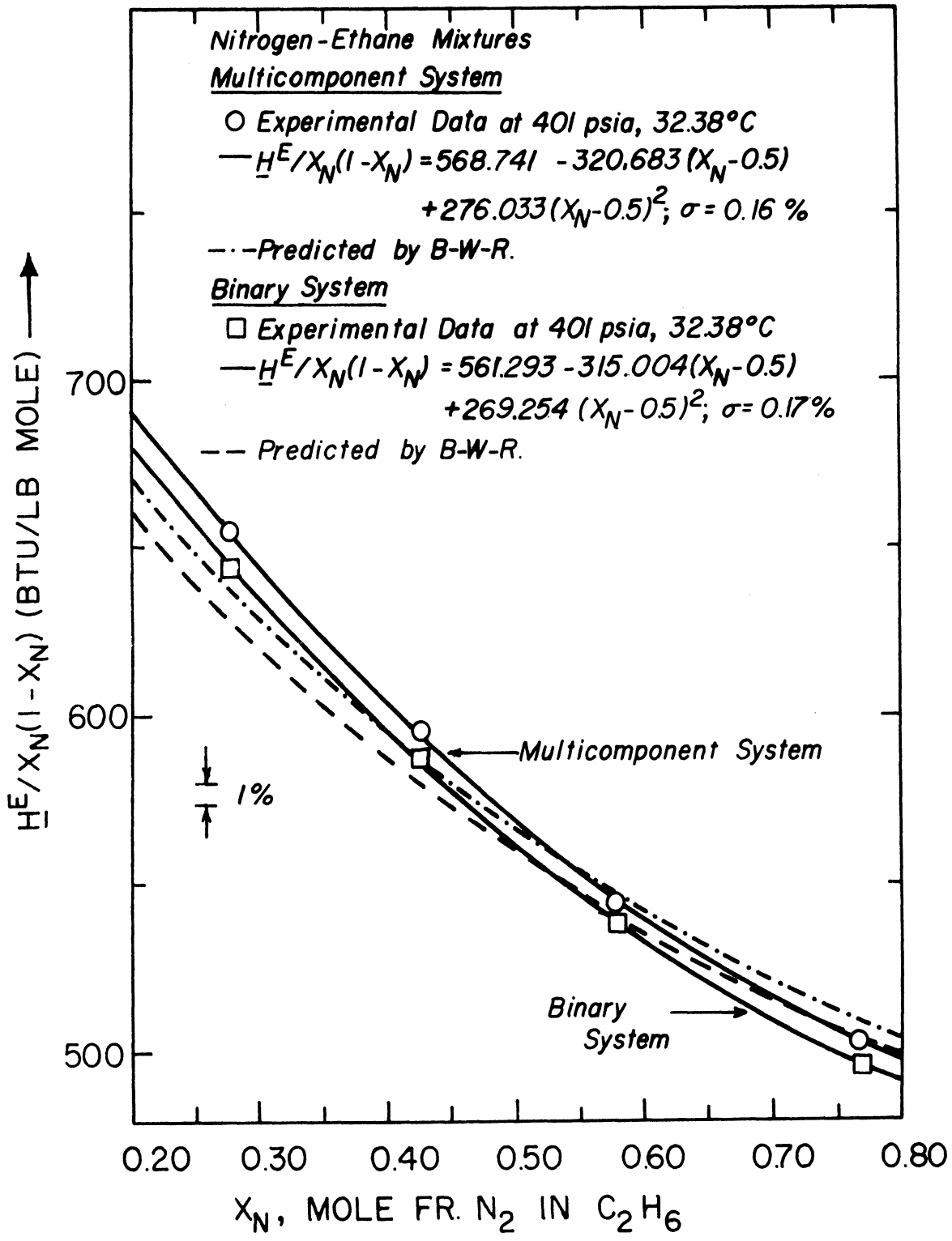

Figure 14. Excess Enthalpy Data on Nitrogen-Ethane System and Comparisons with B-W-R Equation of State Predictions.

(solid lines) in Figures 13 and 14 are calculated using Equations (87) and (69) respectively with the constants listed in Table XIV. Based on the critical point for ethane of 708 psia and 32.3°C, this data is at a reduced pressure of 0.57 and at a reduced temperature of unity.

TABLE XIV

REGRESSION COEFFICIENTS FOR SMOOTHING NITROGEN-ETHANE EXCESS ENTHALPIES VERSUS COMPOSITION

System	Regression Coefficients			Percent Arithmetic Average Absolute Deviation from Experimental Points	σ Percent
	a_n	b_n	c_n		
Binary	568.741	-320.683	276.033	0.07	0.16
Multicomponent	561.293	-315.004	269.254	0.07	0.17

Nitrogen-Oxygen System

This is the first system on which enthalpy of mixing measurements were made in this research. There is a greater uncertainty in the accuracy of these measurements than on those on the nitrogen-carbon dioxide and nitrogen ethane systems because the measured excess enthalpies of nitrogen-oxygen mixtures are at least two orders of magnitude smaller than the excess enthalpies of the other two systems. However, the results are included because measurements revealed that unlike the other systems heat is evolved when the two gases are mixed, with a resultant increase in temperature of the exiting gas mixture over the temperature of the inlet gases to the calorimeter. Five measurements were made at the same value of composition, calorimeter outlet pressure and bath temperature of which two were made with and three were made without power input to the calorimeter. The calometric data are detailed in Table XXXVII in Appendix C.

Other differences exist between the measurements on this and the other systems. Improper positioning of a heater resulted in a temperature difference of about 0.01°C between the two inlet gases. Further, the pressure at the calorimeter outlet pressure tap was measured with a Heise bourdon tube gauge and not with the dead weight gauge.

Calculation of the excess enthalpy requires values for the heat capacity and the isothermal Joule-Thompson coefficient of both nitrogen and oxygen. The heat capacities for both nitrogen and oxygen at 26°C are obtained by combining the data of Workman[183] on the ratio of heat capacity under pressure to the heat capacity at one atmosphere, with the tabulated heat capacities at one atmosphere of Din[34] for nitrogen and Weber[180] for oxygen. The variation of heat capacity values with temperature calculated from Din's[34] and Weber's[180] tabulations of heat capacity are employed to correct the heat capacities to 25°C.

The isothermal Joule-Thompson coefficient for nitrogen is obtained by combining Roebuck's[140] Joule-Thompson coefficient value with the he t capacity for nitrogen. For oxygen, the isothermal Joule-Thompson coefficient is determined from Equation (41), from tabulated values of the volume and the differentials $(\partial P/\partial \rho)_T$ and $(\partial P/\partial T)_\rho$ calculated by Weber[180] from his own accurate PVT measurements. The values for the thermodynamic properties determined in this way are listed in Table XLIII in Appendix C. The accuracies of the C_P and φ values are believed to be three percent and five percent respectively. Details of the reduction of the nitrogen-oxygen data are given in Table XLII and the results are summarized in Table XV. The mean value of the excess enthalpy based on the five measurements is -1.6 Btu/mole.

The accuracy of the experimental measurements is limited by the small temperature rise of 0.12°C across the calorimeter. Based on an uncertainty of 0.008°C, the accuracy of the temperature difference measurement is estimated to be seven percent. As discussed in Appendix A, the accuracy of the excess enthalpy data on the nitrogen-oxygen system is believed to be 10 percent.

As described, two enthalpy of mixing measurements were made with power being supplied to the calorimeter. The heat capacities of the mixture calculated from the data on these runs are listed in the last column of Table XV. They are based on an average calorimeter outlet temperature of 25.116° ± 0.003°C and are assessed to be accurate to 23 and 77 percent for the low and high power input runs respectively (See Appendix A).

TABLE XV

EXCESS ENTHALPY DATA ON NITROGEN-OXYGEN SYSTEM

Mole Fraction Nitrogen	Power / Flow ($\dot{W}/F$) Btu/lb	Temperature Rise °C	H_o^E Btu/lb	Measured Heat Capacity of Mixture Btu/lb °F
Nominal Experimental Conditions: 25°C and 1001 psia				
0.522	0.0	0.117	-0.0548	
0.522	0.0	0.119	-0.0554	
0.522	0.0070	0.128	-0.0529	0.318
0.522	0.0214	0.159	-0.0532	0.277
0.522	0.0	0.113	-0.0530	
Mean H_o^E = -0.054 Btu/lb or -1.6 Btu/mol				
σ = 2.2%				

Linear interpolation with respect to composition between the heat capacities of nitrogen and oxygen in Table XLIII yields 0.262 Btu/lb°F. The discrepancy of 21 percent and 5.7 percent between this and the measured value of heat capacity is within the estimated experimental accuracy of the heat capacity measurement.

Discussion of Results

Part of the data that have been obtained on the nitrogen-carbon dioxide system are used to check on the performance of the calorimeter. The probable maximum inaccuracy of the results is summarized based on the error analysis of Appendix A. Comparisons are made with a prediction method and with the experimental results of other investigators.

Check on the Assumption of Adiabaticity

In the mathematical development which utilizes the first law of thermodynamics in the chapter entitled "Thermodynamic Relations," it is assumed that the measurements are made under adiabatic conditions. Mathematically this is expressed by Equation (31) as

$$\dot{Q} = 0 \qquad (31)$$

implying that there is zero heat transfer between the calorimeter and its surroundings.

The check on this assumption of adiabaticity is based on a principle suggested by Montgomery and DeVries. They show that for measurements in a flow calorimeter, if the heat capacity, or as in this case the excess enthalpy, is independent of flow rate then the heat leak is negligible.

Ten measurements were made as a function of flow rate at 40°C and 500 psia on the nitrogen-carbon dioxide system between 0.481 and 0.525

mole fraction nitrogen. The results are listed in Table XI and may be seen as the cluster of points at 0.50 mole fraction in Figures 7 and 8. After normalization to 0.50 mole fraction nitrogen, the excess enthalpy values are plotted as a function of reciprocal flow rate in Figure 15.

The mean value of the ten points in Figure 15 is 83.48 Btu/mol and the standard deviation is 0.31 percent. The same data were fitted by a regression analysis to a linear equation:

$$\underline{H}^E = 83.74 - \frac{0.0215}{F} \frac{\text{Btu}}{\text{mol}} \qquad (90)$$

with a standard deviation of 0.31 percent--which represents no improvement over the standard deviation of the ten points from the mean value. The effect of heat leak should vanish at infinite flow rate: at $1/F = 0$ the intercept is 83.74 Btu/mol. The intercept differs from the mean value by 0.31 percent and this percent difference is the same as the experimental precision. Hence it seems reasonable to draw a horizontal line as shown in Figure 15 and assume that the heat leak, $\dot{Q}$, is smaller then experimental uncertainty of these measurements.

It is possible to obtain the minimum operating flow rate for a flow facility from this kind of flow rate dependency study. This minimum flow rate is chosen so that the heat leak does not affect the accuracy of the results and, simultaneously, the cost of operating the facility is minimized. For the present experiments, this flow rate independence study was only partially completed. The lowest flow rate that could be achieved on this facility was limited not by the heat leak but by a practical difficulty encountered with the equipment. At low flow rates, the response time of the system to changes in conditions decreased disproportionately with the decrease in flow rate. Consequently the economic benefit of operating at low flow rates was cancelled by the longer

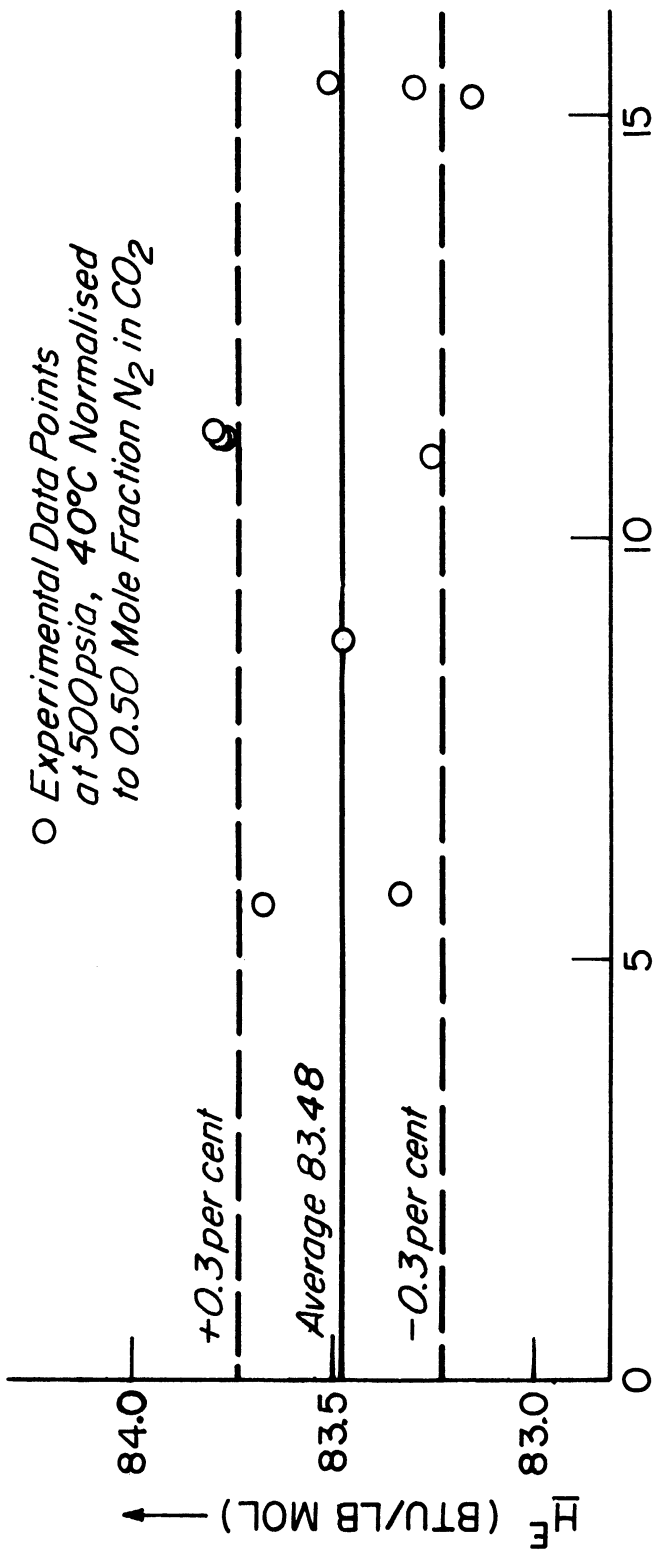

Figure 15. Excess Enthalpy Measurements on Nitrogen-Carbon Dioxide System as a Function of Reciprocal Flow Rate.

operating times required to attain steady state conditions. Hence, the measurements of the excess enthalpy of nitrogen-carbon dioxide mixtures and nitrogen-ethane mixtures were performed at flow rates of about 0.1 lb/minute (1/F = 10). For the nitrogen-oxygen system, the mixture flow rate was about 0.3 lb/minute.

Accuracy of the Results

There are two factors which affect the accuracy of the experimental measurements. They are: 1. Inaccuracies in the instruments and the experimental techniques, and 2. Errors introduced by data interpretation.

The four prime experimental measurements are pressure, temperature, electrical power input and flow rate. The techniques for measuring pressures, temperatures and electrical power are well established and their application to flow calorimetry have been discussed here and by previous investigators.[45,71,101] The estimated accuracies of the pressure and temperature measurement have been described in the chapter entitled "Apparatus and Experiments" and are listed in Table XVI. The accuracy of the power and flow measurements are discussed in Appendix A. The estimated accuracy of the composition and power per unit flow depend on the latter two measurements and are given in Table XVI.

The measurement of flow rate poses the greatest uncertainty. Hence a gas density analytical technique was used to check on the compositions calculated from the flow meter calibrations for the nitrogen-carbon dioxide system. The results of the comparison are given in Table XLIX in Appendix C. The accuracy of the composition calculated from a knowledge of the flow rates is believed to be 0.002 to 0.003 mole fraction whereas the limiting accuracy is estimated to be 0.000 mole fraction for the gas

TABLE XVI

ESTIMATED LIMIT OF ACCURACY OF THE EXPERIMENTAL MEASUREMENTS

System	Uncertainty In					
	Pressure psia	Temperature °C	Composition mol fr N_2	Power / Flow Percent	Primary Corrections Percent	Secondary Corrections Percent
Nitrogen-Carbon dioxide	0.3	0.04	0.002-0.003	0.7	0.1-0.3	0.1-1.1
Nitrogen-Ethane (Multicomponent)	0.3	0.04	0.003	0.8-1.1	0.2	0.3-0.4
Nitrogen-Ethane (Binary)	0.3	0.04	0.003	0.8-1.1	0.6-0.7	0.3-0.4
Nitrogen-Oxygen	1	0.04	0.007	1.5	10	

density technique. The estimation of the accuracy of both methods for composition measurements are discussed in detail in Appendix A. There is good agreement between the two tabulated sets of compositions in Table XLIX within the combined accuracy of the two sets of measurements.

There are two sources from which errors may stem while applying primary and secondary corrections during data interpretation. One is the inaccuracies in the experimental measurements of pressure, pressure drop, temperature and temperature difference in the calorimeter. The other is the inaccuracies in the thermodynamic properties used in making corrections. These have been estimated (neglecting the effect of the uncertainty in composition) and the resultant range of errors due to primary and secondary corrections given in Table XXI and XXII in Appendix A and are summarized in Table XVI.

The accuracy of the enthalpy of mixing data on the nitrogen-oxygen system is believed to be ten percent. For the other two systems, if the errors in the primary and secondary corrections are added to the errors in the power/flow ratio (See Table XVI) then the range of accuracies of the excess enthalpies at outlet conditions, $\underline{H}_o^E$, and the normalized excess enthalpies, $\underline{H}_n^E$, are

1. For the nitrogen-carbon dioxide system: 0.8 to 1.0 percent for $\underline{H}_o^E$ and 0.9 to 2.1 percent for $\underline{H}_n^E$
2. For the nitrogen-ethane system: 1.0 to 1.3 percent for $\underline{H}_o^E$ and 1.3 to 1.7 percent for $\underline{H}_n^E$ of the multicomponent system, and 1.4 to 1.8 percent for $\underline{H}_o^E$ and 1.7 to 2.2 percent for $\underline{H}_n^E$ of the binary system.

There are two other factors which affect the accuracy of the results. The first one is the uncertainty introduced by heat leak to the surroundings from the calorimeter. An upper bound has been placed on

this quantity by the flow rate independence check described in the previous section. The other factor is inhomogenities in the gas mixture at the calorimeter outlet due to inadequate mixing in the calorimeter. The reversal of flow and especially the sparging of the gas mixture from one baffle to the other along with additional time for equilibration in the helical tube leading to the calorimeter outlet is designed to eliminate composition gradients in the outlet mixture. The flow rate independence study furnishes some proof since the residence time varies from two to six seconds over the range of flow rates illustrated in Figure 15. It is felt that in the future an independent test should be made for further confirmation. It is suggested that a coiled length of tubing be used to extend the flow path of the gas before it leaves the vacuum chamber. If the gas temperature is the same at the end of this coil as the gas temperature at the outlet measuring station then the mixture exiting the mixing chamber is homogeneous.

Ultimately, however, there is only one method by which the accuracy of these measurements may be checked and that is to compare this data with the data obtained independently in another laboratory. It would be preferable if a different method is used--for example the closed-system technique used in measuring excess enthalpies of liquids.

Comparisons

There is no data available in the literature on the nitrogen-ethane system. The data on the nitrogen-oxygen system may be compared with the measurements of Knoester *et al.*[82] on a similar system. They report the excess enthalpy of a mixture containing 52 mole percent argon in nitrogen to be -2 Btu/mol at 1320 psia and 20°C. This suggests that the excess enthalpy of the nitrogen-oxygen system measured in this research is of the correct sign and magnitude.

For the data on nitrogen-carbon dioxide mixtures, a more accurate comparison can be made with the data of Lee and Mather[90] at 40°C. The excess enthalpy values, which they estimate to be better than four percent accurate, are plotted in Figures 8 and 9. As described in an earlier chapter entitled "Experience of Previous Investigators" these data were taken under relatively unsteady state conditions and smoothed versus pressure and composition at a given temperature. The values plotted as squares in Figures 8 and 9 are their reported values and were not interpolated by this author. Based on the interpolation technique for composition, it is felt that errors due to it are least at 0.5 mole fraction where the excess enthalpy does not vary excessively with composition. Further, since the excess isothermal Joule-Thompson coefficient is smaller at 500 psia than at 950 psia, the errors from pressure smoothing should be correspondingly lesser at the lower pressure. As anticipated, the agreement between the two sets of data is better at 500 psia than at 950 psia and is best at 0.50 mole fraction nitrogen at both pressures.

Comparisons are also made with excess enthalpies calculated by the original Benedict-Webb-Rubin equation of state using various sets of constants for the nitrogen-carbon dioxide system: For nitrogen the constants of Crain and Sonntag,[27] Stotler and Benedict[160] and Bloomer and Rao;[19] for carbon dioxide the constants of Eakin and Ellington[37] and Cullen and Kobe.[29] The mixing rules used are those suggested by Benedict et al.[13] Various combinations of the constants predicted approximately similar values of the excess enthalpy. However, the constants of Bloomer and Rao[19] for nitrogen, and Cullen and Kobe[29] for carbon dioxide (See Table XLV) give values that are closestto the experimental data reported here. The dotted lines in Figures 8, 9, 11 and 12

represent calculations using these constants. The constants used for predicting the excess enthalpies of both the binary and the multicomponent nitrogen-ethane system are those of Bloomer and Rao[19] for nitrogen and Benedict et al.[15] for ethane (See Table XLV).

RECOMMENDATIONS FOR IMPROVEMENT OF EXPERIMENTAL TECHNIQUES IN SUBSEQUENT STUDIES

1. It is felt that flow rates should be reduced by an order of magnitude in order to reduce operating costs. Flow meters suitable for use at low flow rates have already been designed and built. However, before incorporating them in the facility, it will be necessary to make improvements in the system to reduce the time required to achieve steady state conditions. It is believed that the four suggestions that follow this one will remedy the present situation.
2. The preconditioning of the gases before they enter constant-temperature baths or before they are throttled should be carried out in coils immersed in controlled temperature baths rather than with the present arrangement of wrapping electrical heating tapes around the tubes that convey the gas.
3. The valves and pressure regulators used in controlling flows should be placed in a heated box whose temperature is thermostatically controlled.
4. Automatic control on the D.C. power supply which provides the electrical energy input to the calorimeter will reduce the time required to achieve isothermal conditions in the calorimeter and will also assist in reducing the magnitude of the correction for temperature differences across the calorimeter.
5. The accuracy and speed of the measurement of pressure level in and pressure drop across the calorimeter should be improved by using null and differential transducers, respectively.
6. Bath temperatures should be measured with a more accurate device such as a platinum resistance or a quartz crystal thermometer.

7. Tests should be performed to confirm that the mixture exiting the calorimeter is of uniform composition.

8. A data interpretation technique should be developed to replace the secondary corrections which are used to normalize the data. It is suggested that a numerical method be used which relies on the experimental measurements of this very research and does not need an enthalpy prediction technique to predict excess properties. This will necessitate taking a larger volume of data over a finer grid of pressures and temperatures but would eliminate the inaccuracies introduced by the predicted excess properties.

SUMMARY AND CONCLUSIONS

1. A flow calorimetric facility was designed and built for the measurement of the enthalpy of mixing of binary gaseous mixtures at elevated pressures.

2. Data was obtained on three systems:

   (a) The nitrogen-carbon dioxide system at 31°C, 500 and 950 psia, and at 40°C at the same pressures at a minimum of four compositions.

   (b) The nitrogen-ethane system at 32.38°C and 401 psia at four compositions.

   (c) The nitrogen-oxygen system at 25°C and 1001 psia at one composition.

   The systems investigated are of both industrial and theoretical importance: Mixtures of nitrogen with oxygen and carbon dioxide can be used to evaluate engine and fuel performance of combustion engines; nitrogen, ethane and carbon dioxide are constituents of natural gas. The data on the nitrogen-carbon dioxide system at 31°C and on the nitrogen-ethane system at 32.38°C represent the first direct calorimetric data obtained at a reduced temperature of unity of the heavy component in the mixtures.

3. Ten repetitive measurements on the nitrogen-carbon dioxide system at 40°C, 500 psia and 0.5 mole fraction nitrogen were shown to be independent of flow rate indicating that the heat leak was less than the experimental precision (0.5 percent).

4. The accuracy of the data is believed to be between 0.8 and 2.1 percent for the data on mixtures of nitrogen with ethane and carbon dioxide and ten percent for the data on nitrogen-oxygen mixtures.

5. It was concluded that before obtaining further data on this facility, the operating flow rates should be reduced by an order of magnitude. However, modifications should be made to improve the time required to achieve steady state conditions before low flow rates are used.

APPENDIX A

ERROR ANALYSIS

The accuracy of data of the kind obtained in this research is difficult to evaluate. However, an estimate can be made of the maximum errors caused by the measuring techniques and the data interpretation. To perform a detailed error analysis, it is necessary to assess the uncertainties in the instruments as well as the inaccuracies in data obtained from the literature. The latter is much more difficult than the former, hence this error analysis is based largely on instrument error with the inaccuracies in the data being accounted for wherever possible.

Compounding of Errors

Various techniques for compounding errors have been discussed by Faulkner,[45] Jones,[71] and Manker[98] for heat capacity measurements with a flow calorimetric method very similar to the present one.

If a dependent variable Z is related to a number of independent variables $(z_1, z_2, \ldots z_n)$ by the equation

$$Z = Z(z_1, z_2, \ldots z_n) \tag{91}$$

then the absolute error $e(Z)$ in Z is given by[118]

$$e(Z) = \sum_{i=1}^{n} \left| \left(\frac{\partial Z}{\partial z_i} \right)_{Z_{j \neq i}} e(z_i) \right| \tag{92}$$

where $e(z_i)$ is the absolute error in the variable z_i. Dividing through by Z, the fractional error is obtained:

$$\frac{e(Z)}{Z} = \sum_{i=1}^{n} \left| \frac{1}{Z} \left(\frac{\partial Z}{\partial z_i} \right)_{Z_{j \neq i}} e(z_i) \right| \tag{93}$$

In this analysis, the errors are assumed to be random errors. This method of compounding errors does not allow for the subtraction of

errors of opposite sign and it estimates the limit of accuracy of the experimental results.

Power Input Measurement

The scheme employed in supplying electrical energy input to the calorimeter has been described earlier and the equation for calculating the power input, $\dot{W}$, has already been derived as

$$\dot{W} = \left(\frac{R_s+R_e}{R_e}\right) V_e \left(\frac{V_i}{R_i} - \frac{V_e}{R_e}\right) \tag{74}$$

The quantity $\frac{V_e}{R_e}$ is much smaller than $\frac{V_i}{R_i}$ and R_s is much larger than R_e, hence the purposes of error analysis, this equation is approximated as

$$\dot{W} = \frac{R_s}{R_e R_i} V_i V_e \tag{94}$$

Performing the manipulation described in Equation (93) on the last equation yields

$$\frac{e(\dot{W})}{\dot{W}} = \frac{e(R_s)}{R_s} + \frac{e(V_i)}{V_i} + \frac{e(V_e)}{V_e} + \frac{e(R_e)}{R_e} + \frac{e(R_i)}{R_i} \tag{95}$$

The estimated maximum percent errors in the independent variables are listed in Table XVII. Compounding the errors as indicated in the last equation and adding the uncertainty in the power supply regulation and standard cell voltage yields an estimated accuracy of 0.1 percent.

Flow Rate Measurement

The measurement of the flow rate of the two gases to the calorimeter involves three steps. The first one is the volume determination of the calibration tank. The next is the calibration of the flow meters and the final step is calculating the flow rate of each gas from the correlation of the calibration data and the measurements on the flow meters.

TABLE XVII

ERRORS IN DETERMINATION OF POWER INPUT TO CALORIMETER

Variable	Instrument	Reading	Error	Percent Error
Power Supply	Kepco Power Supply			0.01
Resistance	Standard Resistors	R_i=1 ohm R_e=10 ohms R_s=10,000 ohms		0.01 0.01 0.01
Standard Cell	Leeds and Northrup #7309			0.01
Calorimeter Heater Voltage, V_e	K-3 Potentiometer and Resistor, R_e	0.022 volts	5 micro volts	0.023
Calorimeter Heater Current, V_i	K-3 Potentiometer and Resistor, R_i	0.16 volts	36 micro volts	0.023

Measurement of Volume of Calibration Tank

For purposes of this analysis, the relation used to determine the volume of the calibration tank, V_{ct}, may be approximated by the ideal gas law. The experimental measurements along with estimated errors are listed in Table XVIII. Excluding uncertainties in the second virial coefficient of nitrogen the errors in the individual measurements sum to 0.27 percent. At the low final pressure in the calibration tank (45 inches Hg), it is unlikely that errors in the reliable volumetric data of Otto[126] will appreciably affect the accuracy of the results.

A check on the present measurements is the volume measurement on the same tank performed by Mage.[96] He determined the volume to be 6.416 ± 0.002 ft^3 by weighing the amount of water required to fill the tank at a measured temperature. Adding 0.0041 ft^3 for the volume of the

TABLE XVIII

ERRORS IN VOLUME DETERMINATION OF CALIBRATION TANK

Measurement	Instrument	Reading	Error	Percent Error
Pressure, P_{ct}	36-inch King Manometer	15 inches Hg	0.05 inches	0.16*
	Barometer	30 inches Hg	0.02 inches	
Vacuum	McLeod Gauge	20 microns Hg	5 microns Hg	0.0007*
Temperature, T_{ct}	Thermometer	20°C	0.03°	0.043
	Thermocouples		0.10°	
Mass, m_{ct}	Balance	320g	0.2g	0.07

*Percent error based on 45 inches Hg final pressure in tank.

manometer well and the gas lines outside the tank to the calibration tank volume measured by Mage yields 6.420 ft^3. The excellence of the agreement of this value with the mean value of $V_{ct} = 6.422$ ft^3 given in Table XXIII may be fortuitous. However, it provides some justification for assuming the probable error in the measurement of the volume of the calibration tank to be ± 0.2 percent.

Flow Meter Calibration

Four quantities are required for the correlation of the results of flow meter calibrations using Equation (86) given earlier. They are: the pressure drop across the flow meters, ΔP_F, the flow rate, F, obtained from measurements on the calibration tank, and the density, ρ_F, and viscosity, η_F, of the gas in the flow meters.

For purposes of this error analysis, the quantity $\frac{F}{\sqrt{\rho_F \Delta P_F}}$ is equated to Y

$$Y = \frac{F}{\sqrt{\rho_F \Delta P_F}} \tag{96}$$

Also, for this analysis the relation for determining the mass of gas in the calibration tank is approximated by the ideal gas law. The flow rate may then be calculated from the approximate equation:

$$F = \frac{1}{\theta} \frac{(P_{ctf}-P_{cti})V_{ct}}{R\, T_{ct}} \tag{97}$$

where θ is the time period of gas collection, P_{cti} is the pressure in the initially evacuated tank and P_{ctf} is the final pressure in the filled tank. Substituting for the flow rate F from the last equation into Equation (96) yields:

$$Y = \frac{1}{\sqrt{\rho_F \Delta P_F}} \frac{1}{\theta} \cdot \frac{(P_{ctf}-P_{cti})V_{ct}}{R\, T_{ct}} \tag{98}$$

Using the method of analysis described by Equation (93), the fractional error in Y is given by

$$\frac{e(Y)}{Y} = \frac{1}{2}\frac{e(P_F)}{P_F} + \frac{1}{2}\frac{e(\Delta P_F)}{\Delta P_F} + \frac{e(\theta)}{\theta} + \frac{e(P_{ctf})}{(P_{ctf}-P_{cti})} + \frac{e(P_{cti})}{(P_{ctf}-P_{cti})} + \frac{e(V_{ct})}{V_{ct}} + \frac{e(T_{ct})}{T_{ct}} \tag{99}$$

noting that the error in the density has been replaced by the error in the measurement of pressure in the flow meter.

The estimated error in the various measurements are listed in Table XIX. The Heise pressure gauges are calibrated against the dead weight gauge before and after every calibration or enthalpy of mixing run. The 1 psi variation of Table XIX includes this deviation as well as the uncertainty of $\pm$ 0.02 inches Hg in the barometric pressure measurement. The fluctuations of pressure and pressure drop during a calibration run are less than the uncertainties listed in Table XIX. The measurements

TABLE XIX

ERRORS IN FLOW METER CALIBRATION MEASUREMENTS

Measurement	Instrument	Reading	Error	Percent Errors Low Flows	Percent Errors High Flows
Measurements on Flow Meters					
Pressure, P_F	Heise Gauge	1100 psia	1 psi	0.09	0.09
Pressure Drop, ΔP_F	Manometer and Cathetometer	15 to 95 cm	0.04 cm	0.26	0.04
Flow Meter Bath Temperature	Mercury-in-Glass Thermometer	45°C	0.03°C		
Flow Rate Determination					
Time of flow through Solenoid Valve, θ	Timer	1000 to 400 sec	0.1 sec	0.01	0.03
Pressure in Calibration Tank, P_{ctf}	Manometer	28 in di butyl phthalate (sp. gr. 1.04)	0.05 in dbp	0.07*	0.07*
	Barometer	30 in Hg	0.02 in Hg		
Pressure in Evacuated Calibration Tank, P_{cti}	Vacuum Manometer	20 mm Hg	0.5 mm Hg	0.07*	0.07*
Temperature in Calibration Tank, T_{ct}	Thermometer Thermocouples	20°C	0.03°C 0.1°C	0.04	0.04

*Percent error based on approximately 30 inches Hg final pressure in tank.

on the calibration tank for determination of flow rate are similar to those listed in Table XVIII with two exceptions: the vacuum in the tank is measured with a vacuum manometer and a timer is used to measure the time interval of gas collection, θ .

The volume of the calibration tank is taken as fixed for all the calibration runs. Therefore, it affects the accuracy but not the precision of the measurements. Neglecting the error in the volume of the calibration tank and substituting the percent errors from Table XIX in the last equation yields an estimated precision for the experimental measurements of 0.28 to 0.37 percent between high and low flow rates, respectively.

Indeterminacies in the viscosity (η_F) and density (ρ_F) of the gas in the flow meters have so far been neglected. Since the flow meters have been calibrated at the conditions at which they will be used in the calorimetric measurements, errors in the absolute values of these quantities will not affect the accuracy of the results appreciably. The effect of pressure on the density of di butyl phthalate is also eliminated by replicating conditions in this way.

Errors in the second virial coefficient data on nitrogen,[126] carbon dioxide[113] and ethane[116] do not appreciably alter the precision or accuracy of the results because the data is believed to be reliable and because at the approximately atmospheric pressure in the calibration tank there is only a small deviation from ideal gas behavior.

There are two more factors which can affect the precision of the flow calibration results. The first represents deviations from the friction factor relation, Equation (75), chosen to correlate the data. The second is drifts in the true calibration line with time which has been experienced by other investigators.[48,101] The latter effect is

minimized by repeating calibration runs over the period of time that the enthalpy of mixing runs are performed. In the case of the carbon dioxide flow meter, however, it is believed that the true calibration line drifted upwards.

The combined affect of all the factors on the precision of the flow rate is reflected in the standard deviation from the regression line. For the nitrogen and carbon dioxide flow meters this standard deviation is 0.18 and 0.25 percent respectively (See Tables XXIV, XXV and Figures 16, 17 in Appendix B). This is less than the estimated upper limit of errors in the experimental measurements hence the maximum precision of these calibrations is taken to be 0.28 to 0.37 percent for the nitrogen-carbon dioxide system.

Four ethane flow meter calibration points give a standard deviation of 0.63 percent (See Table XXVI and Figure 18 in Appendix B). This large value is due to one calibration point which deviates by 0.68 percent from the regression line. This point was not repeated because of an insufficient supply of ethane. Hence the precision of the ethane flow meter calibrations is taken as 0.65 percent.

For the nitrogen-oxygen system it is felt that due to the limited number of calibration points (See Table XXVII in Appendix B) a reasonable estimate of the precision is one percent for each gas.

The accuracy of the flow rate measurements depends not only on the flow meter calibrations but on the accuracy of the calibration tank volume determination. Combining the estimated 0.2 percent error in the latter with the error in the flow meter calibrations yields:

1. Nitrogen-carbon dioxide system: The accuracy of the flow meter calibrations for each gas should be 0.48 to 0.57 percent.

2. Nitrogen-ethane system: The accuracy of the nitrogen flow meter calibrations is 0.48 to 0.57 percent and the corresponding value for ethane is 0.85 percent.
3. Nitrogen-oxygen system: The accuracy of each flow meter calibration is 1.2 percent.

Calculation of Flow Rate

The error in the flow rate calculation is determined by compounding the errors in the pressure and pressure drop measurements on the flow meter with the estimated errors in the flow meter calibrations. This error is obtained from the equation

$$\frac{e(F)}{F} = \frac{e(Y)}{Y} + \frac{1}{2}\frac{e(\Delta P_F)}{\Delta P_F} + \frac{1}{2}\frac{e(P_F)}{P_F} \qquad (100)$$

For the nitrogen and carbon dioxide flow meters, the error at low flow rates is 0.75 percent and at high flow rates is 0.55 percent. Similar calculations on the ethane flow meters which operated at 500 psia yield estimates of 0.97 to 1.1 percent which may be rounded off to one percent. For the nitrogen-oxygen system the pressure drop in each of the flow meters was about 20 cm Hg during enthalpy of mixing determinations and the resultant accuracy is estimated as 1.4 percent for each gas flow rate.

Gas Composition

The error in the composition determination due to inaccuracies in the flow rate calculation and the error in the gas density technique are estimated.

Composition from Flow Rates

The mass fraction of component A, w_A, is calculated from the mass flow rates of the two constituents A and B of the mixture:

$$w_A = \frac{F_A}{F_A+F_B} \tag{101}$$

Performing the manipulations in Equation (92), the absolute error in the mass fraction is expressed as

$$e(w_A) = w_A(1-w_A)\left[\frac{e(F_B)}{F_B} + \frac{e(F_A)}{F_A}\right] \tag{102}$$

For the nitrogen-carbon dioxide system the mass fraction of nitrogen varies between 0.23 and 0.73. When combined with the accuracy of the flow rate determinations for the two gases, the error for nitrogen-lean mixtures is 0.0023 mass fraction and for nitrogen-rich mixtures is 0.0026 mass fraction. The corresponding absolute error in the mole fraction is 0.003 to 0.002 mole fraction, respectively. In the case of the nitrogen-ethane system, the error is 0.003 mass or mole fraction. The uncertainty in the composition of the nitrogen-oxygen system is 0.007 mass or mole fraction.

Composition from Gas Density Analysis

The error in the composition is obtained by compounding the error in the initial step of can volume determination with the error in the final step of gas density measurements. The estimated instrument errors are listed in Table XX.

The mathematical relation for calculating the volume of the aerosol can may be simplified to the ideal gas relation. The overall maximum error of 0.14 percent is obtained as the sum of the errors in the individual measurements listed in Table XX.

Gas density measurements yield the molecular weight, M , of the unknown mixture

$$M = \frac{m_{ac}RT_{ac}}{P_{ac}V_{ac}} \tag{103}$$

TABLE XX

ERRORS IN GAS DENSITY ANALYSIS MEASUREMENTS

Measurement	Instrument	Reading	Error	Percent Error
Determination of Can Volume				
Mass, m_{ac}	Balance	1.8g	1 mg	0.056
Pressure, P_{ac}	Manometer Barometer	100 in Hg 30 in Hg	0.05 in 0.02 in	0.054
Temperature, T_{ac}	Thermometer	25°C	0.1	0.033
Gas Density Determination				
Mass, m_{ac}	Balance	2.5g*	1 mg	0.04
Pressure, P_{ac}	Manometer Barometer	100 in Hg 30 in Hg	0.05 0.02	0.054
Temperature, T_{ac}	Thermometer	25°C	0.1	0.033

*For equimolar mixture of nitrogen and carbon dioxide.

again assuming ideal gas behavior for the purpose of error analysis. The fractional error in the molecular weight $e(M)/M$ is the sum of the errors in the individual measurements for gas density determinations given in Table XX combined with the uncertainty in the volume of the can. Evaluated thus, the estimated accuracy is 0.27 percent. The composition of the gas mixture is dependent on its molecular weight

$$x_N = (M-M_{CO_2})/(M_N-M_{CO_2}) \qquad (104)$$

where M_N and M_{CO_2} are molecular weights of nitrogen and carbon dioxide respectively. The absolute error in composition measurement obtained by performing the operations in Equation (92) on the last equation is

$$e(x_N) = \frac{e(M)}{M}\left(\frac{M}{M_N - M_{CO_2}}\right) \qquad (105)$$

For an average molecular weight of $M = 36$ the maximum error in composition is 0.006 mole fraction.

The second virial coefficients used in these calculations are given in Table XLVIII in Appendix C. It is difficult to estimate the error in these low pressure volumetric properties. However, it seems likely that the error introduced is small compared to the uncertainties in the experimental measurements.

Excess Enthalpy Determinations

The errors introduced by the data reduction procedure are evaluated for the nitrogen-carbon dioxide and the nitrogen-ethane systems. The nitrogen-oxygen system is treated separately.

Power per Unit Flow

The power/flow ratio is determined from the equation

$$(\dot{W}/F) = \frac{\dot{W}}{F_A + F_B} \qquad (106)$$

Using the previous analysis, the fractional error in the power/flow ratio is

$$\frac{e(\dot{W}/F)}{(\dot{W}/F)} = \frac{e(\dot{W})}{\dot{W}} + \left(\frac{F_A}{F_A+F_B}\right)\frac{e(F_A)}{F_A} + \left(\frac{F_B}{F_A+F_B}\right)\frac{e(F_B)}{F_B} \qquad (107)$$

where the terms with the ratio of flow rates represent the mass fractions of the two components.

For the nitrogen-carbon dioxide system, the mass fraction of nitrogen varies between 0.23 and 0.73. The corresponding error in power/flow ratio should then be 0.71 to 0.72 percent. The range of error for nitrogen-ethane mixtures is estimated to be 1.1 to 0.75 percent for

nitrogen-lean and nitrogen-rich mixtures respectively. For an estimated error of 0.1 percent in the power input for the nitrogen-oxygen system, the inaccuracy in the power/flow ratio is 1.5 percent.

Primary Corrections

The estimated errors due to primary corrections for the data on nitrogen-carbon dioxide mixtures at 40°C and 500 psia are detailed in Table XXI(a). All the percent errors listed are based on the power/flow ratio, $(\dot{W}/F)$. The estimated range of error of 0.19 to 0.27 percent are the sum of the columns of minimum and maximum errors, respectively.

The estimated errors in the primary corrections at the other experimental conditions, are summarized in Table XXI(b). The error in the individual variables, $e(z)$, is assumed to be identical with the estimates in Table XXI(a) except for a 15 percent uncertainty in the isothermal Joule-Thompson coefficient at 31°C and 950 psia.

Based on the uncertainties in the individual variables, $e(z)$, in Table XXI(b), the estimated errors in the primary corrections for the multicomponent nitrogen-ethane system are 0.22 to 0.23 percent. The additional inaccuracy in the binary nitrogen-ethane system due to an estimated 30 percent uncertainty in the impurity correction causes this error estimate to rise to 0.55-0.71 percent.

Secondary Corrections

The errors due to the variables that affect the secondary corrections for the nitrogen-carbon dioxide system are listed in Table XXII in a manner similar to the previous Table XXI for primary corrections. The percent errors in this table are based on the excess enthalpy at outlet conditions, $\underline{H}_O^E$. For the data at 500 psia, both at 31°C and 40°C, the uncertainty in the excess properties, φ^E and C_p^E , is believed to

TABLE XXI

ESTIMATED ERRORS INTRODUCED BY PRIMARY CORRECTIONS
FOR NITROGEN-CARBON DIOXIDE MIXTURES

(a) For measurements at 40°C and 500 psia

Correction for	Percent Correction to Power/Flow Ratio min	max	Variable z	Estimate of Error in Variable, e(z)	Error in H_o^E Fractional Contribution	Percent Error min	max
Pressure Drop	0.03	0.22	φ	5%	$\Delta P\ e(\varphi)/(\dot{W}/F)$	0.002	0.011
			ΔP	1 cm di butyl phthalate*	$e(\Delta P)\varphi/(\dot{W}/F)$	0.023	0.023
Temperature Difference	0.04	1.20	C_p	5%	$\Delta T\ e(C_p)/(\dot{W}/F)$	0.002	0.060
			ΔT	0.006°C	$e(\Delta T)C_p/(\dot{W}/F)$	0.149	0.149
Impurities	0.30	0.58	Composition	5%	$e(\Delta I_{corr})/(\dot{W}/F)$	0.015	0.029
				Range of Errors due to Primary Correction: (sum of minimum and maximum errors)		0.19%	0.27%

(b) For measurements at other conditions

Experimental Conditions T_n °C	P_n psia	Percent Error in H_o^E min	max
40	950	0.12	0.19
31	500	0.26	0.27
31	950	0.13	0.19

*1 cm di butyl phthalate = 0.015 psi.

TABLE XXII

ESTIMATED ERRORS INTRODUCED BY SECONDARY CORRECTIONS
FOR NITROGEN-CARBON DIOXIDE MIXTURES

(a) For measurements at 40°C and 500 psia

Correction for	Percent Correction of $\underline{H}^E_o$ min	max	Variable z	Estimate of Error in Variable z e(z)	Error in $\underline{H}^E_n$ Fractional Contribution	Percent Error min	max
Pressure Level	0.01	0.58	φ^E	10%	$e(\varphi^E)\Delta P_o/\underline{H}^E_o$	0.001	0.058
			ΔP_o	0.3 psi	$\varphi^E e(\Delta P_o)/\underline{H}^E_o$	0.071	0.071
Temperature Level	0.00	0.07	C^E_P	10%	$e(C^E_P)\Delta T_o/\underline{H}^E_o$	0.000	0.007
			ΔT_o	0.04°C	$C^E_P e(\Delta T_o)/\underline{H}^E_o$	0.072	0.072
			Range of Errors due to Secondary Corrections: (sum of minimum and maximum errors)			0.14	0.21

(b) For measurements at other conditions

Experimental Conditions T_n °C	P_n psia	Percent Error in $\underline{H}^E_n$ min	max
40	950	0.34	0.72
31	500	0.23	0.33
31	950	0.63	1.1

be 10 percent. For the remainder of the data and also for the nitrogen-ethane system the errors in the excess properties are estimated to be 30 percent. The range of error is estimated to be 0.26 to 0.36 percent for both the binary and the multicomponent nitrogen-ethane data.

Nitrogen-Oxygen System

The maximum possible error in the measurement of the temperature difference between the inlet oxygen and outlet mixture is 0.006°C (See chapter entitled "Apparatus and Experiments"). The error in the temperature difference between the inlet gases, nitrogen and oxygen, is 0.004°C as the 0.002°C error in the bath temperature control can be neglected. Hence the uncertainty in the temperature difference between inlet nitrogen and outlet mixture is 0.010°C. The average uncertainty for the equimolar mixture is ± 0.008°C which corresponds to a 6.9 percent error. Compounded with a three percent uncertainty in the heat capacity values, the estimated uncertainty in the excess enthalpy measurement is about 10 percent.

The accuracy of the heat capacity values is also limited by the ± 0.003°C uncertainty in the mixture outlet temperature and the ± 0.006°C uncertainty in the temperature difference measurement. Compounded with the 1.5 percent inaccuracy in the power/flow ratio, the uncertainty for the measurement at the low power input is estimated at 77 percent and at 23 percent. The error due to heat leakage in the calorimeter is estimated to be less than the experimental uncertainties for both the excess enthalpy and the heat capacity measurements.

APPENDIX B

CALIBRATIONS

TABLE XXIII

RESULTS OF VOLUME DETERMINATIONS ON CALIBRATION TANK

Determination Number	Measured Volume ft^3	Percent Deviation from Average Volume
1	6.412	-0.16%
2	6.436	0.22%
3	6.429	0.11%
4	6.411	-0.17%
Average Volume =	6.422 ft^3	
σ =	0.20%	

TABLE XXIV

DATA OF CALIBRATIONS FOR NITROGEN FLOW METER

$\ln\left\lvert\frac{\rho\Delta P}{\eta^2}\right\rvert$	$\frac{F}{\sqrt{\rho\Delta P}} \times 10^{-2}$	Date
10.8581	0.47348	Oct 12, 1969
11.1328	0.48046	Feb 22, 1969
11.4457	0.49192	Jan 8, 1970
11.6912	0.49946	Feb 23, 1969
11.7095	0.49881	Apr 10, 1969
11.7183	0.50144	Nov 16, 1969
11.9434	0.50709	Mar 28, 1970
12.3812	0.52123	Feb 25, 1969
12.7131	0.53304	Feb 25, 1969
12.9873	0.54245	Sep 8, 1969

$$\frac{F_N}{\sqrt{\rho_F \Delta P_F}} = 0.118757 \times 10^{-2} + 0.325670 \times 10^{-3} \left(\ln\left[\frac{\rho_F \Delta P_F}{\eta_F^2}\right] \right)$$

Average Deviation = 0.14%; σ = 0.18%

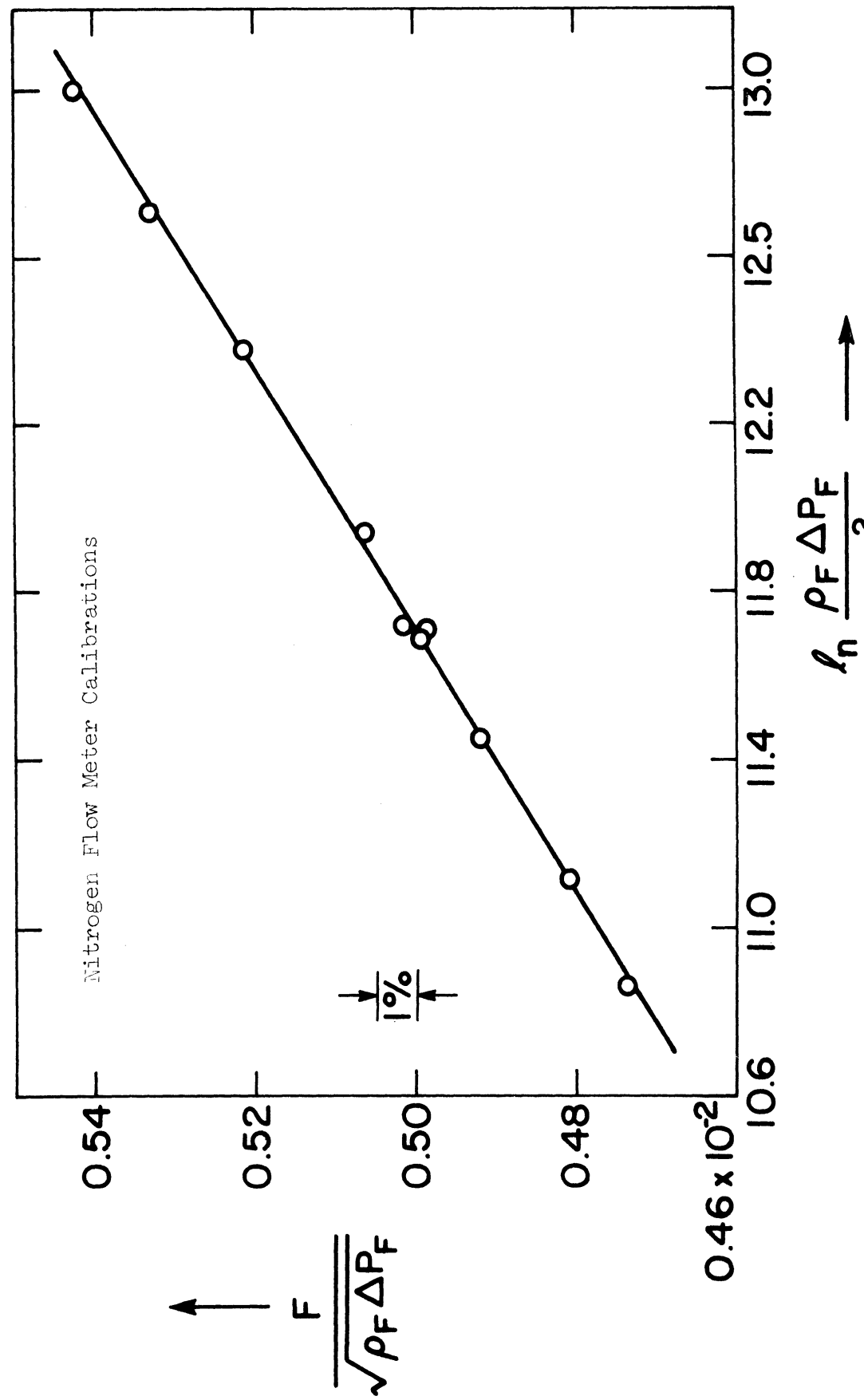

Figure 16. Flow Meter Calibrations for Nitrogen.

TABLE XXV

DATA OF CALIBRATIONS FOR CARBON DIOXIDE FLOW METER

$\ln\left[\frac{\rho\Delta P}{\eta^2}\right]$	$\frac{F}{\sqrt{\rho\Delta P}} \times 10^{-2}$	Date
11.9286	0.51121	Oct 13, 1969
12.0813	0.51833	Feb 14, 1969
12.4421	0.52793	Nov 27, 1969
12.4434	0.53062	Feb 15, 1969
12.4528	0.52853	Dec 10, 1969
12.4982	0.53019	Jan 7, 1970
12.5352	0.53106	Apr 5, 1969
13.0713	0.54743	Feb 16, 1969
13.5173	0.56004	Apr 4, 1969
13.5313	0.55767	Jan 7, 1970
13.8371	0.56796	Feb 17, 1969
13.9072	0.56901	Sep 8, 1969

$$\frac{F_{CO_2}}{\sqrt{\rho_F \Delta P_F}} = 0.174145 \times 10^{-2} + 0.284626 \times 10^{-3} \left(\ln\left[\frac{\rho_F \Delta P_F}{\eta_F^2}\right] \right)$$

Average Deviation = 0.17% σ = 0.25%

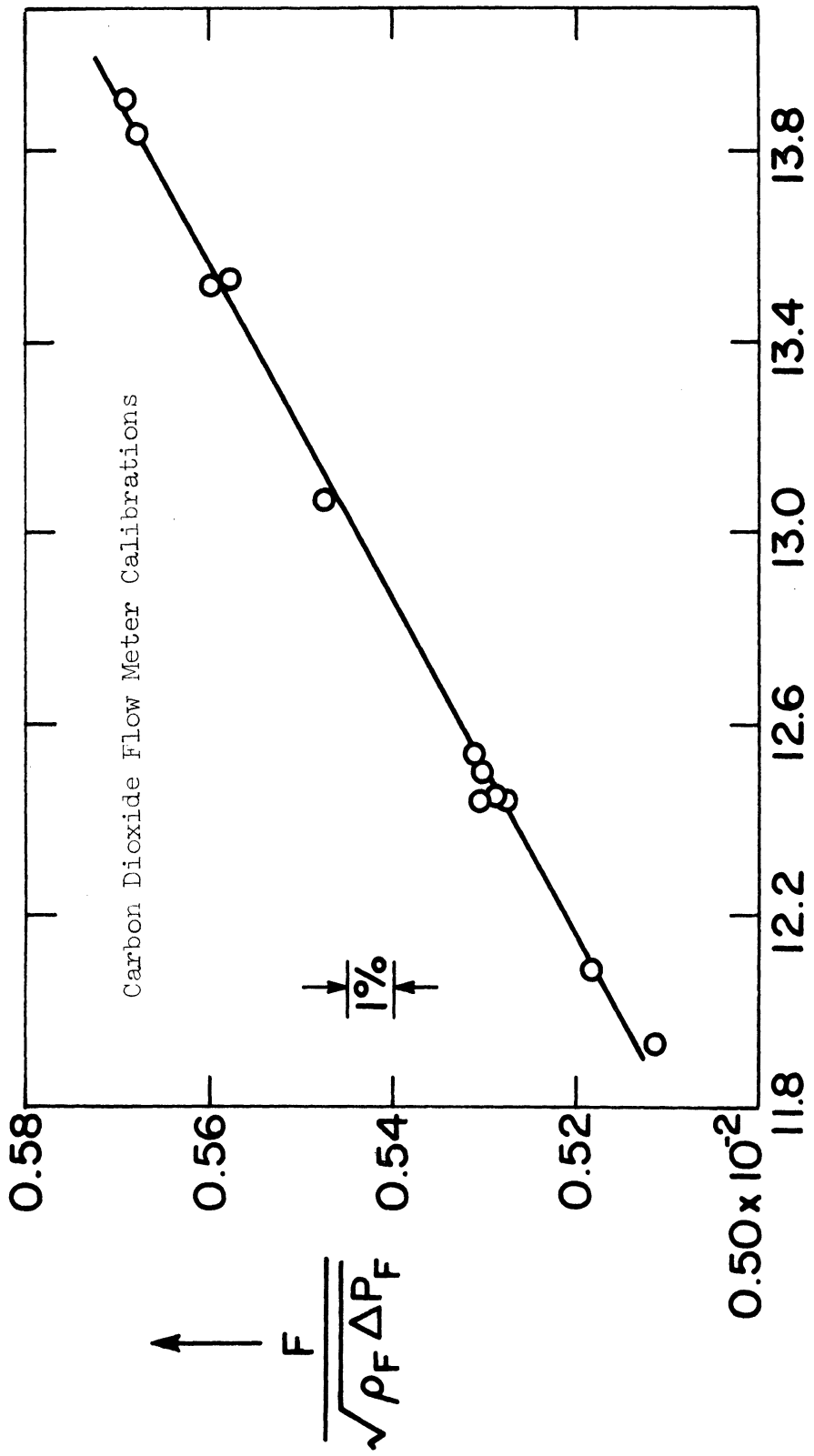

Figure 17. Flow Meter Calibrations for Carbon Dioxide.

TABLE XXVI

DATA OF CALIBRATIONS FOR ETHANE FLOW METER

$\ln\left[\frac{\rho\Delta P}{\eta^2}\right]$	$\frac{F}{\sqrt{\rho\Delta P}} \times 10^{-2}$	Date
12.1287	0.51777	Mar 18, 1970
13.1561	0.55060	Mar 23, 1970
13.6413	0.56044	Mar 24, 1970
13.8746	0.56342	Mar 19, 1970

$$\frac{F_{C_2H_6}}{\sqrt{\rho_F \Delta P_F}} = 0.194744 \times 10^{-2} + 0.267658 \times 10^{-3} \left(\ln\left[\frac{\rho_F \Delta P_F}{\eta_F^2}\right] \right)$$

Average Deviation = 0.39% σ = 0.63%

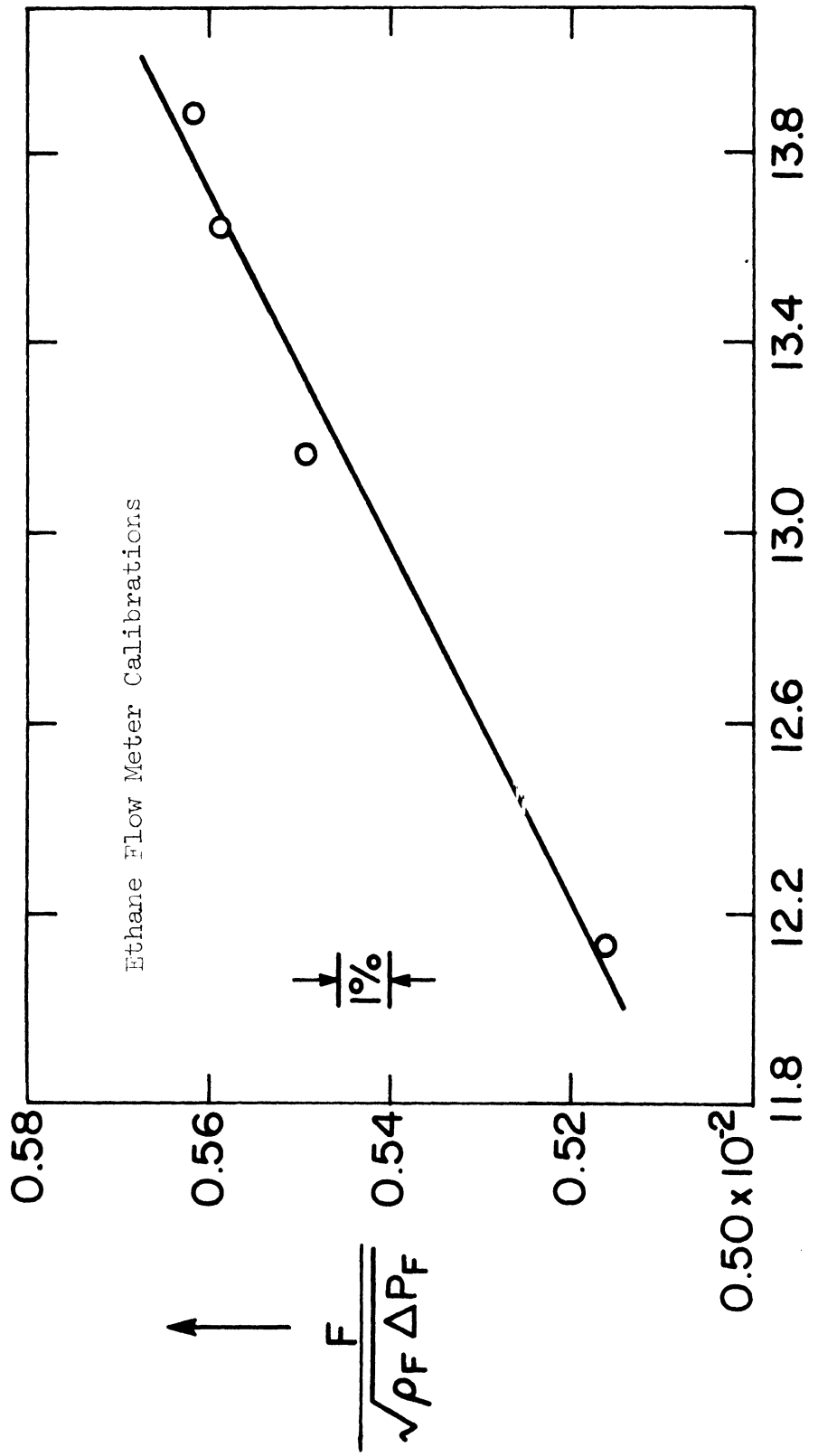

Figure 18. Flow Meter Calibrations for Ethane.

TABLE XXVII

DATA OF CALIBRATIONS FOR NITROGEN AND OXYGEN FLOW METERS USED IN MEASUREMENTS ON NITROGEN-OXYGEN SYSTEM

Gas	$\ln\left[\frac{\rho\Delta P}{\eta^2}\right]$	$\frac{F}{\sqrt{\rho\Delta P}} \times 10^{-1}$	Date
Nitrogen	11.4665	0.20152	May 22, 1968
	12.3205	0.20676	May 21, 1968
Oxygen	11.3686	0.20354	May 24, 1968
	12.2762	0.20838	May 24, 1968

Nitrogen: $$\frac{F_N}{\sqrt{\rho_F \Delta P_F}} = 0.131085 \times 10^{-1} + 0.614258 \times 10^{-3} \left(\ln\left[\frac{\rho_F \Delta P_F}{\eta_F^2}\right]\right)$$

Oxygen: $$\frac{F_O}{\sqrt{\rho_F \Delta P_F}} = 0.143003 \times 10^{-1} + 0.532507 \times 10^{-3} \left(\ln\left[\frac{\rho_F \Delta P_F}{\eta_F^2}\right]\right)$$

TABLE XXVIII

CALIBRATION OF DEAD WEIGHT GAUGE

Type: Mansfield and Green WG-13Q
Serial No.: 1872
Calibrated by: Mansfield and Green

Nominal Pressure psi	True Pressure psi	Difference psi	Percent Deviation
200	199.978	-0.022	-0.011
400	399.978	-0.022	-0.006
600	600.004	+0.044	+0.007
800	800.044	+0.044	+0.006
1000	1000.044	+0.044	+0.004
1200	1200.044	+0.044	+0.004
1400	1400.088	+0.088	+0.003

TABLE XXIX

CALIBRATION OF MERCURY BAROMETER

Measured Pressure* inches Hg	True Pressure** inches Hg	Difference inches Hg
29.24	29.192	-0.048
29.23	29.195	-0.035
29.24	29.197	-0.043
29.24	29.194	-0.046
29.23	29.194	-0.036
29.24	29.192	-0.048
29.24	29.191	-0.049
29.30	29.263	-0.037
29.30	29.267	-0.033
29.31	29.262	-0.048
29.31	29.253	-0.052
29.31	29.262	-0.048

Zero Error = -0.04 ± 0.006 inches Hg

*Both the measured and the true atmospheric pressure noted here have been corrected for mercury and scale expansion.

**True pressure is read on a calibrated mercury barometer manufactured by H. J. Green Company, New York, belonging to the Meteorology and Oceanography Department, University of Michigan.

TABLE XXX

CALIBRATION OF MERCURY-IN-GLASS THERMOMETER

Type: Fisher Scientific Mercury-in-glass thermometer
Marked: Fisher 3C3642
Range: -1 to +51°C in 0.1°C
Calibrated by: NBS

Thermometer Reading °C	True Temperature °C
+0.02	0.00
10.00	9.97
20.00	19.97
30.00	30.03
40.00	40.02
50.00	50.00

Estimated uncertainties do not exceed 0.03°C up to 51°C.

TABLE XXXI

CALIBRATION OF THERMOPILE

Tagged G27724A and G33950

Temperature °C	EMF microvolts
-196	-33350
-183	-32004
-120	-23627
-100	-20345
-80	-16795
-60	-12971
-40	-8890
-20	-4568
0	0
+20	4776
+40	9764
+60	14948
+80	20323
+100	25886
+120	31613

Calibrated by: NBS

TABLE XXXII

CALIBRATED RESISTANCES OF STANDARD RESISTORS

Designation in Figure 5	Leeds and Northrup Catalog No.	Serial No.	Resistance at 25°C, R_{25} abs ohms	Accuracy R_{25} (Percent)	Date of Calibration	Temperature Coefficients α	β
R_i	4020-B	1745730	1.000008	0.001	Dec '68	+0.000006	-0.0000005
R_e	4025-B	1648097	10.0000	0.005	Jun '64	+0.000009	-0.0000005
R_s	4040-C	1227969	9999.8	0.005	Apr '57	+0.000001	-0.0000005

Resistance, $R_{T_{res}}$, at temperature T_{res} °C given by

$$R_{T_{res}} = R_{25}(1+\alpha(T_{res}-25)+\beta(T_{res}-25)^2)$$

TABLE XXXIII

CALIBRATION OF POTENTIOMETER STANDARD CELLS

Eppley Serial No.	EMF	Date	Calibrated by
768338	1.01930 @ 23°C	Oct '63	Eppley Lab.
	1.01926 @ 23°C	Aug '66	NBS
	1.01923 @ 24°C	Apr '69	NBS
813229	1.01926 @ 23°C	Dec '67	Eppley Lab.

TABLE XXXIV

CHARACTERISTICS OF LEEDS AND NORTHRUP MODEL K-3 NULL POTENTIOMETER

Measuring Ranges

High (X1)	Range 0 - 1.6110 volts
Medium (X0.1)	Range 0 - 0.16110 volts
Low (X0.01)	Range 0 - 0.016110 volts

Limits of Error*

High Range (X1):	± (0.01% + 20 microvolts)
Medium Range (X0.01):	± (0.015% + 2 microvolts)
Low Range (X0.01):	± (0.015% + 0.5 microvolts)

Thermal emf

On operation of switches: Less than 0.1 microvolts of very short duration.
On operation of slide wire: Not more than 0.3 microvolts of very short duration.
Residual emf: Not more than 0.3 microvolts.

Guarding and Shielding

1. The potentiometer is guarded for high humidity operation.
2. The potentiometer is shielded to eliminate electrostatic problems.

*Values apply for both measuring and standardizing, and include the effect of residual thermal emf's at 90% relative humidity.

TABLE XXXV

EXPERIMENTAL ENTHALPY OF MIXING DATA ON NITROGEN-CARBON DIOXIDE SYSTEM

Run Number	Flow Rate N_2 lb/min	Flow Rate CO_2 lb/min	Power (W) watts	Temperature N_2 Inlet (T_1) °C	Temperature Outlet (T_o) °C	Temperature Difference (T_1-T_o) °C	Pressure Drop N_2 Inlet -Outlet (P_1-P_o) psi	Pressure Drop CO_2 Inlet -Outlet (P_2-P_o) psi	Pressure at Outlet P_o psia
4.001	0.03567	0.05549	3.696	40.03	40.037	-0.007	0.089	0.063	499.5
5.001	0.03578	0.05422	3.678	40.02	40.064	-0.044	0.088	0.062	496.9
5.002	0.03577	0.05432	3.678	40.02	40.049	-0.029	0.088	0.062	497.7
5.003	0.03579	0.05470	3.738	40.01	40.068	-0.058	0.088	0.063	500.2
6.001	0.02896	0.11308	4.869	40.00	40.001	-0.002	0.142	0.144	503.1
6.002	0.03073	0.09437	4.589	40.00	40.011	-0.011	0.121	0.113	500.0
6.003	0.04073	0.08251	4.951	40.00	40.037	-0.037	0.137	0.112	499.7
6.004	0.04338	0.07075	4.660	40.00	40.014	-0.014	0.131	0.097	500.7
7.001	0.04956	0.05767	4.331	40.01	40.036	-0.026	0.136	0.088	500.1
7.002	0.07001	0.05423	4.566	40.00	40.015	-0.015	0.217	0.120	500.0
9.001	0.07170	0.10233	7.084	40.01	40.013	-0.003	0.311	0.225	499.2
9.002	0.07177	0.10531	7.174	40.03	40.033	-0.003	0.317	0.232	498.5
11.1	0.02437	0.04144	2.668	40.00	40.017	-0.017	0.050	0.034	500.2
11.2	0.02432	0.04111	2.661	39.99	40.033	-0.043	0.049	0.034	498.1
11.3	0.02423	0.04075	2.648	40.00	40.001	-0.001	0.049	0.033	501.4
13.1	0.02149	0.12034	16.589	40.00	40.088	-0.088	0.059	0.062	949.6
13.2	0.03339	0.09425	17.772	39.99	39.955	0.035	0.063	0.054	952.5
13.3	0.05799	0.08564	19.919	40.02	40.105	-0.085	0.107	0.074	946.1
13.4	0.07262	0.04184	11.705	40.01	39.991	0.019	0.110	0.054	945.8
14.1	0.02264	0.12150	4.873	30.99	31.023	-0.033	0.128	0.139	500.0
14.2	0.03311	0.09146	5.491	31.00	31.009	-0.009	0.119	0.107	502.4
14.3	0.05549	0.09267	6.983	31.00	30.994	0.006	0.204	0.155	502.9
14.4	0.07252	0.04232	4.387	31.00	30.990	0.010	0.204	0.102	498.2
15.1	0.02529	0.12695	27.942	31.00	31.064	-0.064	0.064	0.064	947.1
15.2	0.02603	0.09135	23.277	30.99	31.003	-0.013	0.046	0.041	949.5
15.3	0.05343	0.08804	28.166	31.01	31.047	-0.037	0.094	0.067	948.7
15.4	0.07231	0.04317	16.236	31.00	31.010	-0.010	0.107	0.052	952.5

TABLE XXXVI

EXPERIMENTAL ENTHALPY OF MIXING DATA ON NITROGEN-ETHANE SYSTEM

Run Number	Flow Rate Nitrogen lb/min	Flow Rate Ethane lb/min	Power ($\dot{W}$) watts	Temperature N_2 Inlet (T_1) °C	Temperature Outlet (T_o) °C	Temperature Difference (T_1-T_o) °C	Pressure Drop N_2 Inlet -Outlet (P_1-P_o) psi	Pressure Drop C_2H_6 Inlet -Outlet (P_2-P_o) psi	Pressure at Outlet P_o psia
16.1	0.07279	0.02375	5.385	32.34	32.370	-0.030	0.234	0.103	401.0
16.2	0.05500	0.04358	8.020	32.34	32.369	-0.029	0.180	0.107	400.6
16.3	0.03983	0.05845	8.653	32.35	32.380	-0.030	0.141	0.106	401.1
16.4	0.02292	0.06482	6.880	32.36	32.381	-0.021	0.093	0.086	401.6

TABLE XXXVII

EXPERIMENTAL ENTHALPY OF MIXING DATA ON NITROGEN-OXYGEN SYSTEM

Run Number	Flow Rate Nitrogen lb/min	Flow Rate Oxygen lb/min	Power ($\dot{W}$) watts	Temperature O_2 Inlet (T_1) °C	Temperature Outlet (T_o) °C	Temperature Difference O_2 Inlet -Outlet (T_1-T_o)°C	Temperature Difference N_2 Inlet -Outlet (T_2-T_o)°C	Pressure Drop N_2 Inlet -Outlet (P_1-P_o) psi	Pressure Drop O_2 Inlet -Outlet (P_2-P_o) psi	Pressure at Outlet P_o psia
17.1	0.1268	0.1325	0.0	25.00	25.117	-0.117	-0.108	0.28	0.39	1001.0
17.2	0.1268	0.1325	0.0	25.00	25.119	-0.119	-0.108	0.28	0.39	1001.0
17.3	0.1268	0.1325	0.03188	25.00	25.128	-0.128	-0.118	0.28	0.39	1001.0
17.4	0.1268	0.1325	0.09771	25.00	25.159	-0.159	-0.150	0.28	0.39	1001.0
17.5	0.1268	0.1328	0.0	25.00	25.113	-0.113	-0.104	0.29	0.39	1000.8

TABLE XXXVIII

PRIMARY CORRECTIONS FOR DATA ON NITROGEN-CARBON DIOXIDE SYSTEM

Run Number	Mole Fraction Nitrogen	Power / Flow (W/F) Btu/lb	Corrections for Pressure Drop Btu/lb	Corrections for Temperature Difference Btu/lb	Corrections for Kinetic Energy Diff. Btu/lb	Impurities Btu/lb	$\underline{H}^E_o$ at (T_o, P_o) after Primary Corrections Btu/lb	$\underline{H}^E_o$ at (T_o, P_o) after Primary Corrections Btu/mol
4.001	0.503	2.304	-0.0014	-0.0035	-0.5E-06	0.0087	2.308	83.0
5.001	0.510	2.322	-0.0014	-0.0211	-0.5E-06	0.0086	2.308	82.8
5.002	0.509	2.320	-0.0014	-0.0140	-0.5E-06	0.0086	2.313	83.0
5.003	0.508	2.347	-0.0014	-0.0281	-0.5E-06	0.0086	2.326	83.5
6.001	0.288	1.948	-0.0037	-0.0007	0.1E-05	0.0113	1.955	77.0
6.002	0.339	2.085	-0.0028	-0.0054	0.4E-06	0.0107	2.087	80.5
6.003	0.437	2.283	-0.0026	-0.0179	-0.6E-06	0.0095	2.272	84.1
6.004	0.491	2.320	-0.0022	-0.0066	-0.7E-06	0.0088	2.320	83.9
7.001	0.575	2.295	-0.0018	-0.0126	-0.6E-06	0.0077	2.288	79.7
7.002	0.670	2.089	-0.0023	-0.0071	0.4E-06	0.0062	2.085	69.4
9.001	0.525	2.313	-0.0048	-0.0013	-0.2E-05	0.0084	2.315	82.5
9.002	0.518	2.302	-0.0050	-0.0015	-0.2E-05	0.0085	2.304	82.3
11.1	0.481	2.304	-0.0008	-0.0083	-0.2E-06	0.0090	2.304	83.7
11.2	0.482	2.311	-0.0008	-0.0209	-0.2E-06	0.0089	2.299	83.4
11.3	0.484	2.315	-0.0008	-0.0004	-0.2E-06	0.0089	2.323	84.3
13.1	0.220	6.646	-0.0031	-0.0730	0.2E-06	0.0545	6.625	268.2
13.2	0.358	7.913	-0.0024	0.0278	-0.2E-06	0.0474	7.985	305.7
13.3	0.516	7.881	-0.0028	-0.0617	-0.5E-06	0.0383	7.855	280.9
13.4	0.732	5.811	-0.0015	0.0122	0.5E-06	0.0235	5.845	188.8
14.1	0.228	1.921	-0.0048	-0.0116	0.2E-05	0.0135	1.918	77.4
14.2	0.363	2.505	-0.0033	-0.0044	-0.3E-07	0.0118	2.509	95.8
14.3	0.485	2.678	-0.0043	0.0032	-0.1E-05	0.0100	2.687	97.4
14.4	0.729	2.171	-0.0023	0.0047	0.1E-05	0.0059	2.179	70.5
15.1	0.239	10.429	-0.0054	-0.0808	-0.5E-08	0.0856	10.429	419.0
15.2	0.310	11.269	-0.0032	-0.0157	-0.1E-06	0.0798	11.330	442.4
15.3	0.489	11.314	-0.0044	-0.0390	-0.5E-06	0.0639	11.334	410.2
15.4	0.725	7.989	-0.0023	-0.0082	0.4E-06	0.0384	8.017	259.9

TABLE XXXIX

SECONDARY CORRECTIONS FOR DATA ON NITROGEN-CARBON DIOXIDE SYSTEM

Run Number	Corrections for Pressure Level Btu/lb	Corrections for Temperature Level Btu/lb	$\underline{H}_n^E$ at (T_n, P_n) after Secondary Corrections Btu/lb	$\underline{H}_n^E$ at (T_n, P_n) after Secondary Corrections Btu/mol
4.001	0.0028	0.0009	2.312	83.1
5.001	0.0166	0.0016	2.326	83.4
5.002	0.0124	0.0012	2.327	83.5
5.003	-0.0008	0.0017	2.327	83.5
6.001	-0.0113	0.0000	1.944	76.6
6.002	0.0001	0.0002	2.087	80.5
6.003	0.0017	0.0009	2.274	84.2
6.004	-0.0035	0.0003	2.317	83.8
7.001	-0.0006	0.0009	2.288	79.7
7.002	-0.0001	0.0003	2.086	69.4
9.001	0.0044	0.0003	2.320	82.6
9.002	0.0078	0.0008	2.313	82.6
11.1	-0.0008	0.0004	2.304	83.7
11.2	0.0099	0.0008	2.309	83.8
11.3	-0.0073	0.0000	2.316	84.0
13.1	0.0083	0.0214	6.654	269.4
13.2	-0.0567	-0.0118	7.917	303.0
13.3	0.0823	0.0247	7.962	284.7
13.4	0.0609	-0.0015	5.905	190.7
14.1	-0.0001	0.0008	1.919	77.5
14.2	-0.0199	0.0004	2.489	95.1
14.3	-0.0256	-0.0003	2.661	96.5
14.4	0.0122	-0.0003	2.191	70.9
15.1	0.1306	0.0394	10.599	425.9
15.2	0.0209	0.0018	11.352	443.3
15.3	0.0547	0.0251	11.414	413.1
15.4	-0.0688	0.0034	7.952	257.8

TABLE XL

PRIMARY CORRECTIONS FOR DATA ON NITROGEN-ETHANE SYSTEM

Run Number	Mole Fraction Nitrogen	Power Flow (W/F) Btu/lb	Corrections for Pressure Drop Btu/lb	Temperature Difference Btu/lb	Kinetic Energy Diff. Btu/lb	Impurities Btu/lb	H_o^E at (T_o, P_o) after Primary Corrections Btu/lb	Btu/mol
Multicomponent System								
16.1	0.767	3.170	-0.0033	-0.0185	0.4E-05	-0.0000	3.148	89.8
16.2	0.576	4.623	-0.0049	-0.0213	-0.7E-06	-0.0000	4.597	133.0
16.3	0.423	5.003	-0.0061	-0.0244	-0.1E-05	-0.0000	4.972	145.5
16.4	0.276	4.456	-0.0059	-0.0190	0.6E-06	-0.0000	4.431	131.0
Binary System								
16.1	0.769	3.170	-0.0033	-0.0185	0.4E-05	-0.0519	3.096	88.2
16.2	0.578	4.623	-0.0049	-0.0213	-0.7E-06	-0.0628	4.534	131.0
16.3	0.425	5.003	-0.0061	-0.0244	-0.1E-05	-0.0560	4.916	143.5
16.4	0.277	4.456	-0.0059	-0.0190	0.6E-06	-0.0404	4.391	129.5

TABLE XLI

SECONDARY CORRECTIONS FOR DATA ON NITROGEN-ETHANE SYSTEM

Run Number	Corrections for Pressure Level Btu/lb	Corrections for Temperature Level Btu/lb	$\underline{H}^E_n$ at (T_n, P_n) after Secondary Corrections Btu/lb	$\underline{H}^E_n$ at (T_n, P_n) after Secondary Corrections Btu/mol
Multicomponent System				
16.1	-0.0001	-0.0005	3.148	89.8
16.2	0.0084	-0.0008	4.605	133.2
16.3	-0.0024	-0.0000	4.970	145.4
16.4	-0.0127	0.0001	4.419	130.7
Binary System				
16.1	-0.0001	-0.0004	3.096	88.2
16.2	0.0083	-0.0008	4.542	131.2
16.3	-0.0024	-0.0000	4.914	143.5
16.4	-0.0125	0.0001	4.379	129.2

TABLE XLII

PRIMARY CORRECTIONS FOR DATA ON NITROGEN-OXYGEN SYSTEM

Run Number	Mole Fraction Nitrogen	Power Flow (W/F) Btu/lb	Corrections for Pressure Drop Btu/lb	Corrections for Temperature Difference Btu/lb	Corrections for Kinetic Energy Diff. Btu/lb	H_o^E at (T_o, P_o) after Primary Corrections Btu/lb	H_o^E at (T_o, P_o) after Primary Corrections Btu/mol
17.1	0.522	0.0	-0.0022	-0.0526	-0.9E-06	-0.0548	-1.65
17.2	0.522	0.0	-0.0022	-0.0532	-0.9E-06	-0.0554	-1.67
17.3	0.522	0.0070	-0.0022	-0.0576	-0.9E-06	-0.0529	-1.59
17.4	0.522	0.0214	-0.0022	-0.0724	-0.9E-06	-0.0532	-1.60
17.5	0.522	0.0	-0.0022	-0.0508	-0.9E-06	-0.0530	-1.60

TABLE XLIII

VALUES OF HEAT CAPACITIES AND ISOTHERMAL JOULE-THOMPSON COEFFICIENTS USED FOR PRIMARY CORRECTIONS

Component	Temperature °C	Pressure psia	Heat* Capacity, C_p Btu/(lb°F)	Isothermal* Joule-Thompson Coefficient, φ Btu/(lb psi)
Oxygen	25	1001	0.247	-0.00697
Nitrogen	25	1001	0.275	-0.00603
	31	500	0.259	-0.00592
		950	0.270	-0.00538
	40	500	0.258	-0.00550
		950	0.268	-0.00501
Carbon Dioxide	31	500	0.287	-0.0395
		950	0.782	-0.086
	40	500	0.275	-0.0312
		950	0.497	-0.0575
Ethane	32.4	401	0.597	-0.0904

*Literature sources for these values given in chapter "Results."

TABLE XLIV

FORMULAE DERIVED FROM BENEDICT-WEBB-RUBIN EQUATION OF STATE
USED IN CALCULATING PROPERTIES

Enthalpy Departure

$$H - H^{O} = \left[B_{O}RT - 2A_{O} - \frac{4C_{O}}{T^{2}}\right]\rho + (2bRT - 3a)\frac{\rho^{2}}{2} + \frac{6a\alpha\rho^{5}}{5} + \frac{c\rho^{2}}{T^{2}}\left[\frac{3(1-e^{-\gamma\rho^{2}})}{\gamma\rho^{2}} - \frac{e^{-\gamma\rho^{2}}}{2} + \gamma\rho^{2}\, e^{-\gamma\rho^{2}}\right]$$

Isothermal Joule-Thompson Coefficient

$$\varphi = \frac{(B_{O}RT - 2A_{O} - \frac{4C_{O}}{T^{2}}) + (2bRT - 3a)\rho + 6a\alpha\rho^{4} + \frac{e^{-\gamma\rho^{2}}}{T^{2}}[5c\rho + 5c\gamma\rho^{3} - 2c\gamma^{2}\rho^{5}]}{RT + 2\rho(B_{O}RT - A_{O} - \frac{C_{O}}{T^{2}}) + 3\rho^{2}(bRT - a) + 6a\alpha\rho^{5} + \frac{e^{-\gamma\rho^{2}}}{T^{2}}[3c\rho^{2} + 3c\gamma\rho^{4} - 2c\gamma^{2}\rho^{6}]}$$

Heat Capacity

$$C_{P} - C_{P}^{O} = -R + \frac{6C_{O}\rho}{T^{3}} - \frac{6c}{\gamma T^{3}} + ce^{-\gamma\rho^{2}}\left[\frac{6}{\gamma T^{3}} + \frac{3\rho^{2}}{T^{3}}\right] + \frac{\left[R\rho + B_{O}R\rho^{2} + bR\rho^{3} + \frac{2C_{O}\rho^{2}}{T^{3}} - e^{-\gamma\rho^{2}}\left(\frac{2c\rho^{3}}{T^{3}} - \frac{2c\gamma\rho^{5}}{T^{3}}\right)\right]^{2}}{R\rho^{2} + 2B_{O}R\rho^{3} - \frac{2A_{O}\rho^{3}}{T} - \frac{2C_{O}\rho^{3}}{T^{3}} + 3bR\rho^{4} - \frac{3a\rho^{4}}{T} + \frac{6a\alpha\rho^{7}}{T} + \frac{e^{-\gamma\rho^{2}}}{T^{3}}[3c\rho^{4} + 3c\gamma\rho^{6} - 2c\gamma^{2}\rho^{8}]}$$

TABLE XLV

CONSTANTS FOR THE BENEDICT-WEBB-RUBIN EQUATION OF STATE

Units: psia, ft^3, lb mole, °R
R = 10.7335
T°R = T°F + 459.63

Constants	Nitrogen*	Carbon Dioxide	Ethylene	Ethane	Propylene	Propane
B_o	0.0407426	0.799496	0.891980	1.00554	1.36263	1.55884
A_o	1.053642	10322.8	12593.6	15670.7	23049.2	25915.4
C_o	8059.	1693.01×10^6	1602.28×10^6	2194.27×10^6	5365.97×10^6	6209.93×10^6
b	0.0023277	1.0582	2.20678	2.85393	4.79997	5.77355
a	0.025102	8264.46×10^6	15645.5	20850.2	46758.6	57428.0
c	728.41	2919.71×10^6	4133.60×10^6	6413.14×10^6	20083.0×10^6	25247.8
α	0.0001272	0.348	0.731661	1.00044	1.87312	2.49577
γ	0.0053	1.384	2.36844	3.02790	4.69325	5.64524
Author	Bloomer & Rao	Cullen & Kobe	Benedict, Webb & Rubin	Benedict, Webb & Rubin	Benedict, Webb & Rubin	Benedict, Webb & Rubin
Reference	(19)	(29)	(14)	(14)	(14)	(14)

*Units: atm, l, g mol, °K

TABLE XLVI

SAMPLE RESULTS OF VOLUME DETERMINATIONS ON CANS USED FOR GAS DENSITY ANALYSIS

Data on Can No. 30

Measurement	Volume of Can cc	Percent Difference from Average Volume
1	372.97	0.13
2	372.21	-0.08
3	372.32	-0.05
Average Volume	372.50 cc	
	0.09%	

Data on Can No. 31

1	371.92	0.10
2	371.28	-0.07
3	371.44	-0.03
Average Volume	371.55 cc	
	0.11%	

TABLE XLVII

GAS DENSITY ANALYSES
OF GRAVIMETRICALLY PREPARED SAMPLES

Can Number	Mole Fraction Nitrogen		
	Gravimetric Analysis	Gas Density Analysis	Difference
14	0.4023	0.4053	+0.0030
30	0.4022	0.4003	-0.0019

TABLE XLVIII

SECOND VIRIAL COEFFICIENTS USED
IN GAS DENSITY ANALYSIS COMPUTATIONS

Temperature = 25°C

Constituent	Second Virial Coefficient cc/mol	Reference
Nitrogen, B_{11}	-4.71	(109)
Carbon Dioxide, B_{22}	-123.6	(109)
Nitrogen-Carbon-Dioxide, B_{12} (Interaction Coefficient)	-42.6	(93)

TABLE XLIX

COMPARISON OF COMPOSITIONS FROM FLOW METER CALIBRATIONS AND FROM GAS DENSITY ANALYSIS

Run Number	Nominal Conditions T_n °C	P_n psia	Mole Fraction Flow Meter Calibrations	Nitrogen from Gas Density Analysis	Difference
6.003	40	500	0.437	0.441	0.004
11.1			0.481	0.484	0.003
11.2			0.482	0.486	0.004
				0.483	0.001
11.3			0.484	0.482	-0.002
				0.485	0.001
6.004			0.491	0.495	0.004
4.001			0.503	0.506	0.003
5.001			0.510	0.510	0.000
9.001			0.525	0.524	-0.001
7.002			0.670	0.669	-0.001
13.1	40	950	0.220	0.222	0.002
				0.224	0.004
13.2			0.358	0.359	0.001
				0.362	0.004
13.3			0.516	0.519	0.003
13.4			0.732	0.732	0.000
				0.733	0.001
14.1	31	500	0.228	0.230	0.002
14.2			0.363	0.363	0.000
14.3			0.485	0.483	-0.002
14.4			0.729	0.728	-0.001
15.1	31	950	0.239	0.242	0.003
15.2			0.310	0.307	-0.002
15.3			0.489	0.493	0.004
15.4			0.725	0.720	-0.005

TABLE L

CONVERSION FACTORS FOR SI UNITS

English Units	SI Units[67]
1 Btu	= 1055.87 Joules
1 psi	= 101325/14.696 Nm^{-2}
1 lb	= 0.453592 Kg

TABLE LI

MOLECULAR WEIGHTS USED IN COMPUTATIONS

Substance	Molecular Weight
Carbon Dioxide	44.011
Ethane	30.07
Ethene	28.05
Nitrogen	28.016
Propane	44.10
Oxygen	32.00
Propane	44.10
Propene	42.08

APPENDIX D

SAMPLE CALCULATIONS

One sample calculation of each of the following are presented here:

1. The volume determination of the calibration tank utilized in calculating the flow rate during flow meter calibrations.
2. Flow meter calibrations on the nitrogen flow meter
3. Enthalpy of mixing measurements on the nitrogen-carbon dioxide system and the impurity correction for the nitrogen-ethane system.

The equipment and procedures used have been described in detail in the chapter entitled "Apparatus and Experiments." The literature sources for the thermodynamic and transport properties used in reducing the flow meter calibration data are referred to in the same chapter. The viscosity data[112] and low pressure[126] and high pressure[34] volumetric data on nitrogen were fit graphically. The resultant formulae used in calculating these properties are given in Table LII. A tabulation of the nomenclature used here is given at the end of this appendix.

Volume Determination of Calibration Tank

The calculation of the volume of the tank from the data in Table LIII involves six steps. They are the calculation of the

1. Temperature in the tank, T_{ctf}
2. Atmospheric pressure, P_R
3. Pressure in the tank, P_{ctf}
4. Compressibility factor of nitrogen, Z_N
5. Mass of nitrogen in the tank, m_{ct}
6. Volume of the tank, V_{ct}

TABLE LII

FORMULAE FOR PROPERTIES OF NITROGEN
USED IN COMPUTER PROGRAMS

Property	Independent Variable	Formula
Compressibility Factor	$70 < P \text{ atm} < 80$ $290 < T\ ^\circ K < 320$	$Z_N = ZL + (ZH-ZL)(T-290)/30$ where $ZL = 0.993974 + 7.98\times10^{-5}(P-70)$ and $ZH = 1.0074 + 2.57\times10^{-4}(P-70)$
Viscosity, poise	$70 < P \text{ atm} < 80$	$\eta_N = (183.2 + 0.22P)10^{-6}$
Second Virial Coefficient, $\frac{cc}{g\ mol}$	$283 < T\ ^\circ K < 318$	$B_N = -301.3 + 51.94 \ln T$

Temperature in Tank

Calculated from data on tank filled with nitrogen

$$T_{th} = T_{ref} + \frac{\Delta E}{C_{th}} \qquad (108)$$

$$= 20.80 + (-38.5 \text{ microvolts}) \left(\frac{^\circ C}{40 \text{ microvolts}}\right)$$

$$= 19.84^\circ C$$

$$T_{ctf} = \frac{T_{th}+T'_{ctf}}{2} \qquad (109)$$

$$= \frac{19.84+19.80}{2}$$

$$= 19.82^\circ C$$

Atmospheric Pressure

Equation suggested by Brombacher et al.[22]

$$P_R = (P'_R-0.04)(G)\left[1 + \frac{(s_{exp}-m_{exp})(T_R-21.1)}{1 + m_{exp}(T_R-21.1)}\right] \qquad (110)$$

TABLE LIII

SAMPLE DATA FOR VOLUME DETERMINATION
OF CALIBRATION TANK

Variable	Value
Mass of Nitrogen Discharged	
Full Cylinder No. 1, m_{c1}	2807.810 g
Empty Cylinder No. 1, m_{c2}	2651.080 g
Full Cylinder No. 2, m_{c3}	2876.917 g
Empty Cylinder No. 2, m_{c4}	2715.338 g
Evacuated Tank	
Room Pressure just prior to evacuation, P'_{Ri}	28.95 in Hg
Room Temperature just prior to evacuation, T_{Ri}	20.2°C
Pressure in evacuated tank,* P_{cti}	11×10^{-3} mm Hg
Thermocouple reading, ΔE	-44.1 microvolts
Reference junction temperature, T_{ref}	20.85°C
Bath fluid temperature, T'_{cti}	19.75°C
Tank Filled with Nitrogen	
Tank Pressure,* P'_{ctf}	15.88 in Hg gauge
Thermocouple reading*, ΔE	-38.5 microvolts
Reference Junction temperature,* T_{ref}	20.80°C
Bath fluid temperature* (Corrected for emergent stem), T'_{ctf}	19.80°C
Room Pressure,* P'_R	29.12 in Hg
Room Temperature,* T_R	18.5°C
Equipment Constants	
Thermocouple calibration constant, C_{th}	40 microvolts/°C
Coefficient of expansion of aluminum, s_{exp}	24.5×10^{-6}/°C
Coefficient of expansion of mercury, m_{exp}	1.82×10^{-4}/°C
Ratio of local to standard gravity, G	0.999645
Volume of 36-inch King manometer well, V_{well}	4.7 in^3
Volume of connecting line, V_{line}	0.79 in^3
Approximate volume of tank, V_{app}	6.43 ft^3
Volume of union between calibration tank and solenoid valve, V_u	0.00017 ft^3
Cross-sectional area of indicating column of 36-inch King manometer, A_m	0.038 in^2
Coefficient of expansion of copper, v_{exp}	5×10^{-5}/°C

*Average of three measurements made over a time period of 15 minutes.

$$P_R = (29.12\text{-}0.04 \text{ in Hg})(0.999645)\left[1 + \frac{(24.5\text{x}10^{-6}\text{-}1.82\text{x}10^{-4})(18.5\text{-}21.1)}{1 + 1.82\text{x}10^{-4}(18.5\text{-}21.1)}\right]$$

$$= 29.08 \text{ in Hg}$$

Pressure in Tank

$$P_{ctf} = P_R + (P'_{ctf})(G)\left[1 + \frac{s_{exp}(T_R\text{-}20)\text{-}m_{exp}(T_R\text{-}0)}{1 + m_{exp}(T_R\text{-}0)}\right] \qquad (111)$$

$$= 29.08 \text{ in Hg}$$

$$+ (15.88 \text{ in Hg})(0.999645)\left[1 + \frac{24.5\text{x}10^{-6}(18.5\text{-}20)\text{-}1.82\text{x}10^{-4}(18.5)}{1 + 1.82\text{x}10^{-4}(18.5)}\right]$$

$$= 44.90 \text{ in Hg}$$

Compressibility Factor of Nitrogen

$$Z_N = 1 + \frac{B_N P_{ctf}}{R T_{ctf}} \qquad (112)$$

where $B_N = -6.0$ cc/g mol is calculated from the formula in Table LII at $T = T_{ctf} + 273.15°K$ or $292.97°K$

$$Z_N = 1 + \frac{(-6 \frac{cc}{g \text{ mol}})(44.90 \text{ in Hg})}{(2455 \frac{\text{in Hg cc}}{g \text{ mol } °K})(19.82+273.15°K)}$$

$$= 0.9998$$

Mass of Nitrogen in Tank

$$m_{ct} = N_{app} + N_{well} + N_{line} + N_{vac} \qquad (113)$$

Intermediate calculations:

1. Mass of gas discharged from cylinders, N_{app}

$$N_{app} = (m_{c1}\text{-}m_{c2}) + (m_{c3}\text{-}m_{c4}) \qquad (114)$$

$$= (2807.810\text{-}2651.080) + (2876.917\text{-}2715.338)g$$

$$= 318.309 \text{ g } \left(\frac{1\text{b}}{453.59\text{g}}\right)$$

$$= 0.70175 \text{ lb}$$

2. Residual gas in manometer well, N_{well}

$$N_{well} = \frac{M_N \, P_{R_i} \, V_{well}}{T_{R_i} \, R} \tag{115}$$

where $P_{R_i} = 28.90$ is calculated by substituting $P'_{R_i} = 28.95$ in Hg and $T_{R_i} = 20.2°C$ in Equation (110).

$$N_{well} = \frac{(28.016 \frac{\text{lb}}{\text{mol}})(28.90 \text{ in Hg})(4.7 \text{ in}^3)}{(20.2+273.15°\text{K})(67961 \frac{\text{in}^3 \text{ in Hg}}{\text{mol } °\text{K}})}$$

$$= 0.00019 \text{ lb of nitrogen}$$

3. Mass of residual gas in line connecting cylinders to calibration tank, N_{line}

$$N_{line} = \frac{V_{line} \, M_N}{R \, T_R} [2P_R - P_{int} - P_{ctf}] \tag{116}$$

where

$$P_{int} = \frac{(m_{c1}-m_{c2}) \, R \, T_R}{V_{app} \, M_N}$$

$$= \frac{(156.73\text{g})(18.5+273.15°\text{K})(39.33 \frac{\text{ft}^3 \text{ in Hg}}{\text{mol } °\text{K}})}{(6.43 \text{ ft}^3)(28.016 \frac{\text{lb}}{\text{mole}})(453.59 \frac{\text{g}}{\text{lb}})}$$

$$= 22 \text{ in Hg}$$

Hence

$$N_{line} = \frac{(0.79 \text{ in}^3)(28.016 \frac{\text{lb}}{\text{mol}})}{(18.5+273.15°\text{K})(67961 \frac{\text{in}^3 \text{ in Hg}}{\text{mol } °\text{K}})} [2(29.08)-22-44.90]$$

$$= -0.000008 \text{ lb of nitrogen}$$

4. Mass of gas in evacuated tank, N_{vac}

$$N_{vac} = \frac{M_N \, P_{cti} \, V_{app}}{R \, T_{cti}} \tag{117}$$

where $T_{cti} = 19.75°C$ is calculated from data on the evacuated tank using procedure detailed in Equations (108) and (109) for calculating T_{ctf}

$$N_{vac} = \frac{(28.016 \frac{lb}{mole})(11x10^{-3} \text{ mm Hg})(6.43 \text{ ft}^3)}{(999 \frac{\text{mm Hg ft}^3}{\text{mol °K}})(19.75+273.15°K)}$$

$$= 0.000007 \text{ lb of nitrogen}$$

5. Mass of gas discharged, m_{ct}, calculated from Equation (113)

$$m_{ct} = 0.70175 + 0.00019 - 0.000008 + 0.000007$$

$$= 0.70194 \text{ lb of nitrogen}$$

Volume of Tank

$$V_t = \frac{m_{ct} \, Z_N \, R \, T_{ctf}}{P_{ctf} \, M_N} \tag{118}$$

$$= \frac{(0.70194 \text{ lb})(0.9998)(19.82+273.15°K)(39.33 \frac{\text{in Hg ft}^3}{\text{mol °K}})}{(44.90 \text{ in Hg})(28.016 \frac{lb}{mol})}$$

$$= 6.4292 \text{ ft}^3 \quad \text{at} \quad T_{ctf} = 19.82°C$$

The volume, V_t, calculated above is corrected for (a) volume of manometer fluid displaced into the indicating column from the well (b) volume of union, V_u, connecting calibration tank to two-way solenoid valve (23 in Figure 3) and (c) thermal expansion to 20°C

$$V_{ctf} = V_t + V_u - (A_m)(P'_{ctf}) \tag{119}$$

$$= 6.4292 + 0.00017 - \frac{(0.038 \text{ in}^2)(15.88 \text{ in})}{(1728 \text{ in}^3/\text{ft}3)}$$

$$= 6.4290 \text{ ft}^3$$

$$V_{ct} = V_{ctf}[1 + v_{exp}(20-T_{ctf})] \qquad (120)$$

$$= 6.4290[1 + 5\text{x}10^{-5}(20-19.82)]$$

$$= 6.429 \text{ ft}^3$$

Flow Meter Calibration

Sample data taken on a single flow meter calibration run with nitrogen are given in Table LIV. Two parameters are calculated from these data: $\left[\frac{F}{\sqrt{\rho_F \Delta P_F}}\right]$ and $\ln\left[\frac{\rho_F \Delta P_F}{\eta_F^2}\right]$. These parameters along with the parameters calculated from other calibration runs are used in correlating the results of the flow meter calibrations. The steps described below are followed in calculating these parameters from the data given in Table LIV.

1. Pressure at the flow meter inlet pressure tap, P_F .
2. Pressure drop across the flow meter, ΔP_F .
3. Mean pressure, P_m , in the flow meter calculated from P_F and ΔP_F .
4. Density of nitrogen, ρ_F , in the flow meter at pressure P_m .
5. Viscosity of nitrogen, η_F , in the flow meter at pressure P_m .
6. Flow rate, F , calculated from measurements on the calibration tank.
7. Calculation of parameters.

Pressure at Flow Meter Inlet

$$P_F = P_{hs}\left[\frac{G\left(1 - \frac{\rho_{air}}{\rho_{brass}}\right)}{1+s_{exp}(T_R-23)}\right] + P_h + P_{corr} + P_{diff} + P_R \qquad (121)$$

Intermediate calculations:

1. Heise gauge calibration correction, P_{diff}

$$P_{diff} = \frac{(1087.6-1089.5)+(1091.3-1092.2)}{2} = -1.4 \text{ psi}$$

TABLE LIV

SAMPLE FLOW METER CALIBRATION DATA

Temperature of Flow Meter bath (corrected for emergent stem), T_F	45°C
Pressure in Flow Meter	
Average pressure in flow meter read on Heise gauge, P_{hs}	1084.8 psig
Heise gauge calibration data:	
Heise gauge reading prior to run	1089.5 psig
Nominal dead weight gauge pressure prior to run	1087.6 psig
Heise gauge reading after run	1092.2 psig
Nominal dead weight gauge pressure after run	1091.3 psig
Temperature of dead weight gauge (assumed room temperature), T_R	27.4°C
Pressure Drop across Flow Meter	
Average cathetometer reading of fluid height, h_H	22.08 cm
Average cathetometer reading of zero, h_L	1.44 cm
Temperature of cathetometer, T_{cath}	26.2°C
Temperature of manometer fluid (assumed room temperature) T_R	27.4°C

Flow Rate Determination

	Evacuated Tank	Filled Tank
Pressure*	P_{cti} = 22.2 mm Hg	P'_{ctf} = 28.95 in dbp**
Thermocouple reading,* ΔE	-56.5 microvolts	-52 microvolts
Reference junction temperature,* T_{ref}	26.26°C	26.34°C
Bath fluid temperature* (corrected for emergent stem)	T'_{ctf} = 24.83°C	T'_{cti} = 25.04°C
Room Pressure,* P'_R		29.13 in Hg
Room Temperature,* T_R		27.4°C
Time period of gas collection, θ		931.6 seconds

Equipment Constants

Density of air, ρ_{air}	0.0012 $\frac{g}{cc}$
Density of brass weights (dead weight gauge), ρ_{brass}	8.4 $\frac{g}{cc}$
Expansion coefficient of stainless steel (dead weight gauge), s_{exp}	1.65×10^{-5}/°C
Head of oil between dead weight gauge and U-leg, P_h	0.075 psi

* Average of three measurements made over a time period of 15 minutes.

**dbp = di butyl phthalate

TABLE LIV (Continued)

Dead weight gauge calibration correction (Table XXVIII), P_{corr}	0.044 psi
Expansion coefficient of aluminum (cathetometer scale) s_{exp}	24.5×10^{-5}/°C
Well factor for high pressure manometer, A_w	0.99077

Values of G, v_{exp}, V_{well} and A_m given in Table LIII and V_{ct} from Table XXIII.

2. True barometric pressure, P_R

P_R = 29.05 inches Hg by substituting P'_R = 29.13 inches Hg and

T_R = 27.4°C from Table LIV in Equation (110).

Hence from Equation (121)

$$P_F = (1084.8 \text{ psig})\left[\frac{0.999645\left(1 - \frac{0.0012 \frac{g}{cc}}{8.4 \frac{g}{cc}}\right)}{1 + 1.65\times10^{-5}(27.4-23)}\right] + 0.075 \text{ psi} + 0.044 \text{ psi}$$

$$- 1.4 \text{ psi} + (29.05 \text{ in Hg})\left(0.4912 \frac{\text{psi}}{\text{in Hg}}\right)$$

$$= 1097.2 \text{ psia}$$

Pressure Drop across Flow Meter

$$\Delta P_F = \frac{(\Delta h)(G)}{\rho^o_{dbp}} [\rho_{dbp} - \rho_N] \qquad (122)$$

where $\Delta h = (h_H - h_L)[1 + s_{exp}(T_{cath} - 21.1)]/A_W$

Intermediate calculations:

1. $$\Delta h = (22.08 - 1.44 \text{ cm}) \frac{[1 + 24.5\times10^{-6}(26.2-21.1)]}{(0.99077)(2.54 \text{ cm/in})}$$

$$= 8.203 \text{ in dbp}$$

2. Variation of density of di butyl phthalate with temperature

$$\rho_{dbp} = \rho^o_{dbp}[1 - 6.16\times10^{-4}(T - 23.3)] \frac{g}{cc} \qquad (123)$$

$$= 1.0408[1 - 6.16\times10^{-4}(27.4-23.3)]$$

$$= 1.0382 \frac{g}{cc}$$

3. Density of nitrogen, ρ_N. Compressibility factor calculated from formulae in Table LII at $P_F = (1097.2/14.696)$atm and $T_R = 27.4 + 273.15°K$ is $Z_N = 0.9994$.

$$\rho_N = \frac{M_N P_F}{Z_N R T_R} \qquad (124)$$

$$= \frac{(28.016 \frac{lb}{mol})(1097.2 \text{ psia})}{(0.9994)(27.4+273.15°K)(19.317 \frac{\text{psia ft}^3}{\text{mol °K}})}$$

$$= 5.298 \frac{lb}{ft^3}$$

Hence from Equation (122)

$$\Delta P_F = \frac{(8.203 \text{ in dbp})(0.999645)}{(1.0408 \frac{g}{cc})} \left[(1.0382 \frac{g}{cc}) - (5.298 \frac{lb}{ft^3})(0.01602 \frac{g}{cc} \frac{ft^3}{lb})\right]$$

$$= 7.511 \text{ in dbp}$$

Mean Pressure in Flow Meter

$$P_m = P_F + \frac{\Delta P_F}{2} \qquad (125)$$

$$P_m = 1097.2 \text{ psia} - \frac{(7.511 \text{ in dbp})(1.0408 \frac{\text{inches dbp}}{\text{inches } H_2O})(\frac{0.4912 \text{ psi}}{\text{inches Hg}})}{(2)(13.595 \frac{\text{inches Hg}}{\text{inches } H_2O})}$$

$$= 1097.1 \text{ psia}$$

Density of Nitrogen in Flow Meter

Compressibility factor of nitrogen from formulae in Table LII at $P_m = 1097.1$ psia and $T = T_F + 273.15°C$ or $318.15°K$ is $Z_N = 1.008$

$$\rho_F = \frac{M_N P_m}{Z_N R T_F} \qquad (126)$$

$$= \frac{(28.016 \frac{lb}{mol})(1097.1 \text{ psia})}{(1.008)(45+273.15°K)(19.317 \frac{\text{psia ft}^3}{\text{mol °K}})}$$

$$= 4.962 \frac{lb}{ft3}$$

Viscosity of Nitrogen in Flow Meter

Calculated from the formula in Table LII at P_m = (1097.1/14.696)atm

$$\eta_F = 199.6 \times 10^{-6} \text{ poise}$$

Flow Rate Determination

The four steps consist of calculating:

(a) Mass of gas in initially evacuated in tank, N_i

(b) Mass of residual gas in manometer well, N_{well}

(c) Mass of gas in tank after stopping gas flow, N_f

(d) Flow rate of nitrogen, F

(a) Mass of gas in evacuated tank

$$N_i = \frac{M_N P_{cti} V_{cti}}{R T_{cti}} \qquad (127)$$

Intermediate calculations:

1. Temperature, T_{cti} , calculated as in Equations (108) and (109)

$$T_{th} = 26.26 + (-56.5 \text{ microvolts})(\frac{°C}{40 \text{ microvolts}})$$

$$= 24.85°C$$

$$T_{cti} = \frac{24.85+24.83}{2} = 24.84°C$$

2. Volume of calibration tank, V_{cti} : corrected for thermal expansion of copper tank to T_{cti} and for volume of manometer well

$$V_{cti} = V_{ct}[1 + v_{exp}(T_{cti}-20)] - V_{well} \qquad (128)$$

$$= 6.422[1 + 5x10^{-5}(24.84-20)] - \frac{(4.7\ in^3)}{(1728\ \frac{in^3}{ft^3})}$$

$$= 6.421\ ft^3$$

Hence from Equation (127):

$$N_i = \frac{(28.016\ \frac{lb}{mol})(22.2\ mm\ Hg)(6.421\ ft^3)}{(24.84+273.15°K)(999\ \frac{mm\ Hg\ ft^3}{mol\ °K})}$$

$$= 0.0134\ lb\ of\ nitrogen$$

(b) Mass of gas in manometer well

$$N_{well} = \frac{M_N\ P_R\ V_{well}}{R\ T_R} \qquad (129)$$

$$= \frac{(28.016\ \frac{lb}{mol})(29.05\ in\ Hg)(4.7\ in^3)}{(27.4+273.15°K)(67961\ \frac{in^3\ in\ Hg}{mol\ °K})}$$

$$= 0.0002\ lb\ of\ nitrogen$$

(c) Mass of gas in filled tank

$$N_f = \frac{M_N\ P_{ctf}\ V_{ctf}}{Z_N\ T_{ctf}\ R} \qquad (130)$$

Intermediate calculations:

1. Temperature, T_{ctf} , calculated as in Equations (108) and (109)

$$T_{th} = 26.34°C + (-52.0\ microvolts)(\frac{1°C}{40\ microvolts})$$

$$= 25.04°C$$

$$T_{ctf} = \frac{25.04+25.04}{2} = 25.04°C$$

2. Pressure, P_{ctf}

$$P_{ctf} = P_R + \frac{P'_{ctf}\,\rho_{dbp}\,G}{\overset{o}{\rho}_{Hg}} \tag{131}$$

$$P_{ctf} = 29.05 \text{ in Hg} + \frac{(28.95 \text{ in dbp})(1.0382 \frac{g}{cc})(0.999645)}{(13.5951 \frac{g}{cc})}$$

$$= 31.26 \text{ inches Hg}$$

3. Compressibility factor, Z_N. The second virial coefficient calculated from the formula in Table LII at $T = T_{ctf} + 273.15°K$ or $298.19°K$ is $B_N = -5.3 \frac{cc}{g\ mol}$

$$Z_N = 1 + \frac{B_N\,P_{ctf}}{R\,T_{ctf}} \tag{132}$$

$$= 1 + \frac{(-5.3 \frac{cc}{g\ mol})(31.26 \text{ in Hg})}{(25.04+273.15°K)(2455 \frac{cc \text{ in Hg}}{g\ mol\ °K})}$$

$$= 0.9998$$

4. Volume of calibration tank, V_{ctf} : corrected for thermal expansion to T_{ctf} and for volume of manometer fluid displaced in well

$$V_{ctf} = V_{ct}[1 + v_{exp}(T_{ctf}-20)] + (A_m)(P'_{ctf}) \tag{133}$$

$$= 6.422[1 + 5x10^{-5}(25.04-20)] + \frac{(0.038 \text{ in}^2)(28.95 \text{ in})}{(1728 \text{ in}^3/\text{ft}^3)}$$

$$= 6.424 \text{ ft}^3$$

Hence, from Equation (130)

$$N_f = \frac{(28.016 \frac{lb}{mol})(31.26 \text{ in Hg})(6.424 \text{ ft}^3)}{(0.9998)(25.04+273.15°K)(39.329 \frac{\text{in Hg ft}^3}{mol\ °K})}$$

(d) Flow rate of nitrogen

$$F = \frac{N_f - N_i - N_{well}}{\theta} \tag{134}$$

$$= \frac{(0.4798 - 0.0134 - 0.0002)\text{lb}}{(931 \text{ sec})} \left(\frac{60 \text{ sec}}{\text{minute}}\right)$$

$$= 0.03003 \frac{\text{lb}}{\text{minute}}$$

Calculation of Parameters

$$\frac{F}{\sqrt{\rho_F \Delta P_F}} = \frac{0.03003 \frac{\text{lb}}{\text{minute}}}{\sqrt{(4.962 \frac{\text{lb}}{\text{ft}^3})(7.511 \text{ inches dbp})}}$$

$$= 0.4919 \times 10^{-2}$$

$$\frac{\rho_F \Delta P_F}{\eta_F^2} = \frac{(4.962 \frac{\text{lb}}{\text{ft}^3})(7.511 \text{ inches dbp})}{(199.6 \times 10^{-6} \text{ poise})^2}$$

$$= 0.9352 \times 10^5$$

$$\ln\left[\frac{\rho_F \Delta P_F}{\eta_F^2}\right] = 11.446$$

Enthalpy of Mixing Measurement

Sample data on run number 4.001 on the nitrogen-carbon dioxide system at the nominal experimental conditions of 40°C and 500 psia are given in Table LV. The equations which will be used for making primary and secondary corrections are those that have been derived in the chapter entitled "Thermodynamics Relations." The necessary heat capacity and isothermal Joule-Thompson coefficient data are given in Table XLIII. Calculations made are:

1. Flow rates
2. Composition

3. Power input
4. Pressure at calorimeter outlet
5. Pressure drops across calorimeter
6. Temperature at calorimeter outlet
7. Excess enthalpy at calorimeter outlet conditions
8. Normalized excess enthalpy
9. Impurity correction for a nitrogen-ethane mixture

Flow Rates

(a) Flow rate of nitrogen stream

The measurements on the nitrogen flow meter are given in Table LV. The density, ρ_F, the pressure, ΔP_F, and the viscosity, η_F, are calculated from this data utilizing the procedures described in the previous sections. The flow rate of nitrogen calculated from the calibration equation given in Table XXIV is

$$F_A = 0.03567 \frac{lb}{min}$$

(b) Flow rate of carbon dioxide stream

The flow rate of carbon dioxide uncorrected for impurities, F_{CO_2}, calculated from the measurements on the flow meter in Table LV and the calibration equation in Table XXV is

$$F_{CO_2} = 0.05552 \frac{lb}{min}$$

The flow rate of impure carbon dioxide corrected for impurities is

$$F_{BM} = (F_{CO_2})\left(\frac{M_{BM}}{M_{CO_2}}\right)$$

$$= (0.05552) \frac{(43.988 \text{ lb/mol})}{(44.011 \text{ lb/mol})}$$

$$= 0.05549 \frac{lb}{min}$$

TABLE LV

SAMPLE DATA ON ENTHALPY OF MIXING MEASUREMENT

Variable	Value
Run Number	4.001
Nominal Temperature, T_n	40°C
Nominal Pressure, P_n	500 psia
Room Pressure, P'_R	29.46 in Hg
Room Temperature, T_R	22.5°C
Nitrogen Flow Meter	
Pressure on Heise gauge, P_{hs}	1080.1 psig
Heise gauge calibration, P_{diff}	0.5 psi
Measured pressure drop, (h_H-h_L)	28.03 cm dbp*
Temperature of cathetometer, T_{cath}	23.8°C
Carbon Dioxide Flow Meter	
Pressure on Heise gauge, P_{hs}	1058.0 psig
Heise gauge calibration, P_{diff}	1.2 psi
Measured pressure drop, (h_H-h_L)	23.55 cm dbp
Power Input	
Voltage drop across 1 ohm resistor, V_i	0.147704 volts
Voltage drop across 10 ohm resistor, V_e	0.025439 volts
Temperature of resistors, T_{res}	26.8°C
Calorimeter	
Pressure at calorimeter outlet pressure tap, P'_{bal}	485.2 psig
Measured pressure drop between:	
Nitrogen inlet and mixture outlet, ΔP_N	6.28 cm dbp
Carbon dioxide inlet and mixture outlet, ΔP_{CO_2}	4.44 cm dbp
Measured temperature, T_b	40.00°C
Temperature of emergent stem, t	32°C
Length of emergent stem, n	10°C
Average reading on thermopile between inlet and outlet, ΔE	-1.7 microvolts
Average reading on thermopile between inlet gases	0.2 microvolts
Additional Data	
Molecular weight of impure inlet CO_2 stream, M_{BM}	43.988
Mass fraction of impurities in inlet CO_2 stream, w_I	0.001
Dead weight gauge calibration correction (See Table XXVIII), P_{corr}	0.0 psi
Differential expansion coefficient for mercury-in-glass in thermometer	0.00016/°C

TABLE LV (Continued)

Variable	Value
Thermometer calibration correction (See Table XXX), T_{corr}	+0.02°C
Isothermal Joule-Thompson coefficient of N_2 , φ_A	-0.0055 $\frac{Btu}{lb\ psi}$
Isothermal Joule-Thompson coefficient of CO_2 , φ_B	-0.0312 $\frac{Btu}{lb\ psi}$
Heat capacity of N_2 , C_{P_A}	0.258 $\frac{Btu}{lb\ °F}$
Heat capacity of CO_2 , C_{P_B}	0.275 $\frac{Btu}{lb\ °F}$
Excess isothermal Joule-Thompson coefficient, φ^E	0.0053 $\frac{Btu}{lb\ psi}$
Excess heat capacity, C_P^E	-0.024 $\frac{Btu}{lb\ °C}$
Cross sectional area of calorimeter inlet gas tubes, A_{in}	0.106 in^2
Cross sectional area of calorimeter outlet gas tube, A_{out}	0.197 in^2
Density of Nitrogen, ρ_N	2.74 $\frac{lb}{ft^3}$
Density of Carbon dioxide, ρ_{CO_2}	4.30 $\frac{lb}{ft^3}$
Density of mixture containing 0.503 mole fraction nitrogen, ρ_{AB}	3.15 $\frac{lb}{ft^3}$
Note: See Table LIV for values of s_{exp}, ρ_{air}, ρ_{brass}, P_h, A_w	

*dbp is dibutyl phthalate.

(c) Flow rate of impurities

$$F_I = w_I \, F_{BM} \tag{135}$$
$$= (0.001)(0.05549 \ \frac{lb}{min})$$
$$= 0.00006 \ \frac{lb}{min}$$

(d) Flow rate of mixture

$$F_{ABM} = F_A + F_{BM} \tag{136}$$
$$= 0.03567 + 0.05549$$
$$= 0.09116 \ \frac{lb}{min}$$

$$F'_{ABM} = F_A + F_{CO_2} \tag{137}$$
$$= 0.03567 + 0.05552$$
$$= 0.9119 \ \frac{lb}{min}$$

Composition

$$X_N = \frac{\left(\frac{F_A+F_I}{M_N}\right)}{\left(\frac{F_{BM}}{M_{BM}}\right) + \left(\frac{F_A}{M_N}\right)} \tag{138}$$

$$= \frac{\left(\frac{0.03567+0.00006 \ \frac{lb}{min}}{28.016 \ \frac{lb}{mol}}\right)}{\left(\frac{0.05549 \ \frac{lb}{min}}{43.988 \ \frac{lb}{mol}}\right)\left(\frac{0.03567 \ \frac{lb}{min}}{28.016 \ \frac{lb}{mol}}\right)}$$

$$= 0.503$$

Power Input

$$\dot{W} = \left(\frac{V_i}{R_i} - \frac{V_e}{R_e}\right)\left(\frac{R_s+R_e}{R_e}\right) V_e \tag{74}$$

where resistances R_i, R_e, R_s calculated at $T_{res} = 26.8°C$ from equation and constants given in Table XXXII. Hence

$$\dot{W} = \left(\frac{0.147704 \text{ volts}}{1.000 \text{ ohms}} - \frac{0.025439 \text{ volts}}{10.00 \text{ ohms}}\right)\left(\frac{9999.8+10.00 \text{ ohms}}{10.00 \text{ ohms}}\right)(0.025439 \text{ volts})$$

$$= 3.696 \text{ watts}$$

Pressure at Calorimeter Outlet

$$P_o = P_{bal} + P_R \qquad (139)$$

Intermediate calculations:

1. Pressure measured with dead weight gauge, P_{bal}. Calculated as in Equation (121) in "Pressure at Flow Meter Inlet" at $P'_{bal} = 485.2$ psig.

$$P_{bal} = 485.2\left[\frac{0.999645\left(1 - \frac{0.0012 \frac{g}{cc}}{8.4 \frac{g}{cc}}\right)}{1 + 1.65\text{x}10^{-5}(22.5-23)}\right] + 0.075 + 0.0$$

$$= 485.04 \text{ psig}$$

2. True barometric pressure obtained by substituting $P'_R = 29.46$ in Hg and $T_R = 22.5°C$ in Equation (110)

$$P_R = 29.40 \text{ in Hg}$$

Hence from Equation (139)

$$P_o = 485.04 \text{ psig} + (29.40 \text{ in Hg})(0.4912 \frac{\text{psi}}{\text{in Hg}})$$

$$= 499.48 \text{ or } 499.5 \text{ psia}$$

Pressure Drops across Calorimeter

Pressure drops calculated are between

(a) Nitrogen inlet and mixture outlet, (P_1-P_o)

(b) Carbon dioxide inlet and mixture outlet, (P_2-P_o)

(a) Pressure drop between nitrogen inlet and mixture outlet

$$(P_1 - P_o) = \frac{(\Delta P_N)(G)}{\rho_{dbp}} [\rho_{dbp} - \rho_N]/A_W \qquad (140)$$

Intermediate calculations:

Density of di butyl phthalate from Equation (123)

$$\rho_{dbp} = 1.0408[1 - 6.16\text{x}10^{-4} (22.5-23.3)] \frac{g}{cc}$$

$$= 1.0413 \frac{g}{cc}$$

$$(P_1-P_o) = \frac{(6.28 \text{ cm dbp})(0.999645)[(1.0413 \frac{g}{cc})-(2.74 \frac{lb}{ft^3})(0.01602 \frac{g}{cc} \cdot \frac{ft^3}{lb})}{(1.0408 \frac{g}{cc})(26.6 \frac{\text{in dbp}}{psi})(2.54 \frac{cm}{inch})}$$

$$= 0.089 \text{ psi}$$

(b) Pressure drop between carbon dioxide inlet and mixture outlet

Calculated from $\Delta P_{CO_2} = 4.44$ cm dbp as in Equation (140):

$$(P_2-P_0) = \frac{(4.44 \text{ cm dbp})(0.999645)[1.0413-(2.74)(0.01602)]}{(1.0408)(26.6)(2.54)}$$

$$= 0.063 \text{ psi}$$

Temperature at Calorimeter Outlet

$$T_o = T_b + T_e + T_{corr} - (T_1-T_o) \qquad (141)$$

Intermediate calculations:

1. Emergent stem correction, T_e

$$T_e = K\, n(T_b-t) \qquad (142)$$

$$= (0.00016(°C)^{-1})(10°C)(40-32°C)$$

$$= 0.01°C$$

2. Temperature difference across calorimeter, (T_1-T_o). The data between 20°C and 80°C in Table XXXIII are fitted to the equation

$$\Delta E = -19.75 + 234.94T + 0.2419T^2 \qquad (143)$$

Temperature difference is calculated from the differentiated form of Equation (143)

$$(T_1 - T_o) = \frac{\Delta E}{234.94 + 0.4838T_b} \qquad (144)$$

$$= \frac{-1.7}{234.94 + (0.4838)(40.00)}$$

$$= -0.007°C$$

Hence from Equation (141)

$$T_o = 40.00 + 0.01 + 0.02 - (-0.007)$$

$$= 40.037°C$$

Excess Enthalpy at Calorimeter Outlet Conditions

$$\underline{H}_o^E = (\dot{W}/F) + \Delta P_{corr} + \Delta T_{corr} + \Delta KE_M + \Delta I_{corr} \qquad (145)$$

Intermediate calculations:

1. Power/Flow ratio, $(\dot{W}/F)$

$$(\dot{W}/F) = \frac{\dot{W}}{F_{ABM}} \qquad (38)$$

$$= \frac{3.696 \text{ watts}}{\left(0.09116 \frac{\text{lb}}{\text{minute}}\right)\left(17.5978 \frac{\text{watts}\cdot\text{minute}}{\text{Btu}}\right)}$$

$$= 2.304 \frac{\text{Btu}}{\text{lb}}$$

2. Pressure drop correction, ΔP_{corr}

$$\Delta P_{corr} = \frac{F_A}{F'_{ABM}} \varphi_A [P_1 - P_o] + \frac{F_{CO_2}}{F'_{ABM}} \varphi_B [P_2 - P_o] \qquad (146)$$

$$= \frac{(0.03567\ \frac{lb}{min})}{(0.09119\ \frac{lb}{min})}\left(-0.0055\ \frac{Btu}{lb\ psi}\right)(0.089\ psi)$$

$$+ \frac{(0.05552\ \frac{lb}{min})}{(0.09119\ \frac{lb}{min})}\left(-0.0312\ \frac{Btu}{lb\ psi}\right)(0.063\ psi)$$

$$= -0.0014\ \frac{Btu}{lb}$$

3. Temperature difference correction, ΔT_{corr}

$$\Delta T_{corr} = \frac{F_A}{F'_{ABM}} C_{P_A}(T_1-T_o) + \frac{F_{CO_2}}{F'_{ABM}} C_{P_B}(T_2-T_o) \qquad (147)$$

Intermediate calculations:

Temperature difference (T_2-T_o) is equated to (T_1-T_o) as thermopile reading of 0.2 microvolts is less than the accuracy of potentiometer ($\pm$ 0.5 microvolts)

$$\Delta T_{corr} = \left[\frac{(0.03567\ \frac{lb}{min})}{(0.09119\ \frac{lb}{min})}\left(0.258\ \frac{Btu}{lb\ °F}\right) + \frac{(0.05552\ \frac{lb}{min})}{(0.09119\ \frac{lb}{min})}\left(0.275\ \frac{Btu}{lb\ °F}\right)\right]\frac{(-0.007°C)}{(1.8\ \frac{°F}{°C})}$$

$$= -0.0035\ \frac{Btu}{lb}$$

4. Kinetic energy difference, ΔKE_M

$$\Delta KE_M = \frac{1}{2}\left[\frac{F_A}{F'_{ABM}}\overline{u}_A^2 + \frac{F_{CO_2}}{F'_{ABM}}\overline{u}_B^2 - \overline{u}_{AB}^2\right] \qquad (148)$$

$$= \frac{1}{2}\left[\left(\frac{F_A}{F'_{ABM}}\right)\left(\frac{F_A}{\rho_N A_{in}}\right)^2 + \left(\frac{F_{CO_2}}{F'_{ABM}}\right)\left(\frac{F_{CO_2}}{\rho_{CO_2} A_{in}}\right)^2 - \left(\frac{F'_{ABM}}{\rho_{AB} A_{out}}\right)^2\right]$$

$$= \left[\left(\frac{0.03567\ \frac{lb}{min}}{0.09119\ \frac{lb}{min}}\right)\left(\frac{0.03567\ \frac{lb}{min}}{(2.74\ \frac{lb}{ft^3})(0.106\ in^2)}\right)^2\right.$$

$$\left. + \left(\frac{0.05552\ \frac{lb}{min}}{0.09119\ \frac{lb}{min}}\right)\left(\frac{0.05552\ \frac{lb}{min}}{(4.3\ \frac{lb}{ft^3})(0.106\ in^2)}\right)^2\right.$$

$$- \left(\frac{0.09119 \ \frac{lb}{min}}{(3.15 \ \frac{lb}{ft^3})(0.197 \ in^2)} \right)^2 \Bigg] 2.3 \times 10^{-4} \ \frac{Btu \ min^2 \ in^4}{lb \ ft^6}$$

$$= -0.5 \times 10^{-6} \ \frac{Btu}{lb}$$

5. Impurity correction, ΔI_{corr}

$$\Delta I_{corr} = \frac{F_{BM}}{F_{AB}} \left[\underline{H}^E_{BM,o} \right] \qquad (50)$$

where the excess enthalpy of the inlet carbon dioxide stream, $\underline{H}^E_{BM,o}$, is given as in Equation (52)

$$\frac{\underline{H}^E_{BM,o}}{y_A(1-y_A)} = \frac{332.22 - 138.65(y_A-0.5) + 187.48(y_A-0.5)^2}{M_{BM}} \ \frac{Btu}{lb}$$

Intermediate calculations:

$$\underline{H}^E_{BM,o} = \frac{(0.0014)(0.9986)}{(43.988 \ \frac{lb}{mol})} \left(332.22 - 138.65(0.0014-0.5) + 187.48(0.0014-0.5)^2 \ \frac{Btu}{mol} \right)$$

$$= 0.01423 \ \frac{Btu}{lb}$$

Hence from Equation (50)

$$\Delta I_{corr} = \left(\frac{0.05549 \ \frac{lb}{min}}{0.09116 \ \frac{lb}{min}} \right) (0.01423 \ \frac{Btu}{lb})$$

$$= 0.0087 \ \frac{Btu}{lb}$$

Hence from Equation (145)

$$\underline{H}^E_o = 2.304 - 0.0014 - 0.0035 - 0.5 \times 10^{-6} + 0.0087$$

$$= 2.308 \ \frac{Btu}{lb}$$

Normalized Excess Enthalpy

$$\underline{H}_n^E = \underline{H}_o^E + \varphi^E(P_n - P_o) + C_P^E(T_n - T_o) \qquad (66)$$

$$= 2.304 \frac{\text{Btu}}{\text{lb}} + \left(0.0053 \frac{\text{Btu}}{\text{lb psi}}\right)(500 - 499.48 \text{ psia})$$

$$+ \left(-0.024 \frac{\text{Btu}}{\text{lb °C}}\right)(40 - 40.037°\text{C})$$

$$= 2.308 + 0.0028 + 0.0009$$

$$= 2.312 \frac{\text{Btu}}{\text{lb}}$$

Impurity Correction for a Nitrogen-Ethane Mixture

The example to be described is run number 16.2 on which data are given in Table XXXVI. The procedures used for all calculations other than the impurity correction are identical with those used on the nitrogen-carbon dioxide mixtures. The interpreted data are given in Tables XL and XLI. The impurity correction is

$$\Delta I_{corr} = \frac{F_I}{F_{AB}}(\Delta H_o) + \frac{F_B}{F_{AB}}(\underline{H}_{BM,o} - \underline{H}_{B,o}) + (\underline{H}_{AB,o} - \underline{H}_{ABM,o})$$

$$+ \frac{F_I}{F_{AB}}(\underline{H}_{BM,o} - \underline{H}_{ABM,o}) \qquad (60)$$

Enthalpy departures are used in place of enthalpy values as discussed in the chapter entitled "Thermodynamic Relations." The data for Equation (60) are

$$\underline{H}_{BM,o} - \underline{H}^o_{BM,o} = -27.848 \frac{\text{Btu}}{\text{lb}}$$

$$\underline{H}_{B,o} - \underline{H}^o_{B,o} = -27.706 \frac{\text{Btu}}{\text{lb}}$$

$$\underline{H}_{AB,o} - \underline{H}^o_{AB,o} = -8.959 \frac{\text{Btu}}{\text{lb}}$$

$$\underline{H}_{ABM,o} - \underline{H}^o_{ABM,o} = -9.027 \frac{\text{Btu}}{\text{lb}}$$

$$\Delta H_o = 4.597 \frac{Btu}{lb}$$

$$\frac{F_B}{F_{AB}} = 0.439 \text{ mass fraction}$$

$$\frac{F_I}{F_{AB}} = 0.00482 \text{ mass ratio}$$

Substituting the above values in Equation (60) yields:

$$\Delta I_{corr} = (0.00482)(4.597) + (0.439)[-27.848+27.706]$$

$$+ [-8.959+9.027] + (0.00482)[-27.848+9.027]$$

$$= 0.022 - 0.062 + 0.068 - 0.091$$

$$= -0.063 \frac{Btu}{lb}$$

Nomenclature for Appendix D

Roman Alphabet

A_m	Cross-sectional area of indicating column of 36-inch King manometer
A_W	Well factor for high pressure Meriam manometer. Needed to correct for depression of fluid level in well below measured zero level, h_L, at finite pressure differences, $h_H - h_L$.
A_{in}	Cross-sectional area of gas inlet tubes in calorimeter
A_{out}	Cross-sectional area of mixture outlet tubes in calorimeter
B_N	Second virial coefficient of nitrogen
C_{P_A}	Heat capacity of nitrogen
C_{P_B}	Heat capacity of carbon dioxide
C_P^E	Excess heat capacity
C_{th}	Calibration constant for thermocouples in calibration tank
ΔE	Microvolt reading on thermopiles or thermocouples
F	Flow rate
F_A	Flow rate of nitrogen calculated from flow meter calibrations
F_{AB}	Flow rate of impurity-free binary nitrogen-ethane mixture
F_{ABM}	Flow rate of impure nitrogen-carbon dioxide or nitrogen-ethane mixture
F'_{ABM}	Flow rate of impure nitrogen-carbon dioxide mixture calculated with uncorrected carbon dioxide flow rate, F_{CO_2}
F_B	Flow rate of impurity free ethane
F_{BM}	Flow rate of impure carbon dioxide stream corrected for impurities
F_{CO_2}	Flow rate of carbon dioxide uncorrected for impurities
F_I	Flow rate of impurities
G	Ratio of local gravity (980.317 gals) to standard gravity (980.665 gals)
$\underline{H}_{AB,o}$	Enthalpy of impurity-free binary nitrogen-ethane mixture at (P_o, T_o)
$\underline{H}^o_{AB,o}$	Zero pressure enthalpy of impurity free binary nitrogen-ethane mixture at (P_o, T_o)

$\underline{H}_{ABM,o}$ Enthalpy of impure nitrogen-ethane mixture at (P_o,T_o)

$\underline{H}^{o}_{ABM,o}$ Zero pressure enthalpy of impure nitrogen-ethane mixture at (P_o,T_o)

$\underline{H}_{B,o}$ Enthalpy of pure ethane at (P_o,T_o)

$\underline{H}^{o}_{B,o}$ Zero pressure enthalpy of pure ethane at (P_o,T_o)

$\underline{H}_{BM,o}$ Enthalpy of impure ethane at (P_o,T_o)

$\underline{H}^{o}_{BM,o}$ Zero pressure enthalpy of impure ethane at (P_o,T_o)

$\underline{H}^{E}_{BM,o}$ Excess enthalpy of impure carbon dioxide stream at (P_o,T_o)

$\underline{H}^{E}_{n}$ Excess enthalpy at nominal experimental conditions, (P_n,T_n)

ΔH_o Experimentally measured enthalpy difference obtained by applying pressure drop, temperature and kinetic energy difference corrections to the power/flow ratio

$\underline{H}^{E}_{o}$ Excess enthalpy at experimentally measured calorimeter outlet conditions, (P_o,T_o)

Δh Measured pressure drop in flow meter corrected for scale expansion and for well factor, A_W .

h_H Average cathetometer reading of fluid level in high pressure manometer

h_L Average cathetometer reading of zero level of fluid in high pressure manometer

ΔI_{corr} Impurity correction applied to enthalpy difference, ΔH_o

K Differential coefficient of expansion of mercury-in-glass for thermometer

ΔKE_M Kinetic energy difference between inlet and outlet gases in calorimeter

M_{BM} Molecular weight of impure carbon dioxide stream

M_{CO_2} Molecular weight of carbon dioxide

M_N Molecular weight of nitrogen

m_{c1} Weight of full cylinder number 1

m_{c2} Weight of empty cylinder number 1

m_{c3} Weight of full cylinder number 2

m_{c4} Weight of empty cylinder number 2

m_{ct} Mass of gas in calibration tank during volume determinations

m_{exp}	Coefficient of volume expansion of mercury
N_{app}	Mass of nitrogen discharged from cylinders into calibration tank
N_f	Mass of gas in filled calibration tank after stopping gas flow
N_i	Mass of gas in evacuated calibration tank prior to starting gas flow
N_{line}	Residual gas in line connecting cylinders to calibration tank
N_{vac}	Mass of gas in initially evacuated calibration tank
N_{well}	Mass of gas in well of 36-inch King manometer
n	Length of emergent stem of thermometer
P	Pressure
(P_1-P_o)	Pressure difference between nitrogen inlet and outlet mixture in calorimeter
(P_2-P_o)	Pressure difference between carbon dioxide inlet and outlet mixture in calorimeter
P'_{bal}	Nominal gauge pressure reading on dead weight gauge
P_{bal}	True gauge pressure reading on dead weight gauge
P_{corr}	Calibration correction for dead weight gauge
ΔP_{corr}	Pressure drop correction applied to power/flow ratio
ΔP_{CO_2}	Measured pressure drop between inlet carbon dioxide and outlet mixture in calorimeter
P'_{ctf}	Measured gauge pressure in filled calibration tank
P_{ctf}	Absolute pressure in filled calibration tank
P_{cti}	Absolute pressure in initially evacuated calibration tank
P_{diff}	Heise gauge calibration correction
P_F	Pressure at flow meter inlet pressure tap
ΔP_F	Pressure drop across flow meter
P_h	Head of oil between dead weight gauge and U-leg
P_{hs}	Average pressure in flow meter read on Heise gauge
P_m	Mean pressure in flow meter

ΔP_N	Measured pressure drop between inlet nitrogen and outlet mixture in calorimeter
P_n	Nominal pressure
P_o	Pressure at calorimeter outlet pressure tap
P'_R	Room pressure measured on barometer
P_R	True barometric pressure obtained from P'_R
P'_{Ri}	Room pressure measured on barometer prior to evacuating calibration tank
P_{Ri}	True barometric pressure obtained from P'_{Ri}
R	Gas constant
R_e	Standard resistor, 10 ohms nominal
R_i	Standard resistor, 1 ohm nominal
R_s	Standard resistor, 10,000 ohms nominal
s_{exp}	Linear coefficient of expansion
T	Temperature
T_1	Temperature of inlet nitrogen to calorimeter
(T_1-T_o)	Temperature difference between inlet nitrogen and outlet mixture in calorimeter
(T_2-T_o)	Temperature difference between inlet carbon dioxide and outlet mixture in calorimeter
T_b	Measured calorimeter bath temperature
T_{cath}	Temperature of cathetometer
T_{corr}	Thermometer calibration correction
ΔT_{corr}	Temperature difference correction applied to the power/flow ratio
T'_{ctf}	Temperature of bath fluid measured when calibration tank is filled
T_{ctf}	Temperature of gas in filled calibration tank
T'_{cti}	Temperature of bath fluid measured when calibration tank is evacuated
T_{cti}	Temperature of gas in evacuated calibration tank

T_e	Emergent stem correction for thermometer
T_F	Temperature of flow meter bath
T_n	Nominal temperature
T_o	Temperature at calorimeter outlet
T_R	Room temperature
T_{ref}	Temperature of reference junction for calibration tank thermocouples
T_{res}	Temperature of standard resistors
T_{R_i}	Room temperature prior to evacuating calibration tank
T_{th}	Temperature measured by thermocouples in calibration tank
t	Temperature of emergent stem of thermometer
$\bar{u}_A$	Mean velocity of inlet nitrogen in calorimeter
$\bar{u}_B$	Mean velocity of inlet carbon dioxide in calorimeter
$\bar{u}_{AB}$	Mean velocity of outlet nitrogen-carbon dioxide mixture in calorimeter
V_{app}	Approximate volume of calibration tank
V_{ct}	Volume of calibration tank normalized to 20°C
V_{ctf}	Volume of calibration tank at T_{ctf}
V_{cti}	Volume of calibration tank at T_{cti}
V_e	Voltage drop across standard resistor R_e
V_i	Voltage drop across standard resistor R_i
V_{line}	Volume of line connecting cylinders to calibration tank
V_t	Uncorrected volume of calibration tank at T_{ctf}
V_u	Volume of union connecting solenoid valve to calibration tank
V_{well}	Volume of well of 36-inch King manometer
v_{exp}	Volume expansion coefficient
$\dot{W}$	Power input to calorimeter
$(\dot{W}/F)$	Power/flow ratio
w_I	Mass fraction of impurity in carbon dioxide stream

x_N Mole fraction nitrogen in mixture exiting calorimeter

y_A Mole fraction nitrogen in carbon dioxide stream

ZH Constant defined in Table LII

ZL Constant defined in Table LII

Z_N Compressibility factor of nitrogen

Greek Alphabet

η_N Viscosity of nitrogen

η_F Viscosity of nitrogen at conditions in flow meter

θ Time period of gas collection

ρ_{AB} Density of nitrogen-carbon dioxide mixture

ρ_{air} Density of air

ρ_{brass} Density of brass

ρ_{CO_2} Density of carbon dioxide

ρ^o_{dbp} Density of dibutyl phthalate at 23.3°C

ρ_{dbp} Density of dibutyl phthalate

ρ_F Density of nitrogen at conditions in flow meter

ρ^o_{Hg} Density of mercury at 0°C

ρ_N Density of nitrogen

φ_A Isothermal Joule-Thompson coefficient of nitrogen

φ_B Isothermal Joule-Thompson coefficient of carbon dioxide

φ^E Excess isothermal Joule-Thompson coefficient of nitrogen-carbon dioxide mixture

BIBLIOGRAPHY

1. Abdullaev, Y. A., Zhur. Fiz. Khim., 13, 986 (1939).

2. Ahlert, R. C., Ph.D. Thesis, Lehigh University (1964).

3. Altunin, V. V. and D. O. Kutznetsov, Teploenergetika, 16 (8), 82 (1969).

4. Amirkhanov, K. I., A. M. Kerimov and B. G. Alibekov, The Application of Ultra-Sound to the Study of Matter, No. 13, Mosk. Obl. Ped. In-t. (1961) p. 89.

5. Amirkhanov, K. I., A. M. Kerimov and B. G. Alibekov, Critical Phenomena and Fluctuations in Solutions, Izd. Akad. Nauk. SSSR (1960) p. 5.

6. Amirkhanov, K. I., N. G. Polikhronidi and R. G. Batyarova, Teploenergetika, 17 (3), 70 (1970).

7. Bakx, I. N. and H. F. P. Knaap, Physica, 39, 1 (1968).

8. Beattie, J. A., C. Hadlock and N. Poffenberger, J. Chem. Phys., 3, 93 (1935).

9. Beattie, J. A., G. J. Su and G. L. Simard, J. Am. Chem. Soc., 61, 926 (1939).

10. Beenakker, J.J.M. and J.M.J. Coremans, Second Symposium on Thermophysical Properties, ASME, New York (1962) p. 3.

11. Beenakker, J.J.M., B. Van Eijnsbergen, M. Knoester, K. W. Taconis and P. Zandbergen, Third Symposium on Thermophysical Properties, ASME, New York (1965) p. 114.

12. Benedict, M., G. B. Webb and L. C. Rubin, J. Chem. Phys., 8, 334 (1940).

13. Benedict, M., G. B. Webb and L. C. Rubin, J. Chem. Phys., 10, 747 (1942).

14. Benedict, M., G. B. Webb and L. C. Rubin, Chem. Eng. Prog., 47, 419 (1951).

15. Bennewitz, K. and N. Andreewa, Z. Phys. Chem., A142, 37 (1929).

16. Bhirud, V. L. and J. E. Powers, Thermodynamic Properties of a 5 Mole Percent Propane in Methane Mixture, Report to the Natural Gas Processors Association, Tulsa, Oklahoma (1969).

17. Bird, R. B., W. E. Stewart and E. N. Lightfoot, Transport Phenomena, John Wiley, New York (1963).

18. Blagoi, Yu. P. and N. S. Rudenko, Izvest. Vysshikh. Ucheb. Zavedinii, Fiz., No. 6, 145 (1958).

19. Bloomer, O. T. and K. N. Rao, Inst. Gas Tech. Res. Bull., 18, (1952).

20. Brewer, J, Determination of Mixed Virial Coefficients, CFSTI, AD 663-448 (1967).

21. Brilliantinov, N. A, Zhur. Tekh. Fiz., 18, 1113 (1948).

22. Brombacher, W. G., D. P. Johnson and J. L. Cross, Mercury Barometers and Manometers, Nat. Bur. Standards Monograph 8 (1964).

23. Calado, J.C.G. and L.A.K. Staveley, Rev. Port. Quim., 11, 65 (1969).

24. Charnley, A., G. L. Isles and J. R. Townley, Proc. Roy. Soc. (London), A218, 133 (1958).

25. Cooper, H. W. and J. C. Goldfranck, Hydrocarbon Process., 46 (12), 14 (1967)

26. Cottrell, T. L., R. A. Hamilton and R. P. Taubinger, Trans. Farad. Soc., 52, 1310 (1956).

27. Crain, R. W. and R. E. Sonntag, J. Chem. Eng. Data, 12, 73 (1967).

28. Cross, J. L., Reduction of Data for Piston Gage Pressure Measurements, Nat. Bur. Standards Monograph 65 (1964).

29. Cullen, E. J. and K. A. Kobe, AIChE J., 1, 452, (1955).

30. Curl, R. F., Jr. and K. E. Pitzer, Ind. Eng. Chem., 50, 265 (1958).

31. Cutler, A.J.B. and J. A. Morrison, Trans. Farad. Soc., 61, 429 (1965).

32. Dana, L. I. and G. H. Zenner, Chem. Eng. Prog. Symp. Ser., 59 (44) 36 (1963).

33. Davies, R. H., A. G. Duncan, G. Saville and L.A.K. Staveley, Trans. Farad. Soc., 63, 855 (1967).

34. Din, F., Thermodynamic Functions of Gases, ed. F. Din, Vol. 3, Butterworths, London (1961).

35. Dodge, B. F. and A. K. Dunbar, J. Am. Chem. Soc., 49, 591 (1927).

36. Duncan, A. G. and L.A.K. Staveley, Trans. Farad. Soc., 62, 548 (1966).

37. Eakin, B. E. and R. T. Ellington, First Symposium on Thermophysical Properties, ASME, New York (1959) p. 195.

38. Eakin, B. E., R. T. Ellington and D. C. Gami, Inst. Gas. Tech. Res. Bull., 26, (1955).

39. Eakin, B. E., K. E. Starling, J. P. Dolan and R. T. Ellington, J. Chem. Eng. Data, 7, 33 (1962).

40. Ellington, R. T., B. E. Eakin, J. D. Parent, D. C. Gami and O. T. Bloomer, First Symposium on Thermophysical Properties, ASME, New York (1959) p. 180.

41. Edwards, A. E. and W. E. Roseveare, J. Am. Chem. Soc., 64, 2816 (1942).

42. Ernst, G., Proceedings of First International Conference on Calorimetry and Thermodynamics, Warsaw, Poland (1969).

43. Eubank, P. T. and B. F. Fort, Can. J. Chem. Eng., 47, 177 (1969).

44. Fastovski, V. G. and Y. V. Petrovski, Zh. Fiz. Khim., 31, 2117 (1957).

45. Faulkner, R. C., Ph.D. Thesis, University of Michigan (1959).

46. Fuchs, P., Z. Physik. Chem., 92, 641 (1918).

47. Fuks, S. and A. Bellemans, Bull. Soc. Chim. Belg., 76, 290 (1967).

48. Furtado, A. W., D. L. Katz, and J. E. Powers, Personal communication, University of Michigan, Sept. (1969).

49. Goldman, K. and N. G. Scrase, Physica, 44, 555 (1969).

50. Goodwin, R. D., Jour. Res. Nat. Bur. Standards--A, 73, 25 (1969).

51. Goodwin, R. D. and L. A. Weber, Jour. Res. Nat. Bur. Standards--A, 73, 1 (1969).

52. Goodwin, R. D. and L. A. Weber, Jour. Res. Nat. Bur. Standards--A, 73, 15 (1969).

53. Grossman, E. D., Ph.D. Thesis, University of Pennsylvania (1965).

54. Gusak, I. M., J. Tech. Phys. (USSR), 7, 796 (1937).

55. Hall, L. A., Nat. Bur. Standards Tech. Note No. 383 (1969).

56. Haney, R.E.D., and H. Bliss, Ind. Eng. Chem., 36, 985 (1944).

57. Head, J. F., Ph.D. Thesis, University of London (1960).

58. Hildebrand, J. H. and R. L. Scott, The Solubility of Non-Electrolytes, Reinhold (1950).

59. Hilsenrath, J. T., et al., Tables of Thermal Properties of Gases, NBS Circular 564 (1955).

60. Hobson, M. and J. H. Weber, Petroleum Process., 12 (9), 153 (1957).

61. Hobson, M. and J. H. Weber, Chem. Eng., 64 (12), 272 (1957).

62. Hoover, A. E., I. Nagata, T. W. Leland, Jr. and R. Kobayashi, J. Chem. Phys., 48, 2633 (1968).

63. Hougen, O. A., K. M. Watson and R. A. Ragatz, Chemical Process Principles., Part II: Thermodynamics, John Wiley, New York (1962).

64. Hsi, C. and B. C-Y. Lu, J. Chem. Eng. Data, 14, 38 (1969).

65. Huff, J. A. and T. M. Reed, J. Chem. Eng. Data, 8, 306 (1963).

66. Hust, J. C., Nat. Bur. Standards Tech. Note No. 137 (1962).

67. International Union of Pure and Applied Chemistry, Info. Bull. No. 32 (1968).

68. Ishkin, I. P. and M. G. Kaganer, Soviet Phys. Tech. Phys., 1, 2255 (1956).

69. Jacobsen, J. A. and R. E. Barieau, Paper presented at the Symposium on Enthalpy of Mixtures, 159th National Meeting of ACS, Houston Texas, Feb. 22-24 (1970).

70. Jeener, J., Rev. Sci. Instr., 28, 263 (1957).

71. Jones, M. L., Jr., Ph.D. Thesis, University of Michigan (1961).

72. Kaminishi, G. and T. Toriumi, J. Chem. Soc. Japan, 69, 175 (1966).

73. Kestin, J., Y. Kobayashi and R. T. Wood, Physica, 32, 1065 (1966).

74. Kestin, J. and W. Leidenfrost, First Symposium on Thermophysical Properties, ASME, New York (1959) p. 321.

75. Keunen, J. P., T. Verschoyle and A. T. Van Urk, Proc. Roy. Soc. (London), 26, 49 (1923).

76. Khazanova, N. E. and L. S. Lensevskaya, Khim. Prom., 41, 344 (1965).

77. Klein, R. R., Ph.D. Thesis, Yale University (1969).

78. Knaap, H.F.P., Physica, 28, 343 (1962).

79. Knaap, H.F.P., M. Knoester and J.J.M. Beenakker, Physica, 27, 309 (1961).

80. Knobler, C. M., H.F.P. Knaap and J.J.M. Beenakker, Physica, 26, 142 (1960).

81. Knobler, C. M., R.J.J. Van Heijningen and J.J.M. Beenakker, Physica, 27, 296 (1961).

82. Knoester, M., K. W. Taconis and J.J.M. Beenakker, Physica, 33, 389 (1967).

83. Koeppe, W., Kältetechnik, 11, 363 (1959).

84. Koppel, L. B. and J. M. Smith, J. Chem. Eng. Data, 5, 437 (1960).

85. Kotousov, L. S. and V. V. Baranyuk, Zh. Tekh. Fiz., 39, 372 (1969).

86. Krichevskii, J. R., N. E. Khazanova, L. S. Lensevskaya and L. Yu. Sandalova, Khim. Prom., 38, 169 (1962).

87. Krichevskii, J. R. and V. P. Markov, Zh. Fiz. Khim., 14, 101 (1940).

88. Lambert, M., Phys. Rev Letters, 4, 555 (1960).

89. Lambert, M. and M. Simon, Physica, 28, 1191 (1962).

90. Lee, J. I. and A. E. Mather, Personal Communication, University of Alberta, Jan. 23 (1970).

91. Liley, P. E., J. Chem. Eng. Data, 4, 238 (1959).

92. Luken, J. A. and J. Johnson, J. Chem. Eng. Data, 4, 176 (1959).

93. Lunbeck, R. J. and A.J.H. Boerboom, Physica, 17, 76 (1951).

94. Lunbeck, R. J., A. Michels and G. J. Wolkers, Appl. Sci. Res., A3, 197 (1952).

95. Mackey, B. H. and N. W. Krase, Ind. Eng. Chem., 22, 1062 (1930).

96. Mage, D. T., Ph.D. Thesis, University of Michigan (1964).

97. Mage, D. T., M. L. Jones, Jr., D. L. Katz and J. R. Roebuck, Chem. Eng. Prog. Symp. Ser., 59 (44), 61 (1963).

98. Manker, E. A., Ph.D. Thesis, University of Michigan (1964).

99. Masi, J. F., Trans. Am. Soc. Mech. Eng., 76, 1067 (1954).

100. Mastinu, G., J. Chem. Phys., 47, 338 (1967).

101. Mather, A. E., Ph.D. Thesis, University of Michigan (1967).

102. Mather, A. E., D. L. Katz and J. E. Powers, Trans. Farad. Soc., 64, 2939 (1968).

103. Mathot, V., Nuovo Cimento, 9, Suppl. No. 1, 356 (1958).

104. Mathot, V., Acad. Roy. Belg. Classe Sci., Mem., Collection in 8°, 33, 32 (1963).

105. Mathot, V., L.A.K. Staveley, J. A. Young and N. G. Parsonage, Trans. Farad. Soc., 52, 1488 (1956).

106. McCullough, J. P. and D. W. Scott, Experimental Thermodynamics. Volume I: Calorimetry of Non-Reacting Systems, Butterworths, London (1968).

107. Michels, A., A. Bijl and C. Michels, Proc. Roy. Soc. (London), A160, 376 (1937).

108. Michels, A., B. Blaise and C. Michels, Proc. Roy. Soc. (London), A160, 358 (1937).

109. Michels, A. and A.J.H. Boerboem, Bull. Soc. Chim. Belg., 62, 119 (1953).

110. Michels, A., A. Botzen and W. Schurman, Physica, 23, 95 (1957).

111. Michels, A. and S. R. De Groot, Appl. Sci. Res., A1, 94 (1948).

112. Michels, A. and R. O. Gibson, Proc. Roy. Soc. (London), A134, 288 (1931).

113. Michels, A. and C. Michels, Proc. Roy. Soc. (London), A153, 201 (1935).

114. Michels, A. and G. W. Nederbragt, Physica, 6, 656 (1939).

115. Michels, A., H. W. Schamp and W. De Graaf, Physica, 20, 1209 (1954).

116. Michels, A., W. Van Straaten and J. Dawson, Physica, 20, 17 (1954).

117. Michels, A., T. Wasenaar, J. M. Levelt and W. De Graaf, Appl. Sci. Res., A4, 381 (1954).

118. Mickley, H. S., T. K. Sherwood and C. E. Reed, Applied Mathematics in Chemical Engineering, McGraw-Hill, New York (1957).

119. Miller, J. G. and R. A. Gorski, J. Am. Chem. Soc., 75, 550 (1953).

120. Mills, J. R. and F.J.L. Miller, Can. Chem. Proc. Ind., 29, 651 (1945).

121. Montgomery, J. B. and T. De Vries, J. Am. Chem. Soc., 64, 2372 (1942).

122. Mrazek, R. V. and H. C. Van Ness, AIChE J, 7, 190 (1961).

123. Nathan, D. I., Brit. Chem. Eng., 12, 223 (1967).

124. Newitt, D. M., M. U. Pai, N. R. Kuloor and J.A.W. Huggill, Thermodynamic Functions of Gases, ed. F. Din, Vol. 1, Butterworths, London (1962).

125. Opfell, J. B., W. G. Schlinger and B. H. Sage, Ind. Eng. Chem., 46, 1286 (1954).

126. Otto, J., Handbuch der Experimental Physik, Vol. III, Part 2, Akademische Verlogsgesellschaft M.B.H., Leipzig (1929).

127. Otto, J. and L. Holborn, Z. Physik., 10, 367 (1922).

128. Pfefferle, W. C., J. A. Goff and J. G. Miller, J. Chem. Phys., 23, 509 (1955).

129. Pollitzer, F. and E. Strebel, Z. Physik. Chem., 110, 768 (1924).

130. Pool, R.A.H., G. Saville, T. M. Herrington, B.C.D. Shields and L.A.K. Staveley, Trans. Farad. Soc., 58, 1692 (1962).

131. Pool, R.A.H. and L.A.K. Staveley, Trans. Farad. Soc., 53, 1186 (1957).

132. Powers, J. E., Proc. Ann. Conv., Nat. Gas Process. Assoc., Tech. Papers, 48, 16 (1969).

133. Prigogine, I., The Molecular Theory of Solutions, North Holland Publ., Amsterdam (1957).

134. Reamer, H. H., R. H. Olds, B. H. Sage and W. N. Lacey, Ind. Eng. Chem., 36, 956 (1944).

135. Reamer, H. H., F. T. Selleck, B. H. Sage and W. N. Lacey, Ind. Eng. Chem., 44, 198 (1952).

136. Rivkin, S. L. and V. M. Gukov, Teploenergetika, 15 (10), 109 (1968).

137. Roebuck, J. R., Proc. Amer. Acad. Arts and Sci., 60, 537 (1925).

138. Roebuck, J. R., Proc. Amer. Acad. Arts and Sci., 64, 287 (1930).

139. Roebuck, J. R., T. A. Murrel and E. E. Miller, J. Am. Chem. Soc., 64, 400 (1942).

140. Roebuck, J. R. and H. Osterberg, Phys. Rev., 48, 450 (1935).

141. Rossini, F. D., et al., Selected Values of Physical and Thermodynamic Properties of Hydrocarbons and Related Compounds, Carnegie Press, Pittsburgh (1953).

142. Sage, B. H. and W. N. Lacey, Some Properties of the Lighter Hydrocarbons, Hydrogen Sulfide and Carbon Dioxide, Am. Pet. Inst., Proj. 37, New York (1959).

143. Sage, B. H., D. C. Webster and W. N. Lacey, Ind. Eng. Chem., 29, 658 (1937).

144. Sass, A., B. F. Dodge and R. H. Bretton, J. Chem. Eng. Data, 12, 168 (1967).

145. Saurel, J. R., Genie Chim., 79 (12), 44 (1958).

146. Savini, C. G., D. R. Winterhalter, L. H. Kovach and H. C. Van Ness, J. Chem. Eng. Data, 11, 40 (1966).

147. Savini, C. G. and D. R. Winterhalter and H. C. Van Ness, J. Chem. Eng. Data, 10, 168, 171 (1965).

148. Scott, R. L., J. Chem. Phys., 25, 193 (1956).

149. Sehgal, I.J.S., V. F. Yesavage, A. E. Mather and J. E. Powers, Hydrocarbon Process., 47, No. 8, 137 (1968).

150. Seligmann, P., D. O. Edwards, R. E. Sarwinski and J. T. Tough, Phys. Rev., 181, 415 (1969).

151. Seshadri, D. N., D. S. Vishwanath and N. R. Kuloor, J. Chem. Eng. Data, 12, 70 (1967).

152. Shan'a, M. Y. and F. B. Canfield, Trans. Farad. Soc., 64, 2281 (1968).

153. Shrock, V. E., N.A.C.A. Tech. Note No. 2838 (1952).

154. Simon, M., Physica, 29, 1079 (1963).

155. Smith, G. E., R. E. Sonntag and G. J. Van Wylen, Advan. Cryogen. Eng., 8, 162 (1962).

156. Smithsonian Physical Tables, Publication 4169, Smithsonian Institute, Washington, D.C. (1954).

157. Sommers, H. S., Jr., W. E. Keller and J. G. Dash, Phys. Rev., 92, 1345 (1953).

158. Sprow, F. B. and J. M. Prausnitz, AIChE J, 12, 780 (1966).

159. Stockett, A. L. and L. A. Wenzel, AIChE J, 10, 557 (1964).

160. Stotler, H. H. and M. Benedict, Chem. Eng. Prog. Symp. Ser., 49 (6), 25 (1953).

161. Swindells, J. F., Calibration of Liquid-in Glass Thermometers, Nat. Bur. Standards Monograph 90 (1965).

162. Tester, H. E., Thermodynamic Functions of Gases, ed. F. Din, Vol. 3, Butterworths (1961).

163. Timrot, D. L. and V. P. Borisoglebskii, Soviet Phys. JETP, 11 (6), 1248 (1960).

164. Trautz, M. and O. Emert, Z. Anorg. Chem., 150, 227 (1926).

165. Tsaturyants, A. B., A. R. Mamedov and R. G. Eivazova, Dokl. Akad. Nauk. Azerb. SSSR, 18, (11), 23 (1962).

166. Tsiklis, D. S., Dokl. Akad. Nauk. SSSR, 79, 289 (1951).

167. Tsiklis, D. S., and A. I. Kulikova, Russian J. Phys. Chem., 39, 928 (1965).

168. Tsiklis, D. S. and E. V. Polyakov, Zh. Fiz. Khim., 41, 3145 (1967).

169. Tsiklis, D. S. and E. V. Polyakov, Soviet Phys. Dokl., 12, 901 (1968).

170. Van Eijnsbergen, B. and J.J.M. Beenakker, Physica, 39, 499 (1968).

171. Voronel', A. V., Yu. R. Chaskin, V. A. Popov and V. G. Simkin, Soviet Phys. JETP, 18, 568 (1964).

172. Vukalovich, M. P. and V. V. Altunin, Thermophysical Properties of Carbon Dioxide, Collet's, London (1968).

173. Vukalovich, M. P., V. V. Altunin, K. Bulle, D. S. Rasskozov and D. Ertel, Teploenergetika, 16 (11), 70 (1969).

174. Vukalovich, M. P., V. V. Altunin, K. Bulle, D. S. Rasskozov and D. Ertel, Teploenergetika, 17 (5), 60 (1970).

175. Vukalovich, M. P., V. V. Altunin and A. N. Gureev, Teploenergetika, 11 (9), 83 (1964).

176. Vukalovich, M. P., V. V. Altunin and A. N. Gureev, Teploenergetika, 12 (7), 75 (1965).

177. Vukalovich, M. P. and A. N. Gureev, Teploenergetika, 11 (8), 112 (1964).

178. Vukalovich, M. P. and Ya. F. Masalov, Teploenergetika, 11 (7), 103 (1964).

179. Vukalovich, M. P. and Ya. F. Masalov, Teploenergetika, 11 (11), 91 (1964).

180. Weber, L. A., Nat. Bur. Standards Report No. 9710A (1968).

181. Wilson, G. M., R. G. Clark and F. L. Hyman, Ind. Eng. Chem., 60, 58 (1968).

182. Winterhalter, D. R. and H. C. Van Ness, J. Chem. Eng. Data, 11, 189 (1966).

183. Workman, E. J., Phys. Rev., 37, 1345 (1931).

184. Yesavage, V. F., A. E. Mather, D. L. Katz and J. E. Powers, Ind. Eng. Chem., 59 (11), 35 (1967).

185. Yu, P., I. M. Elshayal and B. C-Y. Lu, Can. J. Chem. Eng., 47, 495 (1969).

186. Zaalishvili, S. D., Uspekhii Khim., 24, 759 (1955).

187. Zandbergen, P. and J.J.M. Beenakker, Physica, 33, 343 (1967).